ARTIFICIAL NEURAL NETWORK BASED MODELLING AND CONTROL OF A DIRECT EXPANSION AIR CONDITIONING SYSTEM

LI NING

Ph.D

The Hong Kong Polytechnic University

2012

The Hong Kong Polytechnic University
Department of Building Services Engineering

Artificial Neural Network Based Modelling and Control of a Direct Expansion Air Conditioning System

Li Ning

A thesis submitted in partial fulfillment of the requirements

for the Degree of Doctor of Philosophy

June 2012

Certificate of Originality

I hereby declare that this thesis is my own work and that, to the best of my knowledge and belief, it reproduces no material previously published or written, nor material that has been accepted for the award of any other degree or diploma, except where due acknowledgement has been made in the text.

Li Ning

Department of Building Services Engineering

The Hong Kong Polytechnic University

Hong Kong SAR, China

June, 2012

Abstract

Direct expansion (DX) air conditioning (A/C) systems have been increasingly used over the recent decades in buildings, especially in small to medium scaled buildings. This is because they are more energy efficient and more flexible in installation, but cost less to own and to maintain, as compared to large chilled water based central A/C systems. Conventional DX A/C units equipped with single-speed compressor and fan rely on on-off cycling of compressor to maintain the indoor dry-bulb temperature, leading to either a space overcooling or an uncontrolled equilibrium indoor air humidity, and resulting in a reduced level of thermal comfort for occupants and low energy efficiency. With the development of variable-speed drive technology, it becomes possible for DX A/C units to have the speeds of their compressors and supply fans varied, so as to achieve simultaneous control over both indoor air temperature and relative humidity (RH).

On the other hand, artificial neural network (ANN) has been proven to be powerful in modeling the dynamic operating performance of a nonlinear multivariable system, because ANN has a powerful ability in recognizing accurately the inherent relationship between any set of inputs and outputs without requiring a physical model. This ability is essentially independent of the system complexity such as nonlinearity, multiple variables, coupling, with noise and uncertainty. An ANN-based control strategy which could deal with a nonlinear multivariable complex system,

such as a DX A/C system, can then be developed. As an intelligent nonlinear dynamic control method, an ANN-based control strategy offers a viable solution to the control over complex systems.

This Thesis reports on a study of developing a multi-input multi-output (MIMO) control strategy that can simultaneously control indoor air temperature and humidity by varying speeds of both compressor and supply fan in a DX A/C system, using ANN-based modeling and control approaches. The Thesis starts with reporting the development of a two-in two-out ANN-based steady-state model for an experimental variable speed DX A/C system. The model can be used for simulating the steady-state total output cooling capacity (TCC) and Equipment Sensible Heat Ratio (SHR) of the DX A/C system under different combinations of compressor and supply fan speeds. Extensive experiments were carried out to collect data for ANN training and testing, as well as for validating the ANN-based steady-state model developed. The ANN-based steady-state model has been validated experimentally by comparing the measured results of TCC and SHR using the experimental DX A/C system with the predicted results using the ANN-based steady-state model developed. The ANN-based model developed can be used to predict the steady-state operating performance of the experimental DX A/C system with a higher accuracy.

Secondly, the Thesis presents the development of an ANN-based dynamic model for the experimental DX A/C system, linking the indoor air temperature and humidity

controlled by the DX A/C system with the variations of compressor and supply fan speeds. The ANN-based dynamic model has been validated experimentally by comparing the measured results of indoor air dry-bulb and wet-bulb temperatures under different compressor speed and/or supply fan speed using the experimental DX A/C system, with the predicted results using the ANN-based dynamic model developed. The calculated values of average relative error (ARE) and maximum relative error (MRE) when experimentally validating the ANN-based dynamic model developed indicated the high accuracy of the ANN-based dynamic model developed.

Thirdly, using the ANN-based dynamic model developed, an ANN-based controller for controlling simultaneously the indoor air temperature and humidity by varying the compressor speed and supply fan speed in a space served by the experimental DX A/C system was developed. This ANN-based controller was designed using the direct inverse control (DIC) strategy. The controllability tests including command following test and disturbance rejection test were carried out using the experimental DX A/C system, and the test results showed that the ANN-based controller developed was able to track the changes in setpoints and to resist the disturbances, with adequate control accuracy and sensitivity.

Finally, to further address the problem of limited controllable range for the ANN-based controller, which is common to all controllers developed based on system identification, an ANN-based on-line adaptive controller has been developed

and is presented. The ANN-based on-line adaptive controller was able to control indoor air temperature and humidity simultaneously within the entire expected operational range by varying compressor and supply fan speeds. The controllability tests for the controller were carried out using also the experimental DX A/C system. The test results showed that the ANN-based on-line adaptive controller developed was able to control indoor air dry-bulb and wet-bulb temperatures both near and away from the operating condition at which the ANN-based dynamic model in the ANN-based on-line adaptive controller was initially trained, but within the entire range of operating conditions, with a high control accuracy.

Publications Arising from the Thesis

I. Journal Papers

- **Ning Li**, Liang Xia, Deng Shiming, Xiangguo Xu and Ming-Yin Chan. Steady-state operating performance modeling and prediction for a direct expansion air conditioning system using artificial neural network. *Building Services Engineering Research and Technology* , 33(3), 281-292 (2012) (Based on Chapter 5)

- **Ning Li**, Liang Xia, Deng Shiming, Xiangguo Xu and Ming-Yin Chan. Dynamic modeling and control of a direct expansion air conditioning system using artificial neural network. *Applied Energy*, 91(1), 290-300 (2011) (Based on Chapters 6 and 7)

II. Manuscripts

- **Ning Li**, Liang Xia, Deng Shiming, Xiangguo Xu and Ming-Yin Chan. On-line adaptive control of a direct expansion air conditioning system using artificial neural network. Submitted to *Automation in Construction* (Based on Chapter 8)

III. Conference paper

- **Ning Li**, Liang Xia, Deng Shiming, Xiangguo Xu and Ming-Yin Chan. Development of an On-line Adaptive ANN-based Controller for a Direct Expansion Air Conditioning System. *International Refrigeration and Air Conditioning Conference*, Purdue University, USA, July 16-19, 2012

Acknowledgements

I must express my grateful thanks to my Chief Supervisor, Dr. Shiming Deng, Professor, and my Co-Supervisor, Dr. Ming-yin Chan, Assistant Professor, both from the Department of Building Services Engineering (BSE), The Hong Kong Polytechnic University, for their readily available supervision, valuable suggestions, patient guidance, continuous help and encouragement throughout the course of the work.

My special thanks go to The Hong Kong Polytechnic University for financially supporting this project. I would like to also thank Dr. Liang Xia, Dr. Xiangguo Xu, Dr. Minglu Qu, Dr. Dongmei Pan and Dr. Yan Pan for their assistance in my simulation and experimental work. I am also grateful to Dr. Zheng Li and Dr. Qi Qi for the inspirations that I got from their work. In addition, I wish to express my gratitude to the technicians in the Heating Ventilation and Air Conditioning Laboratory of the BSE Department for their supports during my experimental work.

Finally, I would like to express my deepest appreciation to my family members: my father, Fujin Li, my mother, Yun Gao and my younger brother, Ting Li. I could not have finished my work without their on-going loves, supports, patience and understandings.

Table of Contents

List of Figures

Chapter 8

Appendix A

List of Tables

Nomenclature

Variable	Description	Unit
b	Bias of a neuron	ND
E	Difference between the output from a system and the corresponding control reference	ND
k	Counter of control action by the ANN-based on-line adaptive controller	ND
l	Number of data sets used for on-line training the ANN-based dynamic model (l = 10 in the current study)	ND
m_a	Mass flow rate of air	kg/s
N	Total number of the data sets used in training/testing/validation	ND
O	Outputs from an ANN	ND
P	Percentage of the maximum compressor or supply fan speed	%
q	Time delay operator	ND
r	Control reference	^{o}C
R	Mean ratio of the experimental results to the corresponding results predicted by the ANN-based model during testing	ND
t	Time instant (where t is the present time step, (t-1), the time instant at last time step and (t+1), the time instant at next time step, and the time interval between time instant t and (t+1) is Δt)	s
Δt	Time interval between two consecutive control actions by the ANN-based on-line adaptive controller	s
T	Temperature	^{o}C
u	Inputs to a system	ND

U	Uncertainty	%
v	Linear combiner output of a neuron	ND
W	Weights	ND
x	Input to a neuron	ND
X	Data of indoor air dry-bulb and wet-bulb temperatures collected for on-line training of ANN-based dynamic model	^{o}C
y	Output from a neuron or system	ND
Y	Data of compressor and supply fan speeds collected for on-line training of ANN-based dynamic model	%

Greek symbols

δ	Local gradient	ND
η	Learning rate	ND
σ	Standard deviation of the ratios of the experimental results to the corresponding results predicted by the ANN-based model during testing	ND
τ	Time duration starting from the beginning of control to the current time instant	s
φ	Activation function	ND

Note: ND = No Dimensions

Subscripts

C	Compressor
db	Dry-bulb
F	Supply fan
i	Layer number
in	Inlet
I	Total number of layers
j	Neuron number in a layer
J	Total number of neurons in a layer
m	ANN-based dynamic model
n	Data set number
out	Outlet
p	Values of the variables collected at a time
wb	Wet-bulb

List of Abbreviations

A/C	air conditioning
ANN	artificial neural network
ARE	average relative errors
BP	back-propagation
COP	coefficient of performance
DAS	data acquisition system
DDC	direct digital control
DIC	direct inverse control
DS	degree of refrigerant superheat
DX	direct expansion
EEV	electronic expansion valve
FRMA	flow rate measuring apparatus
HVAC	heating, ventilation and air conditioning
IAQ	indoor air quality
IMC	internal model control
LGU	load generating unit
L&C	logging & control
MIMO	multiple-input multiple-output
MRE	maximum relative errors
PC	personal computer
PI	proportional-integral
PID	proportional-integral-derivative
PMV	predicted mean vote
RBF	radial basis function
RE	relative error
RH	relative humidity
SHR	sensible heat ratio
SPM	self-programming module

SSR	solid state relay
TCC	totally output cooling capacity
TEV	thermostatic expansion valve
VRV	variable refrigerant volume
VSD	variable speed drive

Chapter 1

Introduction

Direct expansion (DX) air conditioning (A/C) has been widely used in small- to medium-scaled buildings. A DX A/C system consists of a DX refrigeration plant and an air-distribution sub-system. The DX refrigeration plant is mainly composed of a DX evaporator, a condenser, an expansion valve and a compressor. The evaporator in the DX refrigeration plant is used as a DX air cooling coil in the air-distribution sub-system to simultaneously cool and dehumidify the air passing through the coil. The conditioned air is then supplied to a conditioned space through an air distribution ductwork by a supply fan.

DX A/C systems are more advantageous than conventional chilled water based A/C systems. These include higher energy efficiency and lower cost to own and maintain the systems. However, it is difficult to satisfy both the indoor air temperature control and humidity control simultaneously using a DX A/C system with a single speed compressor and a single speed supply fan. This may hinder the wider use of DX A/C systems.

The traditional method for indoor air humidity control for central A/C systems is via reheating cooled air. This method is costly and energy inefficient since it uses a great deal of energy to overcool the air, and then more energy to reheat the air to a suitable

supply temperature. The use of reheating is however uncommon for DX A/C systems, and controlling indoor humidity at an appropriate level while also maintaining suitable indoor air temperature using a DX A/C system is difficult, since the cooling coil in a DX A/C system must perform both air cooling and dehumidification simultaneously. Most DX A/C systems are currently however equipped with a single-speed compressor and supply fan, relying on on-off cycling compressor as a low-cost approach to maintain only indoor air dry-bulb temperature. This results in either space overcooling or an uncontrolled equilibrium indoor relative humidity (RH) level.

The advancement of variable speed drive (VSD) technology offers tremendous opportunities for improving indoor thermal control and energy efficiency when using DX A/C systems. Compressor speed can be continuously varied to modulate the output cooling capacity to match the space actual thermal load. The supply fan speed can be also altered to affect both sensible heat and latent heat transfer rates across a heat exchanger. Therefore it is possible to simultaneously control indoor air temperature and humidity by varying speeds of both compressor and supply fan in a DX A/C system.

Although there are limited reported studies on simultaneous control of indoor air temperature and humidity in open literatures, most of them treated indoor air temperature control and humidity control separately and ignored the nonlinearity of a

DX A/C system and coupling effect of the system's operating parameters, resulting in poor control performance. On the other hand, artificial neural network (ANN) has been proven to be a useful tool in modeling and controlling the dynamic operating performance of a nonlinear multivariable system. This is because it has been shown that ANN has a powerful ability in recognizing accurately the inherent relationship between any set of inputs and outputs without requiring a physical model. This ability is essentially independent of the system complexity such as nonlinearity, multiple variables, coupling, with noise and uncertainty. An ANN-based control strategy which could deal with a nonlinear multi-input multi-output (MIMO) complex system, based on an ANN-based dynamic model, can then be developed. As an intelligent nonlinear dynamic control method, an ANN-based control strategy offers a viable solution to the control over complex systems. However, no previously related research work on controlling indoor air temperature and humidity simultaneously using a DX A/C system through a control strategy developed using ANN can be indentified in open literatures. Therefore it is necessary to fill the gap and embark on a study on developing an ANN-based control strategy that can simultaneously control indoor air temperature and humidity by varying the speeds of both compressor and supply fan in a DX A/C system, through ANN-based modeling.

In this thesis, to begin with, Chapter 2 reports a detailed literature review on various issues related to the modeling and control of DX A/C systems. An extensive literature review on studies related to the sources of indoor moisture and the effects

of air humidity on human thermal comfort is firstly presented. Then, a review of the modeling and control of DX A/C systems is reported. This is followed by introducing ANN, covering its fundamental concepts, its research history, and its applications to the modeling and control of Heating, Ventilation and Air Conditioning (HVAC) systems. Finally, the rationale to use ANN to model and control DX A/C systems is given.

Chapter 3 presents the research proposal which covers the background, project title, aims and objectives and research methodologies employed for the research work reported in this thesis.

Chapter 4 describes an experimental DX A/C system available to facilitate the research work reported in this thesis. Detailed descriptions of the experimental DX A/C system and its major components are firstly given. This is followed by describing the computerized measuring devices and a data acquisition system (DAS). A computer supervisory program used to operate and control the experimental DX A/C system is also detailed. The availability of the experimental system has been expected to be helpful in successfully carrying out the research work proposed in Chapter 3.

Chapter 5 reports on the development of an ANN-based steady-state model for the experimental DX A/C system. This two-in two-out ANN-based steady-state model

links both its totally output cooling capacity (TCC) and Equipment sensible heat ratio (SHR) with different combinations of compressor and supply air fan speeds, at a fixed inlet air temperature and RH to the system. In this Chapter, the related steady-state experimental conditions are firstly described. The training algorithm used for the steady-state modeling of the DX A/C system is secondly reported. Thirdly, the development of the ANN-based steady-state model is presented. Fourthly, the validation of the ANN-based steady-state model developed by comparing the predicted results using the ANN-based steady-state model developed with the experimental data is reported. Finally, a comparison for the prediction accuracy using the ANN-based steady-state model developed, a steady-state physical-based model and a numerical analysis using bilinear interpolation is presented.

Chapter 6 reports on the development of an ANN-based dynamic model for the experimental DX A/C system, linking its output air dry-bulb temperature and wet-bulb temperature with the variation of its compressor and supply fan speeds at a fixed indoor sensible and latent load. In this Chapter, firstly, the related experimental conditions are specified. Secondly, the development of the ANN-based dynamic model is presented. Finally, the experimental validation of the ANN-based dynamic model developed by comparing the measured open-loop responses for the experimental DX A/C system after being subject to step changes in compressor and supply fan speeds, with the corresponding predicted results using the ANN-based

dynamic model developed is presented.

Chapter 7 presents the development of an ANN-based controller to simultaneous control indoor air temperature and humidity by varying compressor speed and supply fan speed for the experimental DX A/C system, based on the dynamic model reported in Chapter 6. In this Chapter, the ANN training algorithm used in developing the ANN-based controller is firstly introduced. Secondly, the development of the ANN-based controller for the experimental DX A/C system is detailed. Finally, the validation of the ANN-based controller developed by carrying out the controllability tests using the experimental DX A/C system is presented.

In Chapter 8, to address the problem of limited control range experienced by the ANN-based controller reported in Chapter 7, the development of an ANN-based on-line adaptive controller and the results of its controllability tests are presented. Firstly, the development of the ANN-based on-line adaptive controller is detailed. Secondly, the results of controllability tests for the ANN-based on-line adaptive controller including initial start-up stage test, command following test, disturbance rejection test and commanding following with disturbances test using the experimental DX A/C system are presented. Finally, a discussion on related issues in the development of the ANN-based on-line adaptive controller for the experimental DX A/C system is detailed.

Finally, the conclusions of this thesis and the proposed future work are presented in Chapter 9.

Chapter 2

Literature Review

2.1 Introduction

HVAC systems have been widely used in almost all types of buildings, such as industrial, commercial and residential buildings for different purposes. In residential buildings, the most commonly used A/C systems are of DX type [Bordick and Gilbride 2002, Zhang 2002]. In order to improve the indoor thermal comfort in buildings, in particular in those located in hot and humid climates, served by DX A/C units, it is necessary to improve indoor air temperature and humidity control.

The DX A/C systems have been widely used in buildings, particularly in small- to medium-scaled buildings. Compared to chilled-water based central A/C systems, the use of DX A/C systems is more advantageous because they are simpler, more energy efficient and generally cost less to own and maintain. In a DX A/C system, its DX evaporator is used directly as a cooling coil to simultaneously cool and dehumidify the air passing through it. This distinguishes itself from a conventional central chilled-water based A/C system where chilled water is used for cooling and dehumidifying air. Given their simplicity in structure and flexibility in installation, DX A/C systems are widely used in residential buildings. For example, in Hong Kong the annual total sale of DX residential air conditioners was around 400,000 units in 2000 [Zhang 2002]. Air-conditioning is the largest single electricity-consuming end-use accounting for on average 36.8% of the total residential electricity use in Hong Kong [Lam 1996]. According to Department of

Energy in USA, packaged rooftop DX A/C units consumed approximately 60% of the total energy used for cooling [Bordick and Gilbride 2002].

Controlling indoor humidity at an appropriate level in a space is important since it directly affects indoor thermal comfort and indoor air quality (IAQ) [Fanger 2001, Mazzei et al. 2005]. As pointed out in ASHRAE Standard 62.1-2005, indoor RH level should be controlled within a relatively narrow range at between 30% and 60%. However, for most applications where DX air conditioners such as window units or split-type units are used, indoor air temperature is often controlled by on-off cycling the compressor in a DX air conditioner. Hence while indoor sensible load is satisfied through altering the length of on-off period, air dehumidification is only a by-product of removing the indoor sensible load. Therefore indoor humidity is not directly controlled and may fluctuate as a result of changing the match between the output sensible and latent capacities of a DX A/C unit and the space sensible and latent loads. When the output latent capacity is inadequate to meet the space latent load, indoor humidity would increase. In order to improve the indoor thermal environmental control in buildings, in particular in those located in hot and humid climates, it is therefore essential to develop new control strategies that enable the simultaneous control over indoor air temperature and humidity in spaces served by DX A/C systems.

This Chapter presents a literature review on various issues related to the modeling and control for DX A/C systems. An extensive literature review on studies related to the sources of indoor humidity and effects of humidity on human thermal comfort is firstly presented. Then, a review of the modeling and control of DX A/C systems is

reported. This is followed by the introduction of ANN, covering its fundamental concepts, its research history, and its applications to HVAC systems. Finally the rationale to use ANN to model and control DX A/C system is given.

2.2 Fundamental issues for indoor humidity control

For indoor humidity control, it is important to look at the sources of indoor moisture, since the amount of moisture to be removed from an indoor space should be equal to the amount introduced into the space from both externally and internally, to maintain a steady indoor humidity level.

2.2.1 Sources of indoor moisture

The sources of indoor moisture can be categorized into external and internal. The external sources could be further classified into three types. The first and the most important is the outdoor air ventilated through A/C systems. In ASHRAE Standard 62.2P, Ventilation and Acceptable IAQ in Low-rise Residential Buildings, there is a special consideration that the moisture from outdoor air is of particular concern in hot and humid climates [Sherman 1999]. For a conditioned space, it is obvious that the latent cooling load from ventilation air is greater than all other latent cooling loads combined [Brandemuehl and Katejanekarn 2004]. Most residential buildings require the ASHRAE-recommended minimum ventilation rate to ensure IAQ and occupants' thermal comfort [McGahey 1998]. During occupied hours, both sensible and latent cooling loads from ventilation air are continuous. Furthermore, if the latent cooling load from ventilation air is allowed to blend into that of return air

stream, a simple constant-air volume DX A/C unit would have a very difficult time to remove it [Berbari 1998, HarrimanⅢ and Judge 2002]. In particular during part load conditions in hot and humid subtropics, the latent cooling load from ventilation air would have greater influences on indoor humidity than that at full load conditions, and therefore should receive more attentions. Assuming that the minimum outdoor air intake at all time is 20% of the supply airflow rate at design/full load, at half load operation, the ratio of outdoor air would increase to 40% of the supply airflow rate. In other words, ventilation requirement dictates the increased portion of outdoor air during part load operations. At the same time, outdoor air dry-bulb temperature is lower, close to indoor air dry-bulb temperature, but its dew point temperature is higher than that at design condition. Therefore, space sensible cooling load is reduced but space latent cooling load is increased [Shaw and Luxton 1988]. The higher the moisture content of outdoor air, the higher the space latent cooling load a DX A/C unit would have to deal with.

The second is through the infiltration of outdoor air. The amount of moisture accumulated inside a conditioned space as a result of air infiltration is a function of infiltrated air mass flow rate, moisture content difference between incoming air and indoor air. Although the infiltration through a building enclosure is intermittent and unintentional, it has been emphasized that its effects on indoor RH level cannot be overlooked [Straube 2002]. Henderson et al. [1992] concluded that infiltration would have a great impact on space latent cooling load by simulating a typical building in both Miami and Atlanta. At a constant indoor air dry-bulb temperature of 25.5°C, the space latent cooling load would increase from at 11% of the total space cooling at an

average infiltration rate of 0.54 air change per hour to at 17% of the total at that of 1.08 air change per hour.

The third is by water vapor diffusion through building envelope from outdoors. Moisture migrates from a place of high vapor concentration to a place of lower vapor concentration by diffusion through materials. The moisture flowing as a result of diffusion is a function of the difference in vapor pressure between the two sides of a supporting wall in a building, the permeability of construction materials, and the exposed surface area [Shakun 1992]. However, this type of moisture gains cannot be easily determined [Barringer and McGugan 1989].

On the other hand, internal sources for indoor moisture load mainly include the moisture gains from occupants and other indoor activities, such as washing and cooking, etc. ASHRAE Handbook of HVAC Systems and Equipment 2000 correctly points out that the moisture load contributed by human occupancy depends on the number of occupants and the level of their physical activity, and recommends an average rate of moisture generation of 320 g/h for a family of four [ASHRAE 2000].

One source for indoor moisture is related to the operation of a DX A/C system. In most buildings served by a DX A/C system, the supply fan in the DX A/C system is normally run continuously regardless its compressor's operating status. When the compressor is on, moisture is condensed over cooling coil surface and collects in a drain pan. However, if the supply fan is still on when the compressor cycles off, moisture on the wet cooling coil and drain pan may be reintroduced into air stream due to constant air circulation, resulting in an increased RH level in the conditioned

space [Amrane et al. 2003, Shirey and Henderson 2004]. The amount of moisture re-evaporated depends on physical characteristics of the evaporator coil and drain pan, such as fin spacing, pan slope, etc., the thermostat cycling rate and the time constant of air conditioner latent performance at compressor start-up [Henderson 1998].

Part of the moisture from both the internal and external sources becomes directly part of space latent cooling load, while others would be absorbed by internal building envelope and indoor furnishings, which may be regarded as “moisture capacitors”, such as wall paper, furniture and carpet, etc., before a dynamic equilibrium of moisture transfer is achieved between indoor air and these capacitors [Rode et al. 2004]. A number of investigations on improving the prediction accuracy of internal humidity level have been undertaken [Lu 2003, Lu and Viljanen 2009, Mustafaraj et al. 2010]. The study undertaken by Lucas and Miranville [2004] took into account the moisture transfer between walls and the air inside a space, and improved the forecast accuracy of the amount of water condensed on an internal wall surface.

2.2.2 Effects of indoor humidity level on human thermal comfort

It was found in previous studies [Toftum and Fanger 1999, Miro 2005] that the level of indoor humidity could affect human thermal comfort. These studies showed that indoor air RH levels influenced the occupants’ thermal comfort in different ways, both directly and indirectly.

On one hand, high levels of indoor air RH may cause comfort and health problems for occupants. The primary biological health problems related to higher levels of RH are due to the growth of contaminated aerosols produced by spray humidification systems [Arens and Baughman 1996]. Health-related agents in connection with indoor RH level include dust mites, fungi, bacteria, viruses and nonbiological pollutants in general [Arens and Baughman 1996]. It has been shown that an indoor RH level above 50% would help increase dust mite population. An indoor RH level above 70% would provide an excellent environment for the growth of fungi. Fungi and dust mites found inside residences have been identified as the main causes of asthma and hay fever [Arens and Baughman 1996]. All the agents affect human health, primarily through their inhalation of indoor air, although some of them have lesser effects through the skin. The discomfort caused by the uncomfortably high levels of insufficient cooling of the mucous membranes in upper respiratory tract by inhalation of humid and warm air would increase the risk of individuals with allergies [Toftum and Fanger 1999]. In addition, the effects of high RH levels on chemical substances include increased off-gassing of formaldehyde from building and furnishing materials; combination with sulphur dioxide to form aerosols, salts and acids including sulphuric acid and sulphate salts; and increased irritative effects of odor, particles and vapors such as acrolein [Sterling et al. 1985]. Furthermore, from the viewpoint of IAQ, decreasing air RH level results in an improved perception of IAQ; air is fresher, less stale and more acceptable. Therefore, within the comfort zone suggested by ASHRAE, it is recommended to keep moderately low levels of temperature and RH to improve the perceived air quality. This may even help decrease the amount of ventilation required for acceptable perceived air quality. It has been shown that people would perceive the indoor air quality better at 20°C

and 40% RH at a small ventilation rate of 3.5 L/s/person than at 23°C and 50% RH at a ventilation rate of 10 L/s/person [Fanger 2001]. Meanwhile, from the viewpoint of human perception, at a given temperature setpoint, a decreased RH level results in occupants feeling cooler, drier and more comfortable. Also, at lower RH levels, fabrics, clothing and textiles would appear more smooth and pleasant.

On the other hand, a low level of indoor air RH would also have comfort and health impacts on occupants. Firstly, it can lead to the drying of skin and mucous surfaces, promoting the accumulation of electrostatic charges in fabric and others materials in buildings. On respiratory surfaces, drying can concentrate mucous to the extent that ciliary clearance and phagocytic activities will be reduced. Therefore, comfort complaints about dry nose, throat, eyes and skin often occur in low RH conditions, typically when the dew point is less than 0°C. A low RH level can also increase the susceptibility to respiratory disease as well as discomfort, such as asthma. Individuals with allergies, newborns and elderly are more susceptible to respiratory infections [Berglund 1998]. Secondly, a low RH level enhances the formation of ozone indoors. Very high ozone levels, in combination with poorly ventilated equipment, will also produce an irritation effect on the mucous membrane of eyes, nose, throat and respiratory tract. Finally, low RH levels are well known as a general catalyst of chemical interactions resulting in a large variety of irritants and toxic substances commonly referred to as “smog”. Indoor smog could well be responsible for a large proportion of similar symptoms of ozone. The smog is commonly associated with tight building syndrome occurring in office and commercial buildings [Sterling et al. 1985].

The problem of having an unsatisfactory level of indoor humidity can be found in different types of buildings, such as office buildings, supermarkets, libraries, hotels, as well as residential buildings, etc. Very often a building A/C system is unable to properly deal with the thermal load imposed when its latent part is high. The mismatch between space latent cooling load and equipment output latent cooling capacity can result in an inappropriate level of indoor humidity, degrading occupants' comfort and productivity. In buildings, it has been recommended that the suitable range for indoor relative humidity be between 30% and 60%, and the upper limit be set at 60% RH [ASHRAE 2000].

2.3 Modeling of DX A/C systems

Mathematical modeling based studies have gained growing recognition because they could not only save the study cost, but also help easily understand the operating characteristics of a physical system under study over its entire operating range. In the field of HVAC and Refrigeration Engineering, system models have been developed and used in predicting the operational performances, design and optimization, developing control strategies, and detecting and diagnosing operating faults, etc.

Mathematical models developed to simulate system characteristics could be classified into steady-state and dynamic models. Steady-state modeling should be sufficiently accurate for most long-term system simulations or for design optimization. However, it is not suitable for control application where it is necessary to investigate system's transient responses to a sudden disturbance. Dynamic modeling is required when carrying out research work related to controlling a

physical system.

On the other hand, mathematical models could also be classified into two broad categories: physical and empirical models. A physical model is based on detailed information of each component in a physical system and derived from physics laws. Two modeling approaches can be used to develop a physical model: lumped- and distributed-parameter modeling. However, for an empirical model, one tries to estimate the functional form of the relationships amongst variables and their numerical values without requiring detailed information of system components. Examples of empirical modeling include regression analysis, polynomial curve fits and artificial neural networks. Given the difficulty to characterize accurately all the components in an HVAC or refrigeration system and the known general good behavior in time response and accuracy for empirical models, empirical approaches are widely used for modeling HVAC and refrigeration systems [Navarro-Esbri et al. 2007].

A DX A/C system may be considered as consisting of four basic components and a conditioned space. Therefore the models of various components in a DX A/C system are separately reviewed as follows.

2.3.1 Compressor modeling

A compressor is often the most complex component in refrigeration systems [Ndiaye and Bernier 2010]. It turns the low pressure vapor refrigerant into high pressure vapor refrigerant such that it can condense in a condenser to reject heat to a second

fluid, and a refrigeration cycle can go on. There are several types of compressors for air conditioning applications, such as reciprocating compressor, scroll compressor, centrifugal compressor and rotary screw compressor.

Many different models with different degrees of complexity for reciprocating compressors can be found in the literature. There were models of reciprocating compressors in which a compressor was divided into several control volumes for compressor elements such as compression chamber and valves, etc. These models required input data either very difficult to obtain or only known to the manufacturer of a compressor. The space volumes of different elements and the effective surface areas of valves were also required. The transient fluid conservation equations (mass, momentum and energy) were integrated over the entire compressor domain and the energy balance for the refrigerant inside the cylinder was computed for each time step of an operating cycle [Perez-Segarra et al. 2003, Rigola et al. 2003]. The latest studies on modeling reciprocating compressors include those carried out by Ndiaye and Bernier [2010], Link and Deschamps [2011], Negrao et al. [2011], etc.

Modeling scroll compressors [Chen et al. 2002a, 2002b, Winandy et al. 2002] required the knowledge of pocket volumes and perimeters for every six degrees of rotation, the height, thickness and pitch of scrolls that were quite difficult to obtain. In those models, the whole compressor was divided into control volumes and the compression process in every gas pocket was simulated. It required the evaluation of areas, volume, pressure, temperature and specific volume for every crank angle. Mass and energy conservation equations were developed for control volumes.

There have been also many investigations concerning the analysis and modeling of centrifugal compressors and rotary screw compressors, such as Jiang et al. [2006], Seshaiah et al. [2007], Galindo et al. [2008] and Krichel and Sawodny [2011].

Compressor models could be classified into two general categories: steady-state models and dynamic models. Steady-state compressor models included those developed by Cavallini et al. [1996], Winandy et al. [2002], Navarro et al. [2007], etc, which were all simplified steady-state models. However, more complex steady-state models needed very specific proprietary data only available from manufacturers.

Dynamic modeling for compressor was also carried out since a dynamic model could capture the dynamic behavior of a refrigeration system and may be applied to the development of advanced control strategies. Jiang et al. [2006] developed a dynamic model for a centrifugal compressor. The model developed could be used to predict the compressor performance from its geometric information. In their study, the dynamic model for the compressor was programmed into a virtual test bed computational environment as a component of an electrical system, from which the performance curves of the compressor such as outlet pressure, efficiency and losses could be predicted. This model provided an available tool for evaluating the system performance as a function of various operating parameters. In addition, the dynamic characteristics of a variable speed compressor could be predicted by a transient simulation model [Park 2010]. Using the model developed, re-expansion loss, friction loss, mass flow loss and heat transfer loss were estimated as a function of the crankshaft speed in a variable speed compressor. A semi-empirical dynamic

mathematical model to simulate the transient behavior of mass flow rate and input power of reciprocating compressors was developed by Negrao et al. [2011]. In developing this dynamic model, curve fitting method was used based on thirteen calorimeter data sets of two compressors having different capacities, and good agreement between measured and simulated results were found in either cycling or start-up tests.

2.3.2 Heat exchangers modeling

Research work on modeling heat exchangers has always been significant in the studies for HVAC and Refrigeration systems. A number of approaches have been employed to establish the models for evaporators and condensers. The models of heat exchangers can generally be classified into two types: distributed parameter models and lumped parameter models.

Distributed parameter models are those that best fit to the nature of heat exchangers, because variations of the states that are concerned take place not only in time but also in space. Such models are represented by a set of partial differential equations [Zavala-Rio and Santiesteban-Cos 2007]. It has a higher accuracy than a lumped parameter model, but the time needed for simulation becomes longer. A lumped parameter model divides however a heat exchanger into a finite number of control volumes and the parameters in each control volume are lumped. Such a modeling approach is simple but its accuracy may be compromised.

Many investigations on modeling heat exchangers using distributed-parameter models have been carried out. Wang and Touber [1991] suggested that distributed parameter models provided the most complete information and best insight into the dynamic behavior of an evaporator. Jia et al. [1995] presented a distributed parameter model for predicting the transient performance of a DX air cooling evaporator. The model was capable of predicting the distributions of the refrigerant velocity, void fraction, temperature, tube wall temperature, air temperature and humidity, in both location and time domains. The dynamic behaviors of the evaporator were investigated with a response to a step change in the inlet refrigerant flow rate. Simulation results were compared with the experimentally measured data from a commercial evaporator using refrigerant R134a as the working fluid. The comparison results indicated that the model provided a reasonable accurate estimation of the dynamic response of the evaporator. Porkhial et al. [2004] developed a distributed parameter model for predicting the transient performance of an evaporator. The model was capable of predicting the refrigerant temperature distribution, tube wall temperature, inventory mass of refrigerant as a function of location and time.

The lumped parameter model by Deng [2000] used a different approach where for example a condenser was divided into three zones, i.e., two-phase, superheated and sub-cooling. Three zones were modeled separately based on the different heat transfer and fluid flow characteristics. This approach can adequately represent the overall thermal characteristics in a heat exchanger in operation to carry out research work related to control, and its simulation stability and computational speed may well be ensured. He et al. [1997] developed a lumped parameter model for a

two-phase flow heat exchanger, which was described mathematically by a set of complex, coupled and nonlinear partial differential equations based on the principles of mass and energy conservation, with the assumptions that the heat exchanger was a long, thin horizontal tube, and that the refrigerant flowing through the heat exchanger tube was one-dimensional. Other studies on lumped parameter models for heat exchangers were also carried out [Vargas and Parise 1995, Zhang and Zhang 2006].

It is well known that the key operating parameters of a DX cooling coil, such as evaporating temperature, refrigerant mass flow rate, coil face velocity and inlet air temperature, would have significant influence on its performance. Liang et al. [1999] developed a lumped simulation model for a DX cooling coil in which there were three heat transfer zones on its refrigerant side, and two zones on its air side, e.g., dry-cooling zone and wet-cooling zone. The model used a numerical method to calculate the partially wet and totally wet fin efficiency. On the basis of this model, a number of parameters which reflected the characteristics of air cooling coils used in diverse humid environments were analyzed. It was found that the performance of a coil was significantly affected by levels of indoor air relative humidity, which was a very significant parameter in determining the energy requirement and the quality of space cooling in a humid environment. A high humid environment would imply a higher cooling load and hence a higher energy requirement compared to a low humid environment.

2.3.3 Expansion valve modeling

The expansion device in a refrigeration system controls the refrigerant mass flow and balances the system pressure. Various expansion devices such as a capillary tube, a short tube orifice and a thermostatic expansion valve (TEV) are used in small refrigeration systems, such as air-conditioners and heat pumps. Even though capillary tubes and short tube orifices have the advantages of simplicity, low cost and low starting torque for a compressor, they are not appropriate for use in a system that requires precise flow control over a wide range of operating conditions. A TEV adopts a mechanical control method to maintain a constant degree of superheat at evaporator outlet. Therefore, the response time of a TEV is relatively slow, and this slowness may cause an unstable operating condition. However, an electronic expansion valve (EEV) has the advantages of rapid response owing to electronic signal transmission, zero activating degree of superheat, nearly linear valve characteristic, a wide range of flow rates and easy realization of programmed control, etc. It is expected that an EEV would gain a wider future application in DX A/C systems. Therefore, an EEV is indispensable if the advantages of a DX A/C system having a variable-speed compressor are to be maximized. As an essential component in a DX A/C system, an EEV acts as a throttling device where the expansion of refrigerant takes place, and usually regulates the refrigerant flow rate such that a desired degree of superheat at the exit of an evaporator can be maintained.

Commonly, an expansion valve can be represented by a steady-state model due to its very small thermal inertia. Refrigerant expansion is generally treated as an

isenthalpic process when modeling an expansion valve. Refrigerant mass flow passing through an expansion valve is usually calculated by using an empirical correlation. Deng [2000] presented a relatively simple model for an expansion valve. The model simply considered the refrigerant mass flow rate proportional to the degree of refrigerant super heat. However, the actual fluid-flow characteristic in an expansion valve was hard to be represented by the model. Park et al. [2007] developed an empirical correlation for predicting the mass flow rate passing through an EEV by modifying a single-phase orifice equation with consideration of EEV's geometries and operating conditions. Geometric parameters that were included in the empirical correlation were orifice diameter, orifice length and the EEV's opening. One representative model for an expansion valve was developed by Damasceno and Rooke [1990], based on the specifications given by value manufacturer and the empirical fitting for one set of distributor nozzle and tube size.

2.3.4 Supply fan modeling

A model of a constant-speed supply fan that can account for the influence of its inlet vane angle on its operating parameters was established by Carrado and Mazza [1991]. The model normalized the air flow rate, fan total pressure rise and fan power consumption respectively. Fan performance law was directly applied by fitting two polynomials of normalized air flow rate and fan pitch angle. As to a variable speed supply fan, its pressure-volume flow characteristics can be described, in general, by a family of constant-speed curves for pressure rise versus volumetric flow rate. According to the first fan performance law [ASHRAE 2000], for fans operating at similar dynamic conditions, their volumetric flow rates at different speeds are

proportional to the change of fan speed; their fan pressure rises are proportional to the square of, and their fan power consumptions to the cubic of the change of fan speed, respectively. Hence, using the performance data from a fan manufacturer and the well-known least-square curve-fitting technique, the fan characteristics at different speeds can be developed based on the performance data at its rated speed and expressed by a set of polynomials.

The dynamics of a fan-motor system lies in the electromagnetic and mechanical inertia of the system. When a varying voltage is supplied to a fan motor to change fan speed, the fan speed does not immediately reach its steady-state regime mainly due to the electro-motive force induced to the armature of the motor. Therefore when carrying out a control strategy analysis, the dynamics of the fan whose speed is controlled by varying supply voltage, should be taken into consideration. Mei and Levermore [2002] used a first-order differential equation with different time constants in different operational areas to describe the dynamics of a fan-motor system. For a fan whose speed is controlled by varying frequency using variable frequency drive, its dynamics can be neglected due to the fact that the speed of a standard squirrel-cage motor is direct proportional to the input power frequency and fan speed change can reach its steady-state regime in a fraction of second.

2.4 Control of DX A/C systems

The main objective of controlling an A/C system is to ensure that the desired air temperature and/or humidity in a conditioned space served by the A/C system are maintained. If A/C systems were always operated with constant loads, little or no

capacity control would be needed. However, most A/C systems are designed to meet the demands under the hottest or coldest climate conditions, thus for most of time they are operated at part-load condition. Therefore, all DX A/C systems need to be appropriately controlled with regards to their output cooling capacity when operated at different part load conditions.

2.4.1 Control issues for DX A/C system

Two specific issues related to the control of DX A/C systems, capacity control and indoor air humidity control, are discussed in this section.

2.4.1.1 Capacity control

Building heating or cooling loads do not stay unchanged but vary with time. It is therefore important to implement certain capacity control schemes to continuously adjust the output capacity of a DX A/C system to match the varying building loads. Several methods of capacity control have been applied to DX A/C systems.

Firstly, the most commonly used method in small sized residential DX A/C systems is intermittent running of compressor, e.g., on/off cycling. The disadvantage of this method is that it imposes wear and tear on the compressor and hence reduces its life. In addition, it is difficult to maintain a steady indoor air temperature within a suitable range.

Secondly, capacity control can be achieved by using suction-gas throttling, hot-gas by-pass or cylinder-unloading, etc. In the hot-gas by-pass control method, the refrigerant is by-passed from compressor and injected back into the suction line to decrease the cooling capacity, whereas in the cylinder-unloading scheme, one or more cylinders are unloaded to decrease the refrigerant mass flow rate being circulated, hence the cooling capacity. However, with suction gas throttling, the suction gas throttled occupies a large volume at compressor inlet and thus decreases the refrigerant mass flow rate, and hence the system's capacity. A numerical investigation on the above three capacity control methods for HFC-134a refrigeration systems was carried out by Yaqub and Zubair [2001]. The study results showed that the cylinder-unloading method was mostly suitable because of a high coefficient of performance (COP) in comparison with the other two methods. However, the capacity reduction was restricted to about 25%, 50%, or 75% of the total for a 4-cylinder compressor. On the other hand, the hot-gas by-pass scheme will lead to the lowest COP. Moreover, it was not suitable from the thermodynamic point of view. In addition, a very high compressor discharge temperature will restrict the capacity reduction down to around 50%. For the suction-gas throttling method, precise indoor air temperature and humidity control may be achieved and the COP was at between those by the other two methods. Furthermore, the compressor discharge temperature was the lowest, and a wide range of capacity reduction was possible with this method, depending upon the degree of throttling at compressor inlet.

Finally, capacity control may be realized by varying the flow of refrigerant by using variable speed compressors in DX A/C systems. The use of variable speed

compressor coupled with EEV in a variable refrigerant volume (VRV) A/C system can modulate precisely the refrigerant flow rate and hence system's cooling capacity, making the accurate matching between output cooling capacity and varying thermal load possible. It was reported that through the modulation of compressor speed, the output cooling capacity from a residential split-type DX A/C system could be varied between 50 and 100% of its full capacity in proportion to the change in room temperature [Yamamoto et al. 1982]. Currently with the advancement of variable speed compressor and EEV technologies, inverter-aided DX A/C systems can vary their cooling outputs between 20% and 100% of the full load. The use of variable speed compressor for capacity control may offer as well the potential for greater energy savings during part load operations. On the other hand, the energy performance of a conventional DX A/C system with a single speed compressor at part load condition was degraded dramatically [Silver et al. 1990]. During part load operation, the condensing and evaporating pressures/temperatures in a DX A/C system will respectively decrease and increase with a lower compressor speed, which would substantially increase its COP [Scalabrin and Bianco 1994]. Yang and Lee [1991] presented an analysis for an inverter-driven variable speed air conditioning system used in a hot and humid region. The results indicated that the use of variable-speed compressor could provide an annual energy saving of 20%. Furthermore, it can be expected that the pull-down time needed for a DX A/C system to reach a temperature setting during start-up can be reduced because a compressor can operate initially at its highest speed. The energy could be saved on a seasonal basis because the system would operate more efficiently at lower capacity, due to the reduced frictional losses in the compressor and the reduced pressure ratio imposed on the compressor.

In the past, variable speed compressors were generally regarded to be suitable only for use in small-scale A/C systems, but not in medium- or large-scaled A/C systems due to the lack of sufficient development and component integration. Fortunately, in recent years medium- to large-scaled variable speed compressors have gained great improvement in various aspects and been widely used in medium-capacity multi-evaporator A/C systems [Youn et al. 2002]. In order to demonstrate the benefit and feasibility of variable speed technology used in large-scale centrifugal chiller systems, Lenarduzzi and Yap [1998] established a demonstration installation of variable speed compressor in retrofitting a chilled-water based A/C system. The system was monitored for one cooling season and the results showed that variable speed drive technology could also work successfully in large-scale A/C systems. It was estimated that approximately 41% of energy saving could be achieved for this particular site and the power quality and total harmonic distortion problem induced could be neglected. Therefore, the VRV technology featured with variable speed compressor and EEV has been proven to be an energy efficient and practical way to realize capacity control in medium- or large-scaled A/C systems. Qureshi and Tassou [1996] made theoretical and practical comparisons of various capacity control methods at full- and part-load conditions, and the results showed that a variable speed operation was the most energy efficient technique for capacity control in A/C systems.

2.4.1.2 Humidity control

In many residential and commercial buildings, humidity control was found to be

inadequate and unsatisfactory. The traditional principal method for indoor humidity control used in large central HVAC systems is to overcool air to remove more moisture and then to reheat it to a suitable supply temperature. This strategy is inherently costly and inefficient since it uses a great deal of energy to overcool air and then more energy to reheat it. However, reheating is uncommon in DX A/C units, thus the problem of indoor humidity control is often encountered in spaces served by DX A/C units. In a DX A/C unit, dehumidification is less straightforward since a DX A/C unit removes moisture only when cooling the air passing through it. Dehumidification is effected through condensation at a cooling coil. The cooling coil has also a role to play in temperature control, thus this dual role of cooling and dehumidification for the cooling coil makes the controlled variables of temperature and humidity to become coupled. The current trend in designing a DX A/C unit is to have a smaller moisture removal capacity, in an attempt to boost its energy-efficiency rating and COP [Kittler 1996]. One of the methods used to improve efficiency is to increase the heat exchanger surface area. Such a strategy allows a DX A/C unit to run at a higher refrigerant temperature in its evaporator and a lower refrigerant temperature in its condenser, resulting in a lower latent capacity of the unit. Furthermore, when a DX A/C unit is operated at part load conditions, indoor humidity control problem could worsen with on-off cycling its compressor. The compressor will remove the sensible load with very little run-time to easily satisfy the thermostat setpoint and cycle off long before moisture removal can be affected [Hourahan 2004]. Indoor RH would hence rise to above the design level [Shirey and Henderson 2004].

Studies have been carried out on developing control methodologies for reducing high

indoor air humidity during part-load conditions. Chua et al. [2007] compared the following three control strategies for indoor air humidity control using large central chilled water based A/C systems: chilled water flow control, bypass air control and variable air volume control. Simulation results indicated that the use of chilled water flow control strategy resulted in the highest indoor humidity throughout the range of outdoor air conditions studied. The use of variable air volume control could however maintain the indoor humidity at a low and acceptable value as compared to the use of the other two control strategies but there were two distinct disadvantages. One was that the problem of stuffiness and stillness of air in a space may arise as the supply air flow rate dropped during part-load operations. The other was that the supply air flow rate may be reduced to a low value that it cannot provide the required minimum ventilation rate.

Several enhanced dehumidification technologies may be applied to DX A/C systems. These include thermally activated desiccant systems [Nagaya et al. 2006], heat pipe technology [Yau 2007] and dual-path systems that pre-treat ventilation air, etc. Kosar [2006] compared three enhanced dehumidification components in a conventional DX A/C system: a wraparound heat pipe heat exchanger, a desiccant dehumidifier in a wraparound configuration and a post-coil desiccant dehumidifier regenerated by using condenser waste heat. These integrated systems provided the ability to reduce SHR levels for DX A/C systems at ARI-rating conditions of 0.75 to below 0.50 in certain enhanced dehumidification systems while limiting losses in their COP and capacity.

For the selection of a humidity control method, it may depend on the application of

HVAC systems, which defines the load characteristics, operating conditions and system constraints. For example, a lightly populated small office will have thermal loads dominated by envelope heat gains. With a light occupancy, it will have a small ventilation requirement, and thus cooling and dehumidification loads could be met in most climates by a conventional DX A/C system. By contrast, a large lecture hall may have few windows and a very high ventilation demand, resulting in a large dehumidification load relative to sensible cooling load. In such an application, it may make sense to directly condition the ventilation air or use desiccant dehumidification technology.

2.4.2 Indoor thermal environment control using variable speed DX A/C systems

An experimental study by Chuah et al. [1998] concluded that for dehumidification control, airflow rate was of the prime concern. Previous field studies have demonstrated that lowering the airflow across a cooling coil and lowering evaporator coil surface temperature can enhance dehumidification efficiency [Shaw and Luxton 1988, Shirey and Henderson 2004, Hourahan 2004]. Implementing this strategy would lower space humidity level by 10% to 15% RH. The reduction in energy costs associated with various type of A/C units used, would cover the full range of climates, but is the mostly significant in humid and tropical climates [Shaw and Luxton 1988].

While much available open literature focused solely on reducing airflow rate with multi- or variable-speed supply fans, which itself is an improvement for A/C units, there has been relatively little research work looking into varying the speeds of both

the supply fan and the compressor in a DX A/C unit for better indoor environmental control.

For a DX A/C unit, the sensible and latent components of its total output cooling capacity may be altered by varying its supply fan speed and compressor speed simultaneously. One available strategy is to control the space temperature by varying compressor speed and the space RH level by varying supply fan speed, separately. Variation of the two speeds enables variation of the sensible and latent components of the total output cooling capacity of a DX A/C unit [Krakow et al. 1995].

An experimental verification for the feasibility of such a control strategy was carried out by Krakow et al. [1995]. The conditioned space was a 76.5 m^3 room on the ground floor of a large building in Canada. The experimental results illustrated that the space temperature and RH were maintained within ±0.3°C and ±2.5% RH, respectively, of their setpoint values. The sensible and latent components of the A/C unit's output cooling capacity appeared to respond to the variations of the applied and transmitted space cooling loads. The applied space cooling load on the A/C unit consisted of the heat outputs from electrical-resistance space heaters and a humidifier. The transmitted space cooling load consisted of indeterminate amounts of heat conducted through external and internal envelope, etc. A numerical simulation model incorporating Proportional-Integral-Differential (PID) control was also developed. The experimental and simulation results confirmed the feasibility of this control strategy. However, in their study, only simple comparisons and analysis were given. Detailed temperature and RH data and the related energy consumption were not indicated. Moreover, it was further observed from the experimental results

presented that the transient behaviors were poor, as it took approximately 2 hours for indoor RH to return to its original level after increasing the power input to the humidifier.

In addition, in the simulation study carried out by Andrade et al. [2002], a detailed, physically based A/C simulation model was augmented by adding load equations describing space sensible and latent cooling loads experienced by a typical residential building. The simulation results showed that the use of a variable-speed compressor and a variable-speed supply fan can help prevent short on-off cycling and improve indoor humidity control while possibly increasing system efficiency by having different combinations of compressor and fan speeds at the expanse of running a DX A/C unit longer. However, it was a simulation based study and no actual experimental validation was carried out. Also, the compressor was on-off cycled, without continuous control over the condensing unit in the DX A/C unit.

Various control strategies aiming at simultaneously controlling indoor air temperature and humidity by varying the speeds of both compressor and supply fan have been designed for, and employed in DX A/C systems, in addition to the traditional proportional-integral (PI) or PID control strategies [Krakow et al. 1995]. Li and Deng [2007b, 2007c] developed a novel direct digital control (DDC)-based capacity controller for a variable speed DX A/C system to control indoor air temperature and humidity simultaneously. The development of the controller was based on a numerical calculation algorithm using a number of real-time measured system operating parameters. However, using this control strategy, it would take time for the controller to obtain the information required if the space cooling loads

were changed, leading to an unacceptable control sensitivity. Besides, the controller's disturbance rejection ability was also poor because there was no any feedback loop to reflect the controlled process. Xu et al. [2008] developed a new control algorithm, the so-called H-L control strategy, for a variable speed DX A/C system to enable both compressor and supply air fan to operate at high speeds when the indoor air dry-bulb temperature setting was not satisfied and at low speeds otherwise. This control strategy would achieve an improved indoor humidity level and a higher energy efficiency when compared to the use of the traditional on-off control. Qi and Deng [2009] developed a MIMO control strategy for simultaneously controlling the indoor air temperature and humidity by regulating the speeds of compressor and supply fan in an experimental DX A/C system. This MIMO controller took into account the coupling effects among multiple variables of the DX A/C system, based on a dynamic mathematical model for the DX A/C system which was developed using system identification [Qi and Deng 2008]. This MIMO controller can however only perform as expected near the operating point where the governing equations in the model were linearized.

2.5 The application of ANN to the modeling and control of HVAC systems

2.5.1 Fundamental concepts of ANN

Human brain is made up of a vast network of computing elements called neurons. A neuron is a special cell that conducts an electrical signal. There are about 10 billion neurons in a human brain. Neurons interact through contacts called synapses. Brain organizes this huge number of neurons, each with weak computing power, into a

massively parallel complex network, where these neurons interact with each other dynamically to produce a powerful information processor [Haykin 1999]. A brain, at birth, has a great structure and the ability to build up its own rules through "experience". Indeed, experience is built up overtime, with the most dramatic development of a human brain taking place during the first two years from birth, but the development continues well beyond that stage. This plasticity of a neuron permits the developing nervous system to adapt to its surrounding environment [Gurney 1997, Haykin 1999].

Recognizing that a human brain operates in an entirely different way from a conventional digital computer motivate research work on ANN. The brain is a highly complex, nonlinear and parallel information-processing system. It has the capacity to organize the neurons to perform certain computations. Haykin [1999] in his book pointed out that the speed of computations for human brains can be many times faster than the fastest digital computer. For example, the human brain could recognize a familiar face embedded in an unfamiliar scene in approximately 100-200 ms, whereas the same task may take days by a conventional computer [Haykin 1999].

An ANN is a massively parallel distributed processor made up of simple processing units, which has a natural propensity for storing experiential knowledge and making it available for subsequent use. It resembles a human brain in two respects: the knowledge is acquired by the network from its environment through a learning process, and interneuron connection strengths known as synaptic weights (weights in short form) are used to store the acquired knowledge [Schalkoff 1997, Haykin 1999].

The procedure used to perform a learning process is called a learning algorithm, whose function is to modify the weights of an ANN to attain a desired design objective [Gurney 1997, Haykin 1999].

The following description and equations are essentially that of Haykin [1999]. A neuron is an information-processing unit that is fundamental to the operation of an ANN. The diagram of the model of a neuron is shown in Fig. 2.1. There are three basic elements of the neuron model:

- A set of synapses each of which is characterized by a weight of its own. Unlike a synapse in the brain, the synaptic weights of an artificial neuron may lie in a range that includes positive as well as negative values.

- An adder for summing the input signals, weighted by the respective weights of the neurons. The operations described here constitute a linear combiner.

- An activation function for limiting the amplitude of the output of a neuron. The activation function may limit the permissible amplitude range of the output signal to some finite value.

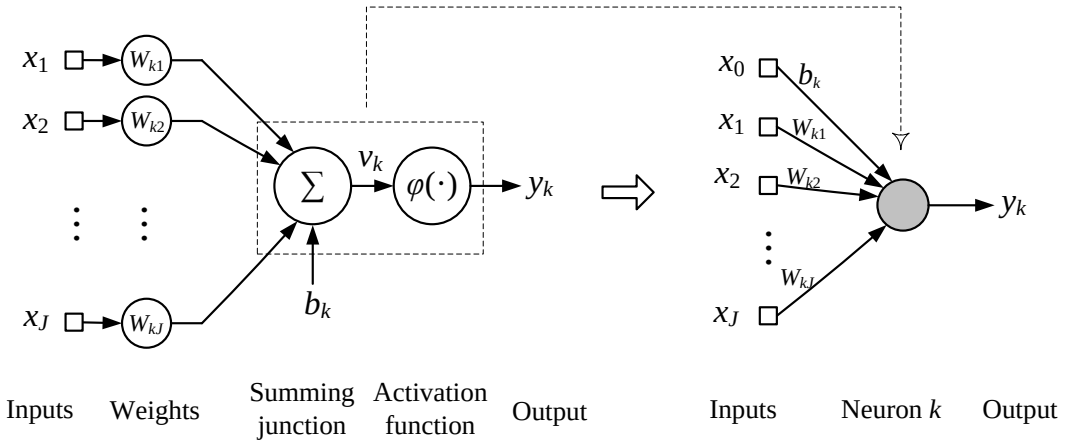

Fig. 2.1 Model of a neuron

In this figure, x_1, x_2, …, x_J are the inputs; W_{k1}, W_{k2}, …, W_{kJ}, the weights of neuron k; b_k, the bias of neuron k; $\varphi(\cdot)$, the activation function, and y_k, the output from neuron k. Input signal x_j ($1 \leq j \leq J$) was inputted to the neuron k with the weight W_{kj} ($1 \leq j \leq J$), and all inputs weighted by their respective weight were summed and then added by b_k as the activation potential of neuron k, v_k, as shown below:

$$v_k = \sum_{j=1}^{J} W_{kj} x_j + b_k \tag{2.1}$$

The bias has the effect of increasing or lowering the input to the activation function, depending on whether it is positive or negative. The activation function used in this paper could be written as:

$$\varphi(v) = \frac{1}{1+e^{-v}} \tag{2.2}$$

This is the logistic sigmoid function which possesses continuous derivatives and is

highly nonlinear. The activation potential of neuron k, v_k, is imported into an activation function φ to derive the output from neuron k, y_k.

$$y_k = \varphi(v_k) = \varphi(b_k + \sum_{j=1}^{J} W_{kj} x_j) \tag{2.3}$$

The input-to-output operation of a neuron described above can be formulized mathematically as follows:

$$y_k = \varphi(\sum_{j=0}^{J} W_{kj} x_j) \tag{2.4}$$

Eqs. (2.3) and (2.4) indicate that the bias b_k can be regarded as a new input, x_0, with its weight to neuron k valued b_k, as shown in Fig. 2.1, which means that $W_{k0} = b_k$.

The neurons as introduced above can then be structured into different patterns of an ANN linking with different learning algorithms used to train the ANN. The ANN structure used and the learning algorithms applied to train the ANN would be introduced in detail when they are applied respectively in Chapters 5 to 8.

2.5.2 Brief history of ANN related research work

An overview of the historical background of the development of ANN is available from Mehrotra et al. [1996], NG [1997] and Haykin [1999]. The modern era of ANN began with the pioneering work of McCulloch, a psychiatrist and neuroanatomist, and Walter Pitts, a mathematical prodigy, in 1943 [Haykin 1999]. McCulloch and

Pitts [1943] described a logical calculus of neural networks that united the studies of neurophysiology and mathematical logic. They showed that, with a sufficient number of such simple units, synaptic connections set properly and operating synchronously, a network so constituted would, in principle, compute any computable function. This was of great significance and with it, it is generally agreed that the disciplines of both ANN and artificial intelligence were born. The basic models of ANN ever existed in history are briefly introduced below [Haykin 1999, Huang et al. 2004, Graupe 2007]:

(1) **McCulloch-Pitts model**. The first mathematical model of a single idealized biological neuron was proposed by Warren McCulloch and Walter Pitts, known as the McCulloch-Pitts model [McCulloch and Pitts 1943];

(2) **Perceptron**. Historically, the earliest ANN was the Perceptron, proposed by a psychologist called Frank Rosenblatt [Rosenblatt 1958]. It was the simplest form of a neural network needed for the classification of a special type of patterns said to be linearly separable. Basically, it consisted of a single neuron with adjustable weights and bias [Haykin 1999, Huang et al. 2004];

(3) **Adaline** (adaptive linear neuron) and **Madaline** (multiple-Adaline). The difference between the Perceptron and the Adaline [Widrow and Hoff 1960] was the training procedure. One of the earliest trainable layered neural networks with multiple adaptive elements was the Madaline proposed by Widrow and his students [Widrow 1962];

(4) **Hopfield neural network**. In this kind of neural network, proposed by John Hopfield [Hopfield 1982], there was no self-connections and it was a fully recurrent network. The Hopfield networks were usually not used for applications involving classification and regression, but were used as associative memories [Huang et al. 2004];

(5) **Self-organizing neural network**. Kohonen [1982] published his paper on self-organizing maps using a one- or two-dimensional lattice structure. As compared to the ANN using supervised learning, a self-organizing neural network using the unsupervised learning resembled more closely the structures of their biological counterparts. Self-organizing neural networks had simple, one-layered structures;

(6) **Multilayer Feedforward neural network**. This kind of ANNs had no feedback connections from the outputs back to the inputs. The multilayer feedforward neural network, which also known as multilayer perceptron or back-propagation network, had a number of hidden layers between the input and output layer [Rumelhart et al. 1986]. Multilayer feedforward ANNs have very quickly become the most widely encountered ANN, particularly within the area of system modeling and control [Narendra and Parthasarathy 1990];

(7) **Radial Basis Function (RBF) neural network**. Broomhead and Lowe [1988] described a procedure for the design of layered feedforward networks using RBF, which provided an alternative to the multilayer feedforward networks. A key feature of RBF networks was that the output layer was merely a linear combination of the hidden layer signal, there being only one hidden layer;

(8) **Cascade-correlation neural network**. This ANN attempted to solve step-by-step problems and moving target problems during back-propagation learning. Its structure and weights may be changed during a supervised type learning [Fahlman and Lebiere 1990];

(9) **Modular and Hierarchical neural network**. A modular neural network [Jacobs et al. 1991] decomposed the computation into two or more modules that operated on distinct inputs. The outputs of these individual modules were then combined by an integrating unit to give the output of a system. Another alternative form of combinatorial network was the Hierarchical neural network [Jordan and Jacobs 1993].

2.5.3 Applications of ANN to modeling and control of HVAC systems

Since 1990s, there has been an explosion of interest in ANN, together with a change in paradigm: there was a greater interest in using ANN as a problem solving method than in developing it as an accurate representation of the human neural system. Accordingly, there have been even wider ranges of problem domains as diverse as Finance [McNelis 2005], Business [Hayashi et al. 2010], Medicine [Lin et al. 2008], transportation [Karlaftis and Vlahogianni 2011], Chemistry [Marini et al. 2008], engineering [Ao and Palade 2011], Astronomy [Friedrich et al. 2008], Agriculture [Huang et al. 2010], etc.

In recent years, studies related to developing intelligent HVAC systems have become

more popular due to the rising concern about indoor environment. In this section, the applications of ANN to modeling and control of HVAC systems will be reviewed.

2.5.3.1 ANN-based modeling for HVAC systems

The applications of ANN to modeling HVAC systems generally covered the following four major aspects:

1) Modeling performances of HVAC system components
2) Modeling performances of HVAC systems
3) Evaluating building thermal loads and energy consumption
4) Analyzing properties of refrigerants

Of all the applications, firstly, the most important one dealt with HVAC system components and their operating performance with a great variety of geometry and at different operational conditions. As a critical component in HVAC systems, heat exchangers have been widely studied using ANN. Yang [2008] introduced the commonly used ANN-based modeling and control methods and reviewed the applications of ANN in the field of thermal science and engineering. In his study, different fin-tube heat exchangers used as evaporators in refrigeration systems were chosen as examples to illustrate the use of ANN for steady-state and dynamic modeling and dynamic control. A series of experiments were carried out under both steady-state and dynamic operational conditions to collect data to train ANNs. ANN-based models were then developed and used for predicting the steady-state and dynamic operating performances of the heat exchangers. In addition, the studies on

dynamic modeling and control of heat exchangers using ANN with genetic algorithms were reviewed [Sen and Yang 2000, Yang and Sen 2000]. Diaz et al. [1996, 1999, 2001a] studied heat exchangers using ANN. In their studies, performances of a single-row fin-tube heat exchanger were firstly simulated using an ANN-based steady-state model to predict its heat transfer rates under different operational conditions [Diaz et al. 1996, 1999]. Then the time-dependent dynamic behaviors of the heat exchanger were also studied using an ANN-based dynamic model [Diaz et al. 2001a]. Yigit and Ertunc [2006] developed an ANN-based model to predict the air temperature and humidity at the outlet of a wire-on-tube type cooling coil. Ertunc and Hosoz [2008] predicted the performances of an evaporative condenser using both ANN and adaptive neuro-fuzzy inference system techniques. In their study, ANN-based models were developed to predict the heat rejection rate, outlet temperature of refrigerant along with dry-bulb and wet-bulb temperatures of the leaving air using experimental data acquired in steady-state operations. There were also a number of previous studies applying ANN to deal with heat transfer analysis and performance prediction of different structured heat exchangers, including a fin-tube heat exchanger [Ding et al. 2002, Ding et al. 2004, Pacheco-Vega et al. 2001a, 2001b, Zhao and Zhang 2010], a wire-on-tube heat exchanger [Yigit and Ertunc 2006, Hayati et al. 2009], a shell-and-tube heat exchanger [Wang et al. 2006, Xie et al. 2007], and a non-adiabatic capillary tube heat exchanger [Islamoglu et al. 2005], etc.

ANN was also applied to studying other HVAC components including compressor, capillary tube, cooling tower and boiler, etc. Yang et al. [2009] developed two ANN-based models to predict the volumetric and isentropic efficiency of both single

and variable speed compressors. A steady-state ANN-based model for a rotary vane compressor was developed by Sanaye et al. [2011] to predict its operating parameters such as refrigerant mass flow rate and compressor power consumption. ANN-based studies for compressors mainly focused on the analysis and prediction of the performances of different kinds of compressors, including reciprocating compressors [Yang et al. 2005, Yang et al. 2009], rotary compressor [Yang et al. 2009, Sanaye et al. 2011], screw compressor [Bao et al. 2006, Yang et al. 2009], centrifugal compressor [Bao et al. 2006, Tirnovan et al. 2008] and scroll compressor [Blunier et al. 2009], etc. Furthermore, ANN has also been used to predict the mass flow rate of refrigerants through capillary tube. A generalized correlation method for predicting the mass flow rate of refrigerant through adiabatic capillary tubes was developed using ANN by Zhang [2005]. Following this work, a generalized ANN-based model has been developed to predict refrigerant mass flow rate through adiabatic capillary tubes and short tube orifices by Zhao et al. [2007]. Other similar work included that by Vins and Vacek [2009]. Hosoz et al. [2007] presented a study on applying ANN to predicting the performance of a cooling tower under a wide range of operating conditions. Gao et al. [2009] predicted the thermal performance of a natural draft counter-flow wet-cooling tower under cross-wind conditions. Wu et al. [2011] applied ANN to predicting the performance characteristics of a reversibly used cooling tower under cross flow conditions for a heat pump heating system in winter. Sainlez and Heyen [2011] applied two types of ANN, a static multilayer perceptron and a dynamic Elman's recurrent neural network, to predicting the high pressure steam flow rate from a heat recovery boiler.

Secondly, ANN has been used to model different HVAC systems for different

purposes. The most widely studied HVAC systems using ANN included refrigeration and heat pump systems, air conditioning and heating systems, etc.

The applications of ANN to modeling refrigeration systems (covering absorption refrigeration systems and vapor compression refrigeration systems) mainly aimed at predicting their operational performances. Sozen and Akcayol [2004] predicted the performances of a solar-driven ejector-absorption refrigeration system with an aqua/ammonia working fluid using ANN. Sencan [2006, 2007] applied ANN to predicting the performances of ammonia-water absorption refrigeration systems. Hosoz and Ertunc [2006a] investigated the applicability of ANN to a cascade vapor compression refrigeration system to predict its various performance parameters. Similarly, the performances of a refrigeration system with an evaporative condenser, in terms of its condenser heat rejection rate, refrigerant mass flow rate, electric power input to the compressor motor and coefficient of performance, were predicted using ANN [Ertunc and Hosoz 2006]. Saidur et al. [2006] predicted the energy consumption of a household refrigerator/freezer using ANN. From the work done by Sahin [2011], ANN was successfully applied to estimating the COP values of a single-stage vapor compression refrigeration system working with R134a, R404a and R407c. ANN has also been used to model the thermodynamic performance of refrigeration systems driven by variable speed compressor [Navarro-Esbri et al. 2007, Kizilkan 2011].

ANN was also applied to modeling heat pumps. Bacthler et al. [2001] used ANN to model the steady-state performance of a vapor compression liquid heat pump. The performance analysis of an ejector absorption heat pump using ozone-safe fluid pair

was achieved using ANN by Sozen et al. [2004a]. Arcaklioglu et al. [2004] predicted the performance of a vapor compression heat pump with different ratios of R12/R22 refrigerant mixtures using ANN. In the studies of Esen and others, the performance of ground coupled heat pump systems, including horizontal ground coupled heat pumps [Esen et al. 2008a, 2008b, 2008c] and vertical ground coupled heat pumps [Esen and Inalli 2009], were modeled using ANN. Mohanraj et al. [2009a, 2009b, 2010] applied ANN to a direct expansion solar assisted heat pump system to predict its performances including power consumption, heating capacity, energy performance ratio and compressor discharge temperature [Mohanraj et al. 2009a] and the exergy destruction and exergy efficiency of the system at different solar intensities and ambient temperatures [Mohanraj et al. 2009b, 2010].

Chiller systems have also been studied using ANN. ANN was used as new approach to modeling the steady-state and dynamic operational performances of vapor compression liquid chillers [Swider et al. 2001, Bechtler et al. 2001]. Manohar et al. [2006] presented a steady-state model for a double effect absorption chiller with steam as heat input using ANN. The model developed was used to predict the chiller performance based on the chilled water inlet and outlet temperatures, cooling water inlet and outlet temperatures and steam pressure. Chang [2007] developed an ANN-based chiller power consumption model to determine optimal chiller sequencing without the requirement to measure the chilled water flow rates for the chillers used in a semiconductor factory. The chilled water supply temperatures were determined through employing ANN to solve the optimal chiller loading problem [Chang and Chen 2009].

ANN was also applied to air conditioning systems to study their operating and control performances. Yang et al. [2003] used ANN to predict the optimal starting time for a heating system in a building. Hosoz and Ertunc [2006b] used ANN to predict various performance parameters of an automotive air conditioning system using HFC134a as refrigerant. An automobile air conditioning system model was also developed by Atik et al. [2010] using ANN to predict system performance under different amounts of refrigerant charge and compressor revolution speeds. Rosiek and Batlles [2010, 2011] modeled a solar-assisted air conditioning system using ANN to predict its operational performance. Furthermore, ANN was applied to studying indoor environment. Lu et al. [2004] developed an ANN-based model for forecasting outdoor air pollutant trends in Mong Kok, Hong Kong. ANN-based evaluation models for indoor thermal comfort were developed [Atthajariyakul and Leephakpreeda 2005, Liu et al. 2007]. Sofuoglu [2008] used ANN to predict the prevalence of building related symptoms of office building occupants. The thermal behaviors in different functioned spaces, in particular indoor air temperature and humidity, have been modeled using ANN [Mustafaraj et al. 2010, Mustafaraj et al. 2011]. Forecasting air-conditioning load using ANN has been undertaken by Hou et al. [2006] and Yao et al. [2006].

Thirdly, ANN was used for the estimation of building thermal loads and the evaluation of building energy consumption. Kusiak et al. [2010] built an ANN-based model to predict the daily steam load in a building using weather data. Kwok et al. [2011] developed an ANN-based model to simulate the total building cooling load in an office building in Hong Kong, in which building occupancy rate was used as an input parameter and played a critical role in building cooling load prediction. Other

studies on predicting or forecasting building thermal loads included those by Ekici and Aksoy [2009] and Li et al. [2009]. ANN was widely used on the evaluation of building energy consumption [Neto and Fiorelli 2008, Wong et al. 2010, Escriva-Escriva et al. 2011]. In the work done by Wong et al. [2010], an ANN-based model was developed for office buildings using day lights under subtropical climates, linking external weather conditions, building envelope designs and day type (i.e. weekdays, Saturdays and Sundays) with the daily electricity use for cooling, heating, electric lighting and for the entire building. Escriva-Escriva et al. [2011] presented an ANN-based method for short-term prediction of the total energy consumption in buildings.

Finally, ANN has been applied to dealing with the thermodynamic property analysis and determination of refrigerants. Arcaklioglu et al. [2004] investigated different possible ratios of refrigerant mixtures, e.g., HFC and HC, and their corresponding performances by using ANN, with the purpose of reducing the use of CFCs by finding a drop-in replacement for pure refrigerants used in domestic and industrial appliances. ANN has been successfully applied to predicting the thermodynamic properties, such as specific volume, enthalpy and entropy in both saturated liquid-vapor region and superheated vapor region of three refrigerant mixtures, R404A, R407C and R508A, by Sozen et al. [2007, 2009, 2010]. Other studies applying ANN to predicting the thermodynamic properties of different refrigerants included those by Kurt and Kayfeci [2009] and Sencan et al. [2011]. Sozen [2004b, 2005] predicted the thermodynamic properties of two alternative refrigerant/absorbent pair, methanol-LiBr and methanol-LiCl, using ANN.

2.5.3.2 ANN-based control for HVAC systems

The applications of ANN to the control of HVAC systems covered generally the following three major aspects:

1) Control performances of HVAC system components
2) Control performances of HVAC systems
3) Control thermal environment and energy consumption

Firstly, for all HVAC system components, heat exchangers were most widely studied using ANN for control purposes. Diaz et al. [2001a] controlled the temperature of the air passing through a heat exchanger system using an ANN-based internal model control (IMC) strategy. Comparing with a standard PI or PID controller, the ANN-based controller developed had less oscillatory behavior, allowing the heat exchanger to reach steady-state operating conditions in the regions where the PI or PID controller cannot perform well. Following this, an adaptive ANN-based controller was developed in which the weights of the ANN could be on-line updated according to different performance criteria such as stability or energy consumption. It has been shown that this adaptive controller was able to both adapt to major structure changes in the system, and to simultaneously minimize the amount of energy used [Diaz et al. 2001b]. To improve the ANN-based controller developed, a modified back-propagation training method was then developed to simultaneously minimize the target error and increase the dynamic stability of the system [Diaz et al. 2004]. In the study by Nanayakkara et al. [2002], a novel ANN architecture characterized by activation functions with dynamic synaptic units was adopted in

controlling an ammonia evaporator. Abbassi and Bahar [2005] modeled an evaporative condenser under both steady state and transient state conditions for controlling its thermal capacity using an ANN-based controller which could better minimize the process error than PID controllers. Varshney and Panigrahi [2005] applied an ANN-based IMC strategy to controlling the temperature inside a test section of a test facility by varying air flow rate over heat exchanger tube surface and water flow inside the heat exchanger tube. Yang [2008] applied the ANN-based IMC strategy to controlling outlet air temperature from a heat exchanger by varying air flow rate. Vasickaninova et al. [2011] applied the ANN-based predictive control to a heat exchanger to maintain the temperature of heated outlet stream at a desired value and to minimize energy consumption.

Other HVAC components have also been studied using ANN for control purpose. For example, the determination of optimal experimental input parameters for a compressor was studied by Cortes et al. [2009] using an ANN-based inverse model. Moghaddam et al. [2011] proposed a decoupled sliding-mode ANN-based variable-bound control system to control rotating stall and surge for compressors. An ANN-based adaptive control scheme for unknown dynamics of a nonlinear plant without using a model was incorporated. In the work done by Ekren et al. [2010], three different control algorithms, i.e., PID control, fuzzy logic control and ANN-based control, were applied to the variable speed compressor and EEV in a chiller system. The comparison results showed that the ANN-based controller helped achieve a lower energy consumption than both PID and Fuzzy controllers. Soyguder [2011] controlled fan speed in a HVAC system to reduce the energy consumption using a wavelet packet decomposition ANN, which confirmed to be more accurate

than a PID controller.

Various HVAC systems, such as refrigeration systems, chilling systems, heating systems and air conditioning systems, were controlled using ANN-based techniques. Tian et al. [2008] designed a fuzzy neural controller, which integrated ANN with fuzzy logics to extract control rules from given data generated online, to control the degree of refrigerant superheat and evaporating pressure of an air cooled refrigeration system. Palau et al. [1999] controlled a gas/solid sorption chilling machine using ANN and expert systems. Chow et al. [2002] achieved the optimal control of an absorption chiller system using ANN and genetic algorithm, where ANN was used to model the system characteristics. To select the parameters for the optimal performance of an absorption chiller and for achieving the required cooling capacity, Labus et al. [2012] developed a control strategy using an inverse ANN on the basis of an ANN-based model developed for a small-scale absorption chiller. Jeannette et al. [1998] improved the performance of an air-handling unit by applying a predictive neural network controller. An ANN-based controller for a hydronic heating system was developed for energy savings while maintaining thermal comfort by Argiriou et al. [2004]. Fargus and Chapman [1998] developed a hybrid PI-ANN controller, in which the ANN could be automatically commissioned, for the control of building services plants. Khayyam et al. [2011] developed an adaptive ANN tuned PID controller to control a vehicle air conditioning system to optimize its energy consumption.

In addition, thermal environment and energy consumption were the targets of applying ANN-based control. Egilegor et al. [1997] implemented a neuro-fuzzy

control strategy, in which ANN was used to adapt the fuzzy control, to maintain the thermal comfort in a dwelling by setting air flow rates of fan coil units in three zones of the dwelling. Zones temperature and humidity were the input variables from which the value of Fanger's thermal comfort index, predicted mean vote (PMV), was calculated and used as a comfort variable. Rock and Wu [1998] developed a CO_2 demand-controlled ventilation scheme using an ANN-based control strategy. Kanarachos and Geramanis [1998] controlled the air temperature in a zone served by a hydronic heating system and the temperature of hot water to be below a maximum value using an ANN-based predictive controller. In the work done by Argiriou et al. [2000], the indoor air temperature of a building served by an electrical heating system was controlled using an ANN-based controller. Argiriou et al. [2004] further developed this controller based on its original concept and applied it to controlling a hydronic heating system. Morel et al. [2001] developed a predictive and adaptive heating controller using ANN to allow the adaptation of the control model to the real conditions, i.e., climate, building characteristics and user's behavior. In the study of Ben-Nakhi and Mahmoud [2002], ANNs were designed and trained using general regression to investigate HVAC system set back control, focusing on energy conservation in air conditioning of public buildings.

2.6 The rationale of choosing ANN in the modeling and control of DX A/C systems

A number of mathematical models have been developed for modeling the operating performances of DX A/C systems by Deng [2000], Chen and Deng [2006], Xia et al. [2008] and Qi and Deng [2008], etc. It can be seen that all these previous models

were constructed by integrating sub-models for the key components in a DX A/C system, which described mathematically the physical processes taking place in these components. Therefore, all these models were considered to be physical-based. To establish a physical-based model, however, all underlying physical processes should be known, requiring a large number of related physical parameters. Very often, the physical processes to be modeled were too complicated to be understood or some of the physical parameters were not readily available, especially for complicated processes. For example, for the above mentioned steady-state physical-based model of a DX air cooling and humidifying coil developed by Xia et al. [2008], a cross-flow DX cooling coil where heat and mass transfer can be much more complicated was simplified to a counter-flow heat exchanger. In addition, previous researchers have also demonstrated the complexity in simulating heat and mass transfer processes when using commercial computational software [Yang 2008]. Even when a complicated physical based model may be established, to find its numerical solution, a trial-and-error approach would be usually needed, inevitably requiring more computational effort and time. In addition, physical-based models can often only describe approximately what actually happened in the real world [Kim et al. 2010]. When developing a physical-based model for a heat exchanger, a number of simplifications would have to be made, for example, constant thermal or fluid coefficients and/or properties and greatly simplified geometrical parameters [Yang 2008].

In addition, various control strategies have been designed for, and employed in DX A/C systems. These include the traditional PI or PID control [Krakow et al. 1995] and other advanced control strategies, such as DDC-based control [Li and Deng

2007b, Li and Deng 2007c], H-L control [Xu et al. 2008], MIMO control [Qi and Deng 2009], etc. However, for PI or PID control strategies, the coupling effect between the output air temperature and humidity from a DX A/C system can only be dealt with by using two decoupled feedback control loops. Hence, the transient control performance of the two decoupled feedback control loops was inherently poor due to the strong cross-coupling between air temperature and humidity [Krakow et al. 1995, Qi and Deng 2008]. For the steady-state DDC-based controller developed by Li and Deng [2007a, 2007b, 2007c], it would take time for the controller to obtain the information required if the space cooling loads were changed, leading to an unacceptable control sensitivity. In addition, the controller's disturbance rejection ability was also poor because there was no any feedback loop to reflect the controlled process. On the other hand, the dynamic MIMO controller developed by Qi and Deng [2009] can only perform as expected near the operating point where the governing equations of the model was linearized.

It has been challenging to model and control a DX A/C system because of its complexity. A DX A/C system is complex. Although there is currently no universally accepted definition of a complex system, many researchers have agreed on many of the characteristics that make a system complex [Loannou and Pitsillides 2008]. Firstly, complex systems are typically composed of several interconnected subsystems which mutually influence one another [Amaral and Ottino 2004]. A DX A/C system consists of many subsystems, such as a DX evaporator, condenser, EEV, compressor and air distribution, each of which will influence, and be influenced by, the others. Actually, even a single component in a DX A/C system may be considered to be complicated and could be categorized as a complex system, for

example, a DX evaporator [Diaz et al. 2004]. Secondly, the presence of nonlinear dynamics in a plant or a process to be controlled would be one significant characteristic of a complex system [Loannou and Pitsillides 2008]. The nonlinearity of a DX A/C system would become more obvious when both indoor air temperature and humidity are controlled simultaneously [Qi and Deng 2009]. Thirdly, other characteristic of complex system would include MIMO, which is still a difficult control problem [Mahmoud and Alajmi 2010, Wong et al. 2010], and uncertainties and time variations [Loannou and Pitsillides 2008]. Therefore, effective and intelligent control strategies for DX A/C systems have been thus studied for decades to satisfy the increasing demands for improved indoor thermal comfort.

On the other hand, computer-based algorithm in a study area known as soft computing has been well developed for the past three decades [Yang 2008]. Soft computing became a formal computer science area of study in the early 1990's [Zadeh 1994]. It is a collection of methodologies, including Fuzzy Systems, Neural Networks and Genetic Algorithms, etc, that exploit tolerance for imprecision, uncertainty and partial truth to achieve tractability, robustness and low solution cost [Zadeh 1996]. Such algorithms generally have the characteristics of very simple computational steps and often need a very large number of repeated computational cycles [Yang 2008]. This is very different from conventional hard computing, which are usually more straightforward in analyzing system performance, with more predictable behavior and higher stability [Ovaska 2004].

ANN is now unquestionably the leading soft computing methodology for general thermal problems [Yang 2008] and appears to be the most popular data-driven

method [Kim et al. 2010]. There are several reasons for this. Firstly, ANN has a powerful ability to recognize accurately the inherent relationship between any set of input and output without requiring a physical model. Meanwhile, ANN results do account for all the physics relating the output to the input [Haykin 1999]. This ability is essentially independent of system complexities, such as nonlinearity, multiple variables, coupling, noise existence and uncertainty. This ability is known as pattern recognition as the results of learning [Yang 2008]. Secondly, ANN has a built-in capability to adapt its synaptic weights to changes in the surrounding environment. Moreover, when an ANN is operating in a changing environment, it can be designed to real time change its weights. Such adaptive capability of ANN makes it a useful tool in dynamic modeling and adaptive control [Haykin 1999, Norgaard et al. 2000]. Thirdly, the ANN-based method is inherently fault tolerant due to the distributed nature of information stored in the network [Yang 2008, Haykin 1999]. Finally, a number of ANN-based control strategies have been developed [Norgaard et al. 2000], such as the inverse-model-based control which included IMC method and direct inverse control (DIC) method [Daosud et al. 2005, Deng et al. 2009], model predictive control [Aggelogiannaki et al. 2007, Kittisupakorn et al. 2009] and optimal control [Becerikli et al. 2003], etc. However, these were developed when the input and output data were available. Therefore, the ANN-based control may be applied when the physical processes to be modeled and/or controlled were complex but the operating data were available or easy to be collected.

Therefore, the use of ANN can offer a viable solution to the modeling and control for DX A/C systems. While the ANN-based modeling and control has been widely used in HVAC systems, no previously reported studies on applying ANN to the modeling

of and the simultaneous control of indoor air temperature and humidity, using a DX A/C system may be identified. Moreover, a DX A/C system appears to be an ideal venue where ANN-based modeling and control techniques may be applied to, because of its nonlinear and MIMO characteristics.

2.7 Conclusions

More and more attentions have been paid to improving thermal environmental control in spaces using A/C systems, due to the pursuing for high quality living and comfortable working environments. DX A/C systems have been widely used in small- to medium- scaled buildings in recent decades. Compared to large central chilled water-based A/C installations, DX A/C systems are simpler, more energy efficient and cost less to own and maintain. However, most DX A/C systems are currently equipped with single-speed compressors and supply fans relying on on-off cycling compressors to maintain only indoor dry-bulb temperature, resulting in either space overcooling or an uncontrolled equilibrium indoor RH level.

A great number of previous studies on the impacts of humidity on human thermal comfort and indoor environmental control indicated that indoor air RH levels influenced the occupants' thermal comfort in different ways both directly and indirectly. Therefore, indoor relative humidity should be controlled within a suitable range for thermal comfort. Indoor moisture which can cause high indoor relative humidity problem may come from both external and internal sources.

Dynamic modeling was of great importance in carrying out research work related to

the control of DX A/C systems. A considerable number of previous investigations have focused on the modeling of DX A/C systems. The dual role of cooling and dehumidification for the cooling coil in a DX A/C system makes the controlled variables of air temperature and humidity to become coupled. Therefore it is necessary to develop a dynamic model for a DX A/C system, which takes the coupling effect between temperature and humidity into account and could be used in the implementation of any new control strategy to be developed.

One of the major issues hindering the wider use of DX A/C systems is the mismatch between their output sensible and latent cooling capacities and the varying sensible and latent cooling loads in the conditioned spaces they serve, leading to possible poor indoor humidity control. Previous studies indicated that capacity control for DX A/C systems can be realized by the intermittent running of a compressor, i.e., on/off cycling compressor. The cooling capacity of DX A/C systems may also be controlled by using suction-gas throttling, hot-gas by-pass or cylinder-unloading. However, the previous studies suggested that varying refrigerant flow using variable speed compressors was the most energy efficient way for capacity control in DX A/C systems.

Previous related studies have also demonstrated that ANN has the ability to recognize accurately the inherent relationship between any set of input and output without requiring a physical model and to account for all the physics relating the output to the input. Furthermore, a number of ANN-based control strategies have been developed and widely used in the field of HVAC engineering. Therefore, the use of ANN offers a viable solution to the modeling and control for DX A/C systems.

While the ANN-based modeling and control has been widely used in HVAC systems as reviewed above, no previously reported studies on applying the ANN-based methods to the modeling and simultaneous control of indoor air temperature and humidity using a DX A/C system may be identified in open literature. Therefore, it is necessary to develop an ANN-based control strategy to simultaneously control the indoor air temperature and humidity in a space conditioned by a DX A/C system, through extensive modeling using ANN. This is to be the target of investigation reported in this thesis.

Chapter 3

Proposition

3.1 Background

From the literature review presented in Chapter 2, it is evident that DX A/C systems are widely used in small- to medium-scaled buildings due to their advantages of simple configuration, a higher energy efficiency and a low cost to own and maintain. When a DX A/C system is however equipped with a single-speed compressor and single-speed supply fan, only indoor air dry-bulb temperature is normally controlled by on-off cycling compressor, resulting in either space overcooling or an uncontrolled equilibrium indoor RH level, thus reducing indoor thermal comfort. This is particular true for buildings located in hot and humid subtropics. Therefore, developing an appropriate indoor thermal environmental control strategy for DX A/C systems has attracted a lot of research attention.

With the fast development of VSD technology in recent years, many DX A/C systems are currently equipped with a variable speed compressor and variable speed supply fan. Previous related investigations suggested that indoor air temperature and humidity may be simultaneously controlled by simultaneously varying compressor speed and supply fan speed.

On the other hand, ANN has been widely used in the field of HVAC engineering for modeling and control purposes, as presented in Chapter 2. ANN is powerful in recognizing accurately the inherent relationship between any set of input and output

without requiring a physical model regardless of the complexity of the underlying physical relation such as nonlinearity, multiple variables, coupling, noise existence and uncertainty. Therefore, a number of control strategies have been developed based on the ANN-based techniques to control nonlinear MIMO complex systems. Consequently, the use of ANN offers a viable solution to the modeling and control of DX A/C systems. While ANN-based modeling and control has been widely used in HVAC systems, no previously reported studies on applying ANN-based techniques to the modeling and simultaneous control of indoor air temperature and humidity using a DX A/C system may be identified in open literature. It was therefore considered necessary to apply ANN to modeling and control of DX A/C systems, with an emphasis on developing an ANN-based control strategy to simultaneously control indoor air temperature and humidity using a variable speed DX A/C system.

3.2 Project title

The thesis focuses on the following major issues related to the modeling and control of an experimental DX A/C system: (1) establishing an ANN-based steady-state model for the DX A/C system, and experimentally validating the ANN-based steady-state model developed; (2) establishing an ANN-based dynamic model for the DX A/C system, and experimentally validating the ANN-based dynamic model developed; (3) designing an ANN-based controller for the DX A/C system based on the ANN-based dynamic model developed, and carrying out controllability tests to validate the ANN-based controller developed; (4) designing an ANN-based on-line adaptive controller for the DX A/C system based on the ANN-based controller developed to solve the problem of limited controllable range, and carrying out

controllability tests to validate the ANN-based on-line adaptive controller developed. The proposed research project is therefore entitled “Artificial neural network based modeling and control of a direct expansion air conditioning system”.

3.3 Aims and objectives

The objectives of the research work reported in this thesis are as follows:

(1) To develop an ANN-based steady-state model to simulate the steady-state operating performance of the experimental DX A/C system, and to validate the ANN-based steady-state model developed by comparing the predicted and experimentally measured results of TCC and equipment SHR of the DX A/C system under different combinations of compressor and supply fan speeds.

(2) To develop an ANN-based dynamic model to simulate the dynamic operating performance of the experimental DX A/C system, and to validate the ANN-based dynamic model developed by comparing the predicted and experimentally measured results of the open loop dynamic responses of the DX A/C system.

(3) To design an ANN-based controller for the experimental DX A/C system based on the ANN-based dynamic model developed to simultaneously control indoor air temperature and humidity in a space served by the experimental DX A/C system through varying compressor speed and supply fan speed; and to carry out controllability tests for the ANN-based controller developed to evaluate its effectiveness and performances.

(4) To design an ANN-based on-line adaptive controller for the experimental DX A/C system to address the issue of limited controllable range for the previously developed ANN-based controller, which is common to all controllers developed based on system identification; and to carry out controllability tests for the ANN-based on-line adaptive controller developed to evaluate its effectiveness and performances.

3.4 Research methodologies

The ANN-based steady-state model for the DX A/C system will be developed by training and testing a multilayer feedforward ANN with the BP learning algorithm, using the experimental data collected which could reflect the steady-state operating performance of the experimental DX A/C system. To validate the ANN-based steady-state model developed, the predicted and experimentally measured results of TCC and Equipment SHR of the DX A/C system will be compared.

The ANN-based dynamic model for the DX A/C system will be developed by training and testing a recurrent ANN which using the previous/present outputs of the system, together with the previous/present inputs to the system, as inputs to the ANN at the current time step using the experimental data collected which could reflect the dynamic characteristics of the experimental DX A/C system. The ANN-based dynamic model developed will be experimentally validated by comparing the predicted and experimentally measured results of indoor air dry-bulb temperature and wet-bulb temperature under different combinations of compressor and supply fan speeds of the DX A/C system.

The ANN-based controller will be designed using the ANN-based DIC strategy, in which the ANN-based dynamic model previously developed is used to reflect the dynamic operating performance of the system controlled, and an ANN-based inverse model is to be developed and used to reduce the measured difference between the control references and the controlled variables by varying compressor speed and supply fan speed. Controllability tests for the ANN-based controller will be carried out with respect to disturbance rejection and command following, respectively, after being subjected to either heat load disturbance in a conditioned space or the changes in indoor air dry-bulb temperature and wet-bulb temperature settings. These tests are to ascertain whether the ANN-based controller developed could behave as expected in simultaneously controlling indoor air dry-bulb and wet-bulb temperatures in the space served by the experimental DX A/C system.

To solve the problem of limited controllable range of the ANN-based controller, an ANN-based on-line adaptive controller for the DX A/C system will be further developed. The ANN-based adaptive algorithms will be applied to on-line training/updating of the ANN-based dynamic model and the ANN-based inverse model in the ANN-based controller to develop the ANN-based on-line adaptive controller. Controllability tests including the initial start-up stage test, command following test, disturbance rejection test and command following with disturbances test for the ANN-based on-line adaptive controller will be carried out to validate the control performances of the ANN-based on-line adaptive controller developed.

Chapter 4

Description of the Experimental rig of DX A/C System

4.1 Introduction

An experimental DX A/C system is available in the HVAC Laboratory of Department of Building Services Engineering in the Hong Kong Polytechnic University. The primary purpose of having the experimental station is to facilitate carrying out the research work related to DX A/C technology.

Advanced technologies such as variable-speed compressor and supply fan, EEV, as well as a computerized data measuring, logging and control system have been incorporated into the experimental DX A/C system.

This Section presents firstly detailed descriptions of the experimental DX A/C system and its major components. This is followed by describing the computerized instrumentation and a data acquisition system (DAS). Finally, a computer supervisory program used to operate and control the experimental DX A/C system is detailed.

4.2 Detailed description of the experimental system and its major components

The experimental DX A/C system is mainly composed of two parts, i.e., a DX refrigeration plant (refrigerant side) and an air-distribution sub-system (air side). The schematic diagrams of both the complete experimental DX A/C system and the DX refrigeration plant are shown in Fig. 4.1 and Fig. 4.2, respectively.

4.2.1 The DX refrigeration plant

As shown in Fig. 4.2, the major components in the DX refrigeration plant include a variable-speed rotor compressor, an EEV, a high-efficiency tube-louver-finned DX evaporator and an air-cooled tube-plate-finned condenser. The evaporator is placed inside the supply air duct to work as a DX air cooling coil whose details are shown in Fig. 4.3. The evaporator's louver fins are made of aluminum and tubes made of copper. A water collecting pan is installed under the evaporator to collect and weight the mass of condensate drained of the cooling coil. The design air face velocity for the DX cooling coil is 2.5 m/s. The nominal output cooling capacity from the DX refrigeration plant is 9.9 kW. The actual output cooling capacity from the DX refrigeration plant can however be modulated from 15% to 110% of the nominal capacity. Other details of the compressor can be found in Table 4.1. The compressor is driven by a VSD. The EEV includes a throttling needle valve, a step motor and a pulse generator. It is used to maintain the degree of refrigerant superheat at the

evaporator exit. The working fluid of the plant is refrigerant R22, with a total charge of 5.3 kg.

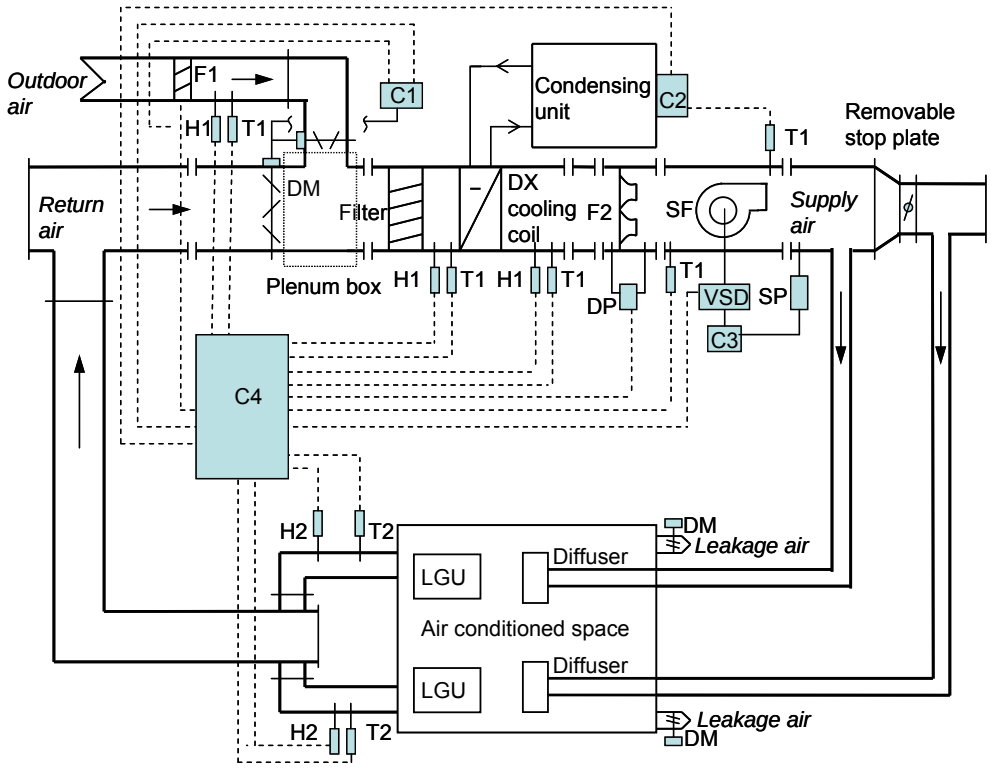

C1-controller of outdoor/return air	C2-controller of condensing unit	C3-controller of supply fan
C4-data acquisition and control unit	DM-damper	DP-differential pressure
F1-hot film anemometer	F2-supply airflow rate measuring	H1-air wet-bulb temperature
H2-air humidity meter	LGU-load generating unit	SF-supply fan with motor outside
SP-static pressure measuring device	T1,T2-air dry-bulb temperature sensor	VSD-variable speed drives

Fig. 4.1 The diagram of the complete experimental DX A/C system

In addition, two three-way connectors and two flexible joints, whose locations are indicated in Fig. 4.2, are reserved in the refrigerant pipeline for the purpose of possibly modifying the system for other related studies. A condenser air duct, which is not normally required in real applications, is used to duct the condenser cooling air

carrying the rejected heat from the condenser away to outside the Laboratory. The condenser fan, housed inside the condenser air duct, can also be variable-speed operated. An electrical heater controlled by a solid state relay (SSR) is used to adjust the temperature of the cooling air entering the condenser for various experimental purposes. A refrigerant mass flow meter is installed upstream of the EEV. Other necessary accessories and control devices, such as an oil separator, a refrigerant receiver, a sight glass and safety devices, are provided in the refrigeration plant to ensure its normal and safe operation.

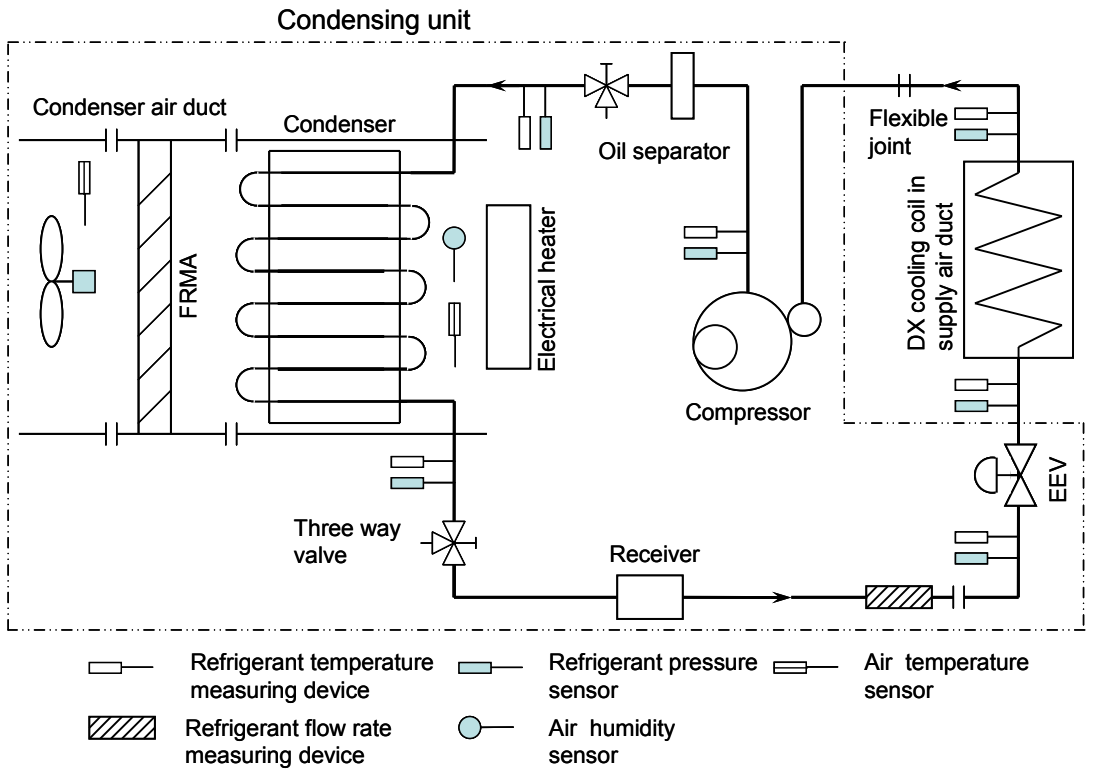

Fig. 4.2 The schematic diagram of the DX refrigeration plant

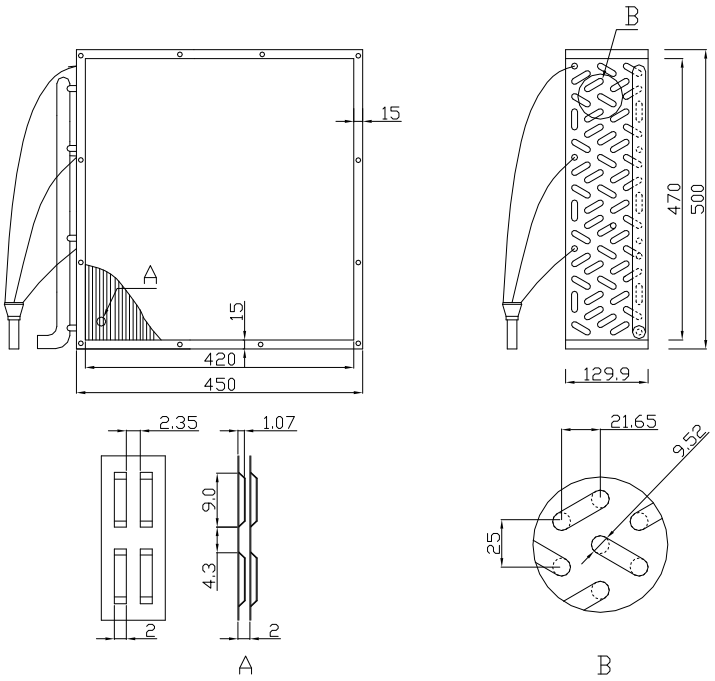

Fig. 4.3 The details of the DX air cooling and dehumidifying coil used in the experimental DX A/C system

Table 4.1 Details of the variable speed rotor compressor

Model	HITACHI THS20MC6-Y
Allowable Frequency range	15~110 Hz
Rated Capacity	9900 W at 90 Hz
Displacement	3.04 ml/rev

4.2.2 The air-distribution sub-system

The air-distribution sub-system in the experimental DX A/C system is schematically shown in Fig. 4.1. It includes an air-distribution ductwork with return and outdoor air dampers, a variable-speed centrifugal supply fan with its motor placed outside the duct, and a conditioned space. The supply fan is driven by a VSD. The details of the

supply fan are given in Table 4.2.

The air conditioned space measures 7.6 m (L)×3.8 m (W)×2.8 m (H). Inside the space, there are sensible heat and moisture load generating units (LGUs). The units are intended to simulate the cooling load in the conditioned space. Its heat and moisture generation rate as regulated by SSR may be varied manually or automatically with a pre-set pattern through operator's programming. In addition, leakage outlets with residual-pressure relief dampers are installed in the space so that a positive internal pressure of not more than 20 Pa can be maintained at all time. In the air-distribution sub-system of the experimental DX A/C system, return air from the space mixes with outdoor air in a plenum box upstream of an air filter. The mixed air is filtrated and then cooled and dehumidified by the DX cooling coil. Afterwards, the cooled and dehumidified air passes through the supply fan, to be supplied to the space to deal with the cooling load from LGUs.

Table 4.2 Details of the variable speed supply fan

Model	KRUGER BSB 31
Nominal flow rate	1700 m^3/h (0.47 m^3/s)
Total pressure head	1100 Pa

4.3 Computerized instrumentation and DAS

The computerized instrumentation for the experimental DX A/C system is also

shown in both Fig. 4.1 and Fig. 4.2. The system is fully instrumented for measuring all of its operating parameters, which may be classified into three types, i.e., temperature, pressure and flow rate. Since all measurements are computerized, all sensors and measuring devices are able to output direct current signal of 4-20 *mA* or 1-5 *V*, which are transferred to a DAS for logging and recording.

4.3.1 Sensors/measuring devices for temperatures, pressures and flow rates

The room temperatures (dry-bulb temperature and wet-bulb temperature) are fundamental parameters in development of the ANN-based modeling and control strategy and the definition of the room temperatures is therefore very important in this study. In the study of Davies [3], the definition of room temperature is given in terms of heat transfer that the loss of heat from a room to ambient at T_0 is normally taken to be proportional to (T_i-T_0), and the index T_i is the room temperature. This room temperature could be obtained through the measures of convective and radiant transfer, which could be combined with various measurable temperatures of the surfaces and the air, possibly with the considerations of heat input. In the current study, in order to simplify the experimental measurement, the air temperature before evaporator was measured and used as the room temperature approximately.

Five sets of air temperature and humidity measuring sensors are located in the air-distribution sub-system of the experimental DX system. Air RH is indirectly

measured via measuring air dry-bulb and wet-bulb temperatures. As shown in Fig. 4.2, there are six temperature sensors for measuring refrigerant temperatures in the DX refrigeration plant. To ensure fast response of the sensors for facilitating the study of transient behaviors of the DX refrigeration plant, these temperature sensors are inserted into the refrigerant circuit, and are thus in direct contact with the refrigerant. The temperature sensors for air and refrigerant are of platinum resistance temperature device type, using three-wire Wheatstone bridge connection and with a pre-calibrated accuracy of ±0.1℃. The specifications of the resistance temperature devices are: CHINO Pt100/0℃-3W, Class A, SUSΦ3.2-150L.

Refrigerant pressures in various locations in the DX refrigeration plant are measured using pressure transmitters with an accuracy of ±0.13% of full scale reading (Model: SETRA C206). The atmospheric pressure is measured with a barometer having an accuracy of ±0.05kPa (Model: VAISALA PTB-101B).

There are two sets of air flow rate measuring apparatus (FRMA) in the air-distribution system. One set of FRMA is used to measure the total supply airflow rate, i.e., the airflow rate passing through the DX cooling coil. The other is for measuring the airflow rate passing through the condenser. The two sets of FRMA are constructed in accordance with ANSI/ASHRAE Standard 41.2, consisting of nozzles of different sizes, diffusion baffles and a manometer with a measuring accuracy of

±0.1% of full scale reading (Model: ROSEMOUNT 3051). The number of nozzles in operation can be altered automatically.

Outdoor airflow rate is measured using a hot-film anemometer with a reported accuracy of ±0.1 m/s (Model: EE70-VT62B5). The anemometer is installed 500 mm, which is longer than the recommended length of entrance of 200 mm by its manufacturer, downstream of the outdoor air inlet, to ensure the measuring accuracy of outdoor airflow rate. The power consumption of the variable-speed compressor is measured using a pulse-width-modulation digital power meter with a reported uncertainty of ±2% of reading (Model: EVERFINE PF9833). The refrigerant mass flow rate passing through the EEV is measured by a Coriolis mass flow meter with a reported accuracy of ±0.25% of full scale reading (Model: KROHNE MFM1081K+F). The supply air static pressure is measured using a manometer with a reported accuracy of ±0.1% of full scale reading (Model: ROSEMOUNT 3051).

In order to ensure the measuring accuracy for the temperatures of the air flowing inside air duct, standardized air sampling devices recommended by the ISO Standard 5151 are used in the experimental DX A/C system.

4.3.2 The DAS

A data acquisition unit (Model: AGLIENT 34970A/34902A) is used in this

experimental DX A/C system. It provides up to 48 channels for monitoring various types of system parameters. The direct current signal from various measuring devices/sensors can be scaled into their real physical values of the measured parameters using a logging & control (L&C) supervisory program which is developed using LabVIEW programming platform. The minimum data sampling interval is one second. It should be noted that the flow rates of both supply air and condenser cooling air are calculated using the air static pressure drops across their respective nozzles. The outdoor airflow rate is evaluated by multiplying the measured air velocity with the sectional area of the outdoor air duct. The output cooling capacity from the DX refrigerant plant is calculated based on the enthalpy-difference of air across the DX cooling coil.

4.4 LabVIEW L&C supervisory program

A computer supervisory program which is capable of performing simultaneously data-logging and parameter-controlling is necessary. It needs to communicate with not only the data acquisition unit, but also conventional standalone digital programmable PI controllers which are to be detailed in Section 4.5. A commercially available programming package, LabVIEW, provides a powerful programming and graphical platform for data acquisition and analysis, as well as for control application.

A data L&C supervisory program has been developed using LabVIEW, with all measured parameters real-time monitored, curve-data displayed, recorded and processed. The program can also perform the retrieval, query and trend-log graphing of historical data for measured parameters. The program runs on a personal computer (PC).

The LabVIEW-based L&C supervisory program enables the PC to act as a central supervisory control unit for different low-level control loops, which will be also discussed in Section 4.5, in the experimental DX A/C system. The PC can therefore not only modify the control settings of those standalone microprocessor-based PI controllers, but also deactivate any of these controllers. The LabVIEW-based L&C supervisory program also provides an independent self-programming module (SPM) by which new control algorithms may be easily implemented through programming. A SPM performs in a similar manner to a central processing unit of a physical digital controller. The variables available from all measured parameters can be input to, and processed according to a specified control algorithm in a SPM to produce required control outputs. Once a SPM is initiated to replace a given standalone controller, the controller must be deactivated, but works as a digital-analog converter to receive the control output from the SPM. An analogue control signal is then produced by the controller to initiate the related actuator for necessary control action.

4.5 Conventional control loops in the experimental system

Totally, there are ten conventional control loops in this experimental DX A/C system. These loops either are activated using the LabVIEW-based supervisory program or use PI controllers which are of digital programmable type with RS-485 communication port (Model: YOKOGAWA UT350-1). Resetting controller's proportional band, integral times and setpoints are allowed.

Among the ten control loops, four are for varying heat and moisture generation rate of the LGUs located inside the space. Electrical power input to the LGU is regulated using SSR according to the instructions from their respective control loops to simulate the space cooling load. In addition, there is one control loop for maintaining the condenser inlet air temperature at its setting through regulating electrical power input by SSR.

The remaining five conventional PI control loops are as follows: supply air temperature by regulating the compressor speed; supply air static pressure by regulating the supply fan speed; condensing pressure by regulating the condenser fan speed; degree of refrigerant superheat by regulating EEV opening; outdoor airflow rate by jointly regulating both outdoor and return air dampers' openings. These five control loops can be activated by using either the conventional physical digital PI controller available in the experimental DX A/C system or a SPM specifically for any new control algorithm to be developed.

The control of supply air temperature is used as an example for illustration. When the conventional PI controller is enabled, the controller measures the supply air temperature using the temperature sensor and then compares the measured with its setpoint. A deviation is processed in the controller according to a pre-set PI control algorithm and an analogue control signal of 4~20 *mA* is produced and sent by the PI controller to the VSD for compressor motor to regulate its speed. On the other hand, such a conventional PI controller may be replaced by a SPM to be specifically developed based on a new control algorithm for compressor speed control. The SPM may take the advantages of using simultaneously multiple input variables, e.g., supply air temperature and its setpoint, evaporating and condensing pressures, degree of refrigerant superheat, etc. Control outputs can then be created by using the SPM according to the new control strategy and algorithm, and communicated to the physical digital PI controller which works only as a digital-analog converter. An analog control signal is then generated and sent to the VSD of compressor for its speed control.

4.6 Conclusions

An experimental DX A/C system is available for carrying out the proposed project. The system consists of two parts: a DX refrigeration plant and an air-distribution sub-system.

The experimental DX A/C system has been fully instrumented using high quality sensors/measuring devices. Totally forty-three operating parameters in the system can be measured and monitored simultaneously and ten conventional PI feedback control loops are provided. Two sets of airflow rate measuring apparatus are constructed in accordance with ANSI/ASHRAE Standard 41.2. Sensors for measuring refrigerant properties are in direct contact with refrigerant, and a Corioli mass flow meter is used for measuring the refrigerant flow rate being circulated in the DX refrigerant plant.

An L&C supervisory program has been developed specifically for this experimental DX A/C system using LabVIEW programming platform. All parameters can be real-time measured, monitored, curve-data displayed, recorded and processed by the L&C program. The LabVIEW-based L&C program provides an independent SPM by which any new control algorithms to be developed may be implemented.

The availability of such an experimental DX A/C system is expected to be extremely useful in developing a multivariable control strategy for simultaneously controlling indoor air temperature and humidity in a space served by a DX A/C system having a variable-speed compressor and supply fan. A multivariable control-oriented dynamic mathematical model for the DX A/C system can be developed and experimentally validated. An ANN-based controller for simultaneous control of

indoor air temperature and humidity can be developed, and the controllability tests for the ANN-based controller carried out using the experimental DX A/C system.

Chapter 5

ANN-based Steady-state Modeling of the Experimental DX A/C System

5.1 Introduction

As presented in Chapter 2, a number of mathematical models have been developed for modeling the steady-state operating performances of DX A/C systems and their components. However, it can be seen that all these models were physical-based and were therefore complicated and often difficult to be established and solved. On the other hand, unlike the physical-based modeling, ANN-based approaches only use experimental data to identify the input-output relationships and thus are always simpler than the approaches used in establishing physical-based models. Therefore, the use of ANN should be preferred when the physical processes taking place in a system to be modeled are complicated. Given that an ANN-based model is able to reveal the inherent relationship of any set of input-output data with a higher accuracy, compared to a conventional physical-based model, even if there could be complexities involving the nonlinearity, multi-variables and uncertainty in modeling processes [Haykin 1999], ANN-based method has become increasingly popular in modeling complicated systems.

Despite of the fact that DX A/C systems have been widely used, there has been a clear lack of using ANN-based technique to model the operational characteristics of DX A/C systems. As a prerequisite of designing effective strategies for simultaneously controlling indoor temperature and humidity, it is essential to have an

accurate understanding of the steady-state operating characteristics of a variable speed DX A/C system [Li and Deng 2007a]. These include the TCC and the Equipment SHR, which is defined as a ratio of the output sensible cooling capacity to the TCC of the DX A/C system, under different combinations of compressor speed and supply fan speed.

Therefore, the objective of this Chapter is, as the first attempt to apply ANN-based modeling method to DX A/C systems, to develop a two-in two-out ANN-based steady-state model for the experimental DX A/C system detailed in Chapter 4, linking both its TCC and Equipment SHR with different combinations of compressor and supply air fan speeds, at a fixed supply air temperature and RH 24^{o}C and 50%, respectively to the system. In this Chapter, the related steady-state experimental conditions are firstly described. The training algorithm used for the steady-state modeling of the DX A/C system is introduced subsequently. Thirdly, the development of the ANN-based steady-state model for the experimental DX A/C system is presented. Fourthly, the validation of the ANN-based steady-state model developed by comparing between the predicted results using the ANN-based steady-state model developed and the experimental data is reported. Finally, a comparison for the prediction accuracy using the ANN-based steady-state model developed, a steady-state physical-based model and a numerical analysis using bilinear interpolation is presented.

5.2 Experimental conditions

During experiments, a fixed inlet air state in terms of indoor air dry-bulb temperature

and RH to the DX cooling coil in the experimental DX A/C system was maintained at 24 ^{o}C and 50%, respectively, using a PID controller. In addition, during the experiments, no outdoor air was introduced by fully closing the outdoor air damper in the experimental DX A/C system so that the space cooling load was fully provided by the LGUs. On the other hand, the condenser cooling air flow rate was maintained constant at 3100 m^3/h at a fixed inlet temperature 35 ^{o}C. The degree of refrigerant superheat was maintained constant at 6 ^{o}C by using the EEV, which was controlled by a built-in conventional PID controller in the DX A/C system.

Given the objective of establishing an ANN-based steady-state model linking its TCC and Equipment SHR at different combinations of compressor and supply fan speed, the two speeds were regarded as the two inputs to, and TCC and SHR as the two outputs from the model.

The equations used to calculate the TCC and Equipment SHR were available from a previous related study [Li and Deng 2007a]. The uncertainties associated with the experimental measurements in calculating the TCC and Equipment SHR were evaluated. All temperatures in the experimental DX A/C system were measured using platinum Resistance Temperature Device type temperature sensors, with a reported accuracy of ±0.1 ^{o}C. The air mass flow rate was measured using a standard nozzle which was constructed in accordance with ANSI/ASHRAE Standard 41.2, with its reported accuracy of ±1.2%.

Hence, the uncertainties in calculating TCC and Equipment SHR, U_{TCC} and U_{SHR}, were evaluated by using the classic root-sum-square formula [Holman 1994]:

$$U_{TCC} = \sqrt{\left(\frac{\partial TCC}{\partial m_a} U_{m_a}\right)^2 + \left(\frac{\partial TCC}{\partial T_{db,in}} U_{T_{db,in}}\right)^2 + \left(\frac{\partial TCC}{\partial T_{wb,in}} U_{T_{wb,in}}\right)^2 + \left(\frac{\partial TCC}{\partial T_{db,out}} U_{T_{db,out}}\right)^2 + \left(\frac{\partial TCC}{\partial T_{wb,out}} U_{T_{wb,out}}\right)^2} \quad (5.1)$$

$$U_{SHR} = \sqrt{\left(\frac{\partial SHR}{\partial T_{db,in}} U_{T_{db,in}}\right)^2 + \left(\frac{\partial SHR}{\partial T_{wb,in}} U_{T_{wb,in}}\right)^2 + \left(\frac{\partial SHR}{\partial T_{db,out}} U_{T_{db,out}}\right)^2 + \left(\frac{\partial SHR}{\partial T_{wb,out}} U_{T_{wb,out}}\right)^2} \quad (5.2)$$

where $T_{db,in}$, $T_{wb,in}$, $T_{db,out}$ and $T_{wb,out}$ are air dry-bulb and wet-bulb temperatures both entering and leaving the DX A/C unit, and m_a the mass flow rate of air, respectively; and U_{TCC}, U_{SHR}, U_{m_a}, $U_{T_{db,in}}$, $U_{T_{wb,in}}$, $U_{T_{db,out}}$, $U_{T_{wb,out}}$ are the uncertainties for TCC, SHR, m_a, $T_{db,in}$, $T_{wb,in}$, $T_{db,out}$ and $T_{wb,out}$, respectively. The calculation results using Equations (5.1) and (5.2) showed that the uncertainties for TCC and Equipment SHR, arising from the measurement errors, ranged from 1.85% to 3.89% and 1.64% to 4.02%, respectively.

All the experimental work reported in this Chapter may be divided into two categories: I) for developing the ANN-based steady-state model; II) for validating the ANN-based steady-state model developed.

Category I experiments

The purpose of Category I experiments was to obtain experimental data linking the outputs from, with the inputs to the DX A/C system under steady-state operating conditions, so as to facilitate the intended ANN-based steady-state model

development. To ensure the greatest possible applicability of the ANN-based model developed for the DX A/C system, the variation of the inputs should cover their entire operation ranges in application [Navarro-Esbri et al. 2007]. Therefore, both percentage of the maximum compressor speed (P_C) and percentage of the maximum supply fan speed (P_F) were varied from 30% to 90% of their respective maximum speeds at a fixed increment of 5%, as shown in Table 5.1. This resulted in a total of 169 (13×13) speed combinations.

Table 5.1 Speed combinations in Category I experiments

P_C (%)						
30	35	40	45	50	55	60
65	70	75	80	85	90	
P_F (%)						
30	35	40	45	50	55	60
65	70	75	80	85	90	

Experiments were carried out at the speed combinations specified in Table 5.1. A total of 169 sets of input-output data (i.e., P_C, P_F - TCC, SHR) were generated. These sets of input-output data were used to train and test the ANN-based steady-state model for the experimental DX A/C system.

Category II experiments

The purpose of Category II experiments was to validate the ANN-based steady-state model developed. These experiments were carried out independent of those in Category I, so as to validate independently the ANN-based steady-state model

developed. This part of experiments was carried out under the same experimental conditions but with different combinations of compressor and supply fan speeds. As shown in Table 5.2, 10 additional sets of experimental data in terms of Equipment SHR and the TCC were obtained by carrying out additional experiments, at 10 randomly selected different combinations of compressor and supply fan speeds. As understood, the output TCC and Equipment SHR data at these 10 additional experimental combinations were not used for either ANN training or testing.

Table 5.2 Speed combinations in Category II experiments

Nos.	1	2	3	4	5	6	7	8	9	10
P_C (%)	38	43	52	53	62	67	73	78	83	87
P_F (%)	37	82	53	67	83	68	43	52	77	47

5.3 Training algorithm in developing the ANN-based steady-state model

The ANN structure chosen was a multilayer feedforword ANN, which was the most commonly used in engineering applications. A multilayer feedforward ANN is constructed by ordering neurons in layers, making each neuron in a layer only take the outputs from neurons in the previous layer or external inputs as input [Norgaard et al. 2000]. In other words, the input signal propagates though the network in forward direction, on a layer-by-layer basis.

A multilayer feedforward ANN has three distinctive characteristics [Haykin 1999]: i) the model of each neuron in a multilayer feedforward ANN includes a nonlinear activation function, whose nonlinearity is smooth (i.e. differentiable everywhere); ii)

the network contains one or more layers of hidden neurons that are not part of the input or output of the ANN; iii) the network exhibits a high degree of connectivity, determined by the weights of the ANN. It is through the combination of these characteristics together with the ability to learn from experience through training that a multilayer feedforward ANN derives its computing power. A general multilayer feedforward ANN is shown in Fig. 5.1, where i ($1 \leq i \leq I$) refers to the layer number and j, the neuron number in each layer, x, input to a neuron, y, output from a neuron, and W, the weights of the ANN. Therefore, the jth neuron in the ith layer of the network is denoted as the neuron (i, j) and J_i refers to the total number of neurons in the ith layer.

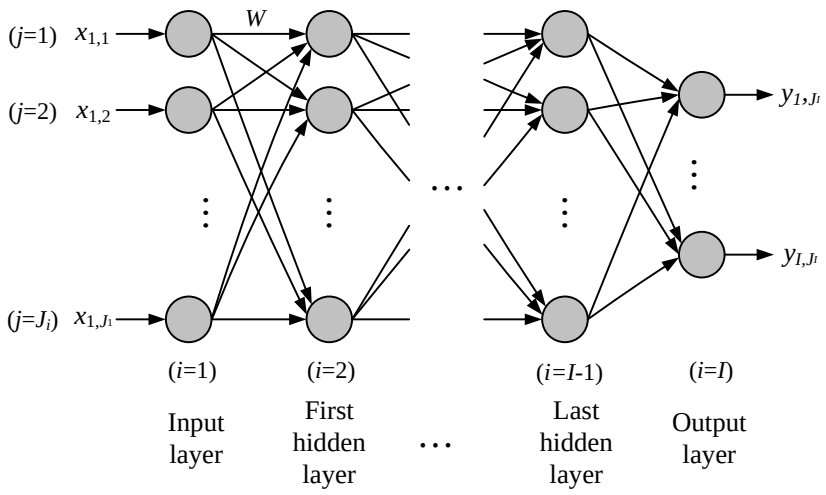

Fig. 5.1 Structure of a general multilayer feedforward ANN

The training algorithm used in the current development was the feedforward back-propagation (BP) algorithm. The training process consisted of two passes: a forward pass and a backward pass. The forward pass was to perform forward calculations using Eqs. (5.3) to (5.4).

$$x_{i,j} = b_{i,j} + \sum_{k=1}^{J_{i-1}} W_{i-1,k}^{i,j} y_{i-1,k} \tag{5.3}$$

$$y_{i,j} = \varphi(x_{i,j}) \tag{5.4}$$

where, $x_{i,j}$ is the input to the neuron (i, j), $b_{i,j}$ the bias of the neuron (i, j), $W_{i-1,k}^{i,j}$ the weight of synaptic connecting the neuron ($i-1$, k) and neuron (i, j), and $y_{i-1,j}$ the output from the neuron ($i-1$, j). The activation function φ used was the logistic sigmoid function, shown in Eq. (5.5):

$$\varphi(x_{i,j}) = \frac{1}{1+e^{-x_{i,j}}} \tag{5.5}$$

When the outputs from the ANN were obtained, the backward pass was to calculate the errors at neurons along the backward direction by using Eq. (5.6):

$$\delta_{i,j} = \begin{cases} (O_{i,j} - y_{i,j}) y_{i,j} (1 - y_{i,j}) & i = I \\ y_{i,j} \left(1 - y_{i,j}\right) \sum_{k=1}^{J_{i+1}} \delta_{i+1,k} W_{i,j}^{i+1,k} & i = 2 \sim (I-1) \end{cases} \tag{5.6}$$

where $O_{i,j}$ is the normalized target output. Once the local gradient, $\delta_{i,j}$, of the output layer was calculated, the computation moved backward layer by layer up to layer 2. After all the values of $\delta_{i,j}$ were known, the changes in the weights and biases would be determined by using the Delta Rule [Haykin 1999], as follows:

$$\Delta W_{i-1,k}^{i,j} = \eta \delta_{i,j} y_{i-1,k} \tag{5.7}$$

where η is the learning rate used to scale down the degree of change made to the connector.

Each time adjusting the weights and biases using Eqs. (5.3-5.7) with one set of training data was called a run. A cycle of training consisted of an adequate number of runs for obtaining weights and biases successively from all training data. The calculations were then repeated over many cycles and the relative error (RE) at the *j*th neuron in the output layer for the *n*th data set at the final cycle, RE_j^n, could be determined by:

$$RE_j^n = \frac{\left| O_{I,j}^n - y_{I,j}^n \right|}{O_{I,j}^n} \tag{5.8}$$

Two further indices i.e., *R*, σ, were used to evaluate the performances of different ANN configurations during the process of testing, relative error and standard deviation sensitivity for all the testing data. They were evaluated by:

$$R = \frac{1}{J_I}\sum_{j=1}^{J_I} R_j = \frac{1}{J_I}\frac{1}{N}\sum_{j=1}^{J_I}\sum_{n=1}^{N} R_j^n = \frac{1}{J_I}\frac{1}{N}\sum_{j=1}^{J_I}\sum_{n=1}^{N}\frac{y_{I,j}^n}{O_{I,j}^n} \tag{5.9}$$

$$\sigma = \frac{1}{J_I}\sum_{j=1}^{J_I}\sigma_j = \frac{1}{J_I}\sum_{j=1}^{J_I}\sqrt{\frac{1}{N}\sum_{n=1}^{N}(R_j - R_j^n)^2} \tag{5.10}$$

where *N* is the total number of the data sets used in training or testing, $O_{I,j}^n$, the target output , and $y_{I,j}^n$, the ANN outputs corresponding to O_I during testing. *R* indicates the average accuracy of the prediction and σ, the degree of scatter of the

ANN prediction [Yang 2008]. The accuracy of the prediction increases with the closeness of R to unity and σ to zero.

5.4 Development of the ANN-based steady-state model

In the current study, 144 data sets (~85% of the totally 169 sets) which were randomly selected were used for training and the remaining 25 data sets (~15% of the totally 169 sets) for testing. It was noted that there were no exact or specific guidelines readily available on allocating the percentage of the total data sets for either training or testing, with however some earlier literatures discussing this issue. For example, Pacheco-Vega et al [2001b] mentioned that when more than 60% of the experimental data were used for training, the final results would be indifferent. Others used 75% [Diaz et al. 1999] and 80% [Anderson et al. 1997] of the data sets for training. In the current study, by reference to these previously reported studies, it was decided to use 85% of the total data for training and the remaining 15% for testing.

In order to select an appropriately configured ANN when modeling the DX A/C system, a large number of different ANN configurations were evaluated by using the four evaluating indices which are explained in Table 5.3. It should be noted that the first two indices were obtained from the training process and the other two the testing process. The first two indices, i.e., average relative error (ARE) and maximum relative error (MRE) were evaluated by:

$$ARE = \frac{1}{J_I}\frac{1}{N}\sum_{j=1}^{J_I}\sum_{n=1}^{N} RE_j^n = \frac{1}{J_I}\frac{1}{N}\sum_{j=1}^{J_I}\sum_{n=1}^{N}\frac{\left|y_{I,j}^n - O_{I,j}^n\right|}{y_{I,j}^n} \tag{5.11}$$

$$MRE = Max\left(RE_j^n\right) \tag{5.12}$$

Table 5.3 Indices used to evaluate the accuracy of different ANN configurations

Index	Definition
ARE	Average relative errors experienced at the final cycle during training
MRE	Maximum relative errors experienced at the final cycle during training
R	Mean ratios of the experimental data to the ANN outputs corresponding to the experimental data during testing
σ	Standard deviation of the ratios of the experimental data to the ANN outputs corresponding to the experimental data during testing

The selection of an ANN configuration was based on accuracy of the ANN during both training and testing processes. An ANN configuration having the 2-6-6-2 structure shown in Fig. 5.2 was finally selected because its ARE and MRE were each at their lowest value of 0.026 and 0.0046, respectively, suggesting the high accuracy when simulating the training data; and its σ was also at its lowest values of 0.0052 and its R close to unit at 0.9985, respectively, suggesting a high averaged accuracy and low degree of scatter for the ANN-based model developed.

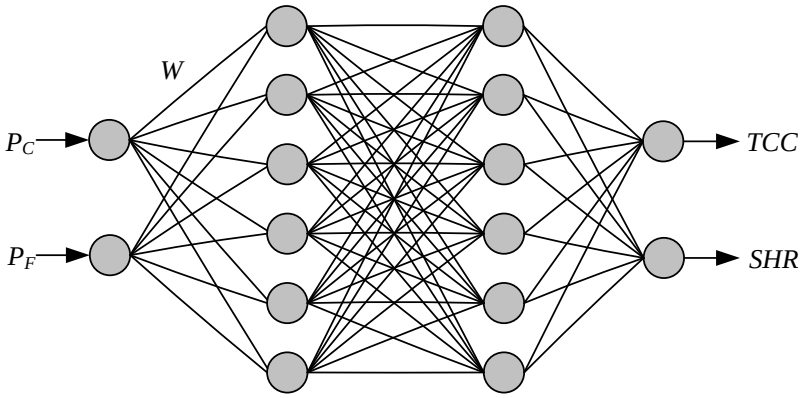

Fig. 5.2 Structure of the selected 2-6-6-2 ANN

The experimental data used in the development of the ANN-based steady-state model are shown in Fig. 5.3 and Fig. 5.4. The 144 data sets used for training are represented by grid points on the two spatial surfaces, while the remaining 25 data sets used for testing by crosses. The calculated results of TCC and SHR under different combinations of P_C and P_F using the ANN-based model developed were compared with the experimental results. For the developed 2-6-6-2 ANN-based model, all the REs during training are shown in Fig. 5.5. As seen, most calculated REs were below 0.015, with only 4 values of RE being greater than 0.015, indicating that the developed ANN-based model for the experimental DX A/C system would be able to predict the operating performance with a high accuracy.

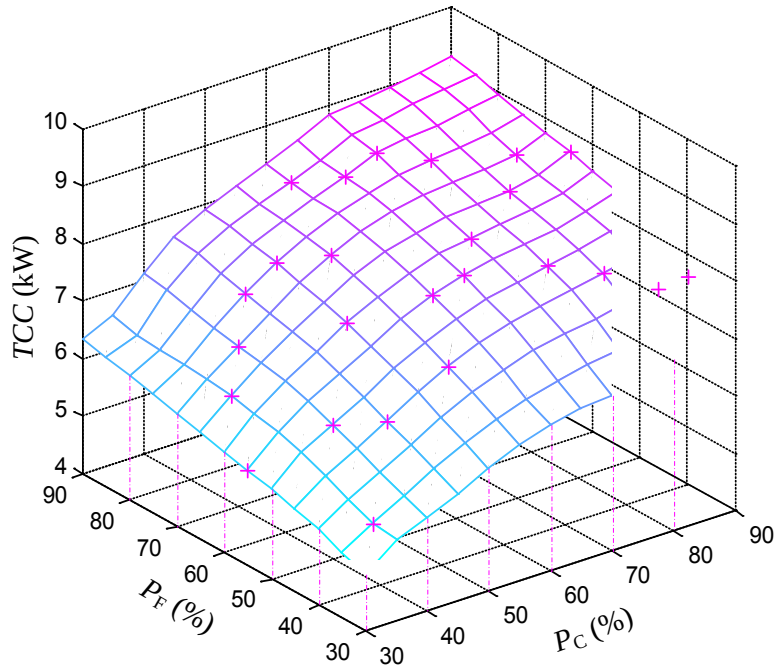

Fig. 5.3 Experimental data of TCC used for training and testing

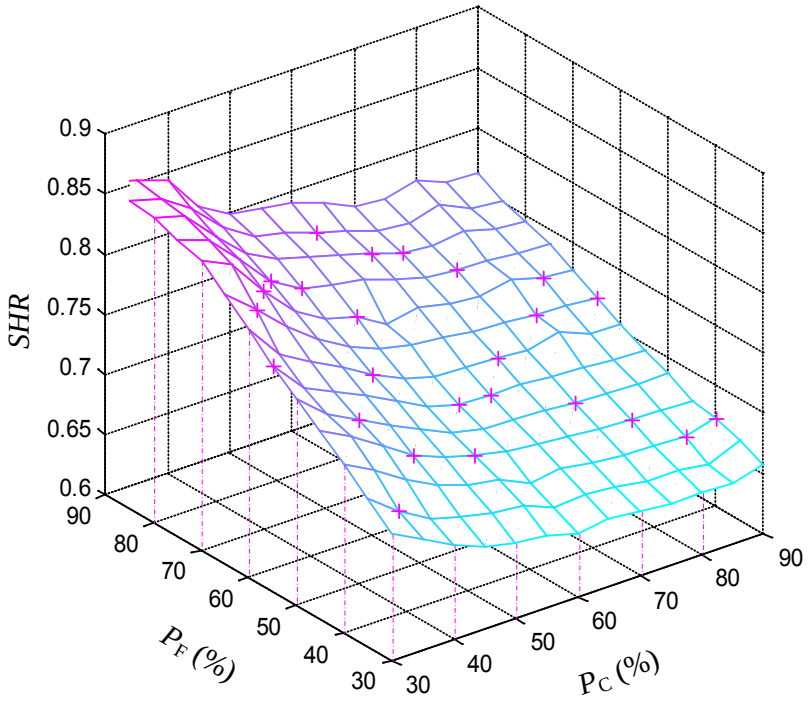

Fig. 5.4 Experimental data of SHR used for training and testing

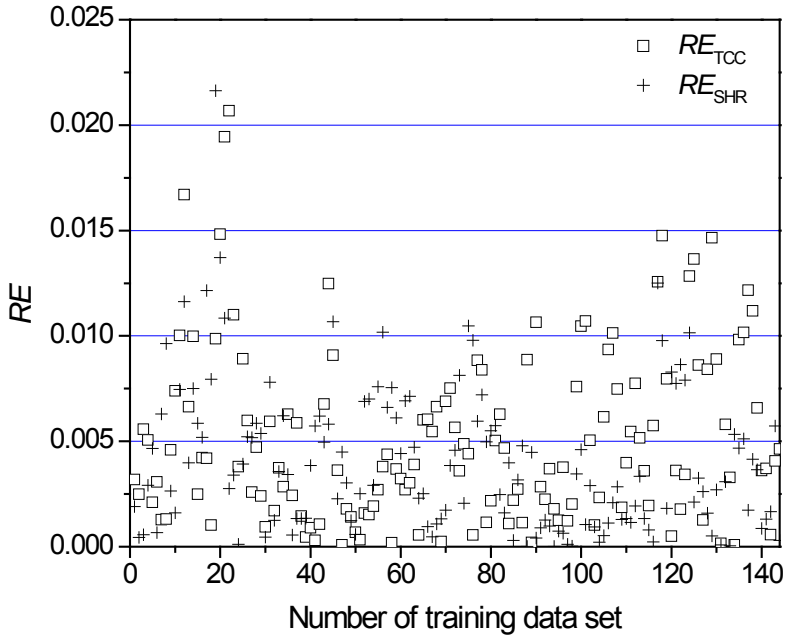

Fig. 5.5 Relative error distribution of the developed 2-6-6-2 ANN-based model

5.5 Validation of the ANN-based steady-state model developed

Using the ANN-based model developed, the Equipment SHR and the TCC of the DX A/C system could be predicted. To exam the prediction accuracy of the ANN-based model developed for the experimental DX A/C system, 10 additional sets of experimental data were obtained, detailed in Section 5.2.

The predicted results using the ANN-based model developed were compared with the corresponding experimental results at these 10 experimental speed combinations to exam the prediction ability of the ANN-based model developed. As given in Table 5.4, all the REs calculated using Eq. (4.8) were lower than 4%, with most of them being lower than 1%.

Table 5.4 REs of predicted results as compared to the experimental results

Nos.	P_C (%)	P_F (%)	RE_{TCC} (%)	RE_{SHR} (%)
1	38	37	0.3141	0.7913
2	43	82	0.3686	1.6348
3	52	53	0.6863	0.2218
4	53	67	1.0145	0.0821
5	62	83	1.6506	1.0782
6	67	68	0.4714	0.3063
7	73	43	0.6205	0.9825
8	78	52	0.7146	0.1237
9	83	77	3.6206	1.6342
10	87	47	0.4266	0.6757

To further prove the prediction ability of the ANN-based model developed, the prediction accuracies using the ANN-based model developed, a steady-state physical-based model and a numerical analysis based on bilinear interpolation were compared.

A physical-based steady-state model for the experimental DX A/C system was previously developed [Xia et al. 2008] although it could only be used to predict Equipment SHR. The prediction accuracy in terms of RE for Equipment SHR using this physical-based steady-state model was about ±6%, which is much higher than the errors shown in Table 5.4, indicating the high prediction accuracy of the ANN-based model developed.

Furthermore, it was worth noting that one more advantage of using an ANN-based model was its simplicity when compared to using a physical-based model which

focused on fundamental physical processes, where a large number of calculation equations were involved and many assumptions were made during its development.

On the other hand, bilinear interpolation is a numerical analysis method, which extends linear interpolation to two dimensions. Using this method, the values of TCC and Equipment SHR on the ten prediction points as specified in Table 5.5 may also be evaluated using experimental data, and the REs between the predicted and the experimental results were calculated. Fig. 5.6 (a) shows the comparison of the REs for TCC and Fig. 5.6 (b) the comparison of REs for Equipment SHR, both between using the ANN-based model and bilinear interpolation. The results of the comparison suggested that the accuracy using the ANN-based model developed was acceptable when compared to using other prediction methods. Therefore, the ANN-based model developed can be used as a good alternative, amongst many others, to simulate a DX A/C system with an acceptable accuracy.

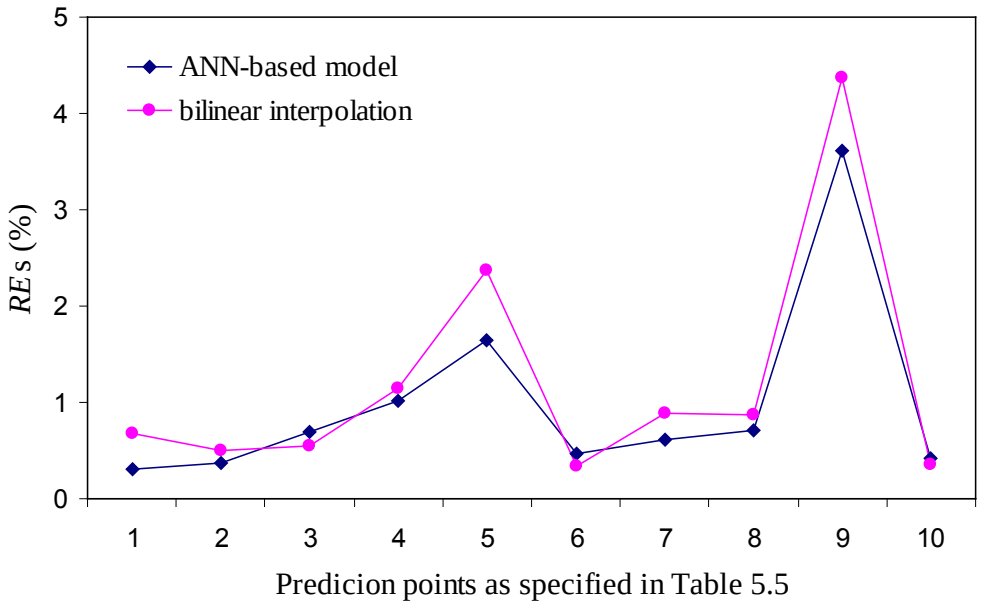

Figure 5.6 (a) Comparison of REs for TCC between using the ANN-based model and bilinear interpolation

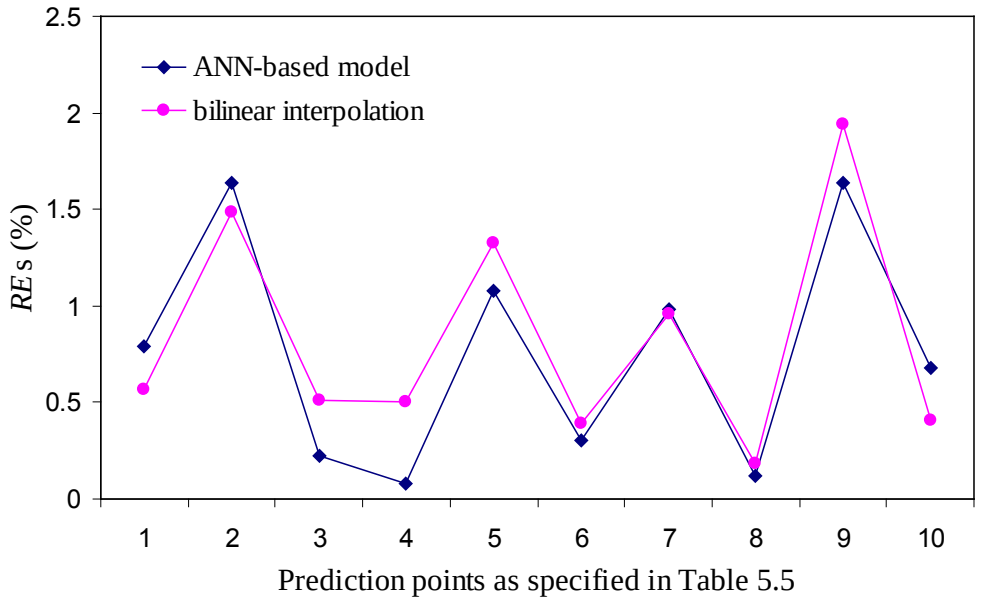

Figure 5.6 (b) Comparison of REs for Equipment SHR between using the ANN-based model and bilinear interpolation

5.6 Conclusions

In this Chapter, a two-in two-out ANN-based steady-state model for an experimental DX A/C system has been developed using BP training algorithm linking its steady-state TCC and Equipment SHR with different combinations of its compressor and supply fan speeds at a fixed inlet air state of 24 ^{o}C and 50% RH, respectively. Totally 144 sets of experimental data were used for ANN training and 25 sets for ANN testing. The ANN-based steady-state model has been validated experimentally by comparing the measured results of TCC and SHR at 10 additional combinations of compressor and supply fan speeds using the experimental DX A/C system with the predicted results using the ANN-based steady-state model developed. All the relative errors when using the developed ANN-based model for prediction were lower than 4%, with most of them being lower than 1%, suggesting the high prediction accuracy of the ANN-based model developed.

The development of the ANN-based steady-state model for the experimental DX A/C system having multivariable inputs and multivariable outputs has clearly suggested that its operating performances can well be represented by using ANN. The ANN-based model developed and reported in this Chapter was the first of its kind applied to a DX A/C system, a highly non-linear complex system. It is expected that the ANN-based steady-state model developed would be very useful in both understanding the operating performances of a DX A/C system and developing an appropriate controller for the DX A/C system to simultaneously control indoor air temperature and humidity in a space served by the DX A/C system, which are to be reported in Chapters 6 to 8 in this Thesis.

Chapter 6

ANN-based Dynamic Modeling of the Experimental DX A/C System

6.1 Introduction

Developing a dynamic model for a DX A/C system to effectively reflect its dynamic operating performances is strongly desirable for control purposes. Firstly, it is well known that the operation of a DX A/C system is dynamic in nature and the coupling effect among its various operating variables is intense [Qi and Deng 2008]. Secondly, all the system components operate in transit conditions in response to the changes in the operating environments and boundary conditions in real applications [Yang 2008]. Thirdly, a good dynamic model which can effectively reflect the dynamic characteristics of a DX A/C system is significantly useful in developing its advanced control strategies, such as capacity control, simultaneous control over indoor air temperature and humidity, etc. [Qi and Deng 2008].

Complexity is a necessary ingredient in physical systems [Mohanraj et al. 2009a]. The complexity of a DX A/C system stems from the fact that it is composed of several interconnected subsystems which mutually influence one another [Amaral and Ottino 2004], and there exist nonlinear dynamics between system inputs and outputs [Loannou and Pitsillides 2008]. In addition, the complexity in controlling DX A/C systems also derives from their MIMO characteristics. As a result, the

control for MIMO systems still presents much difficulty in the current literature [Wong et al. 2010, Mahmoud and Alajmi 2010]. Effective and intelligent control strategies for DX A/C systems have been thus pursued for decades to satisfy the increasingly high requirements for indoor thermal comfort.

Various control strategies have been designed for, and employed in DX A/C systems. These include the traditional PI or PID control strategies. However, for PI or PID control strategies, the coupling effect between the output air temperature and humidity from a DX A/C system can only be dealt with by using two decoupled feedback control loops. Hence, the transient control performance of the two decoupled feedback control loops is inherently poor due to the strong cross-coupling between air temperature and humidity [Krakow et al. 1995, Qi and Deng 2008].

In order to address the coupling effect, other advanced physical-based control strategies have been developed, as detailed in Chapter 2. For these physical-based advanced controllers developed for DX A/C systems, it was necessary to have a physical-based dynamic mathematical model to back up controllers' development. However, because of the complicated inherent interaction among the sub-systems and the nonlinear dynamics in a DX A/C system, developing its physical model of adequate accuracy has always been challenging.

On the other hand, as previously pointed out, ANN has a powerful ability in

recognizing accurately the inherent relationship between any set of input and output without requiring a physical model, while the predicted results using ANN do account for all the physics relating the outputs to the inputs. Therefore, the use of ANN offered a viable solution to the dynamic modeling of complex systems [Angeline et al. 1994]. Using an ANN-based dynamic model, a number of control strategies have been developed, such as the inverse-model-based control which included IMC method and DIC method [Daosud et al. 2005, Deng et al. 2009], model predictive control [Aggelogiannaki et al. 2007, Kittisupakorn et al. 2009] and optimal control [Becerikli et al. 2003], etc.

While the ANN-based modeling and control has been widely used in other engineering systems or processes, no previously reported studies on applying the ANN techniques to the simultaneous control of indoor air temperature and humidity using a DX A/C system may be identified in open literature. On the other hand, a DX A/C system appeared to be an ideal venue where ANN-based modeling and control techniques may be applied to because of its nonlinear and MIMO characteristics. It was therefore considered necessary to develop an ANN-based dynamic model and an ANN-based controller for a variable speed DX A/C system for the simultaneous control of indoor air temperature and humidity in order to fully take the advantage of the advancement in ANN technique.

The development of the ANN-based dynamic model for the experimental DX A/C

system is reported in this Chapter and that of ANN-based controller in Chapter 7. In this Chapter, firstly, the experimental conditions at which experiments were carried out for developing the dynamic model are specified. Secondly, the development of the ANN-based dynamic model for the experimental DX A/C system considering the coupling effect between output air temperature and humidity is presented. Finally, the experimental validation of the ANN-based dynamic model developed by comparing the measured open-loop responses for the experimental DX A/C system after being subject to step changes in compressor and supply fan speeds, with the corresponding predicted results using the ANN-based dynamic model developed is presented.

6.2 Experimental conditions

All the experimental work carried out when dynamically modeling the experimental DX A/C system using ANN may be divided into two categories: I) for developing the ANN-based dynamic model; II) for validating the ANN-based dynamic model developed.

During all experiments, no outdoor air was introduced by fully closing the outdoor air damper in the experimental DX A/C system so that the space cooling load was fully provided by the LGUs. The condenser cooling air flow rate was maintained constant at 3100 m^3/h at a fixed inlet temperature 35 ^oC. The degree of refrigerant

superheat was maintained constant at 6 ºC by using the EEV, which was controlled by a built-in conventional PID controller in the DX A/C system.

Category I experiments

The purpose of Category I experiments was to obtain sufficient amount of experimental data linking the outputs from, with the inputs to the DX A/C system, so as to facilitate the intended ANN-based dynamic model development. In the current study, indoor air dry-bulb temperature and wet-bulb temperature, T_{db} and T_{wb}, were regarded as the outputs from, and the compressor speed and supply fan speed, P_C and P_F, as the inputs to the system.

When carrying out Category I experiments, both indoor sensible load and latent load were kept constant. To achieve this, before recording the experimental data, the speeds of compressor and supply fan were fixed both at 60% of their respective maximums. The outputs from the LGUs were then regulated using the PID controller, so that indoor air dry-bulb temperature and wet-bulb temperature stayed steadily at their respective setpoints, i.e., 24 ^{o}C and 17.1 ^{o}C (or an equivalent of indoor air moisture content of 0.00934 kg/(kg dry air) or a relative humidity of 50%). Then the outputs from the LGUs remained unchanged for the rest of the experimental duration, and the speeds of compressor and supply fan were varied between 30% and 90% of their respective maximum speeds to collect the variation of the experimental results

of T_{db} and T_{wb}. The pattern of input signals were designed as N-samples-constant signals following the methods proposed by Norgaard et al [2000]. Totally 5 groups of experiments, each lasting for 4 hours, were carried out. In each group, there were different combinations of compressor speeds and supply fan speeds which were randomly selected according to the N-samples-constant signal methodology. The experimental data collected from the first four groups were used for training, and those from the last one for testing the ANN-based dynamic model. The sampling interval for experimental data was determined at 1 minute. Totally 960 sets of experimental data were collected to train, and 240 sets of experimental data to test the ANN-based dynamic model. Each set of experimental data included the compressor speed, P_C, supply fan speed, P_F, indoor air dry-bulb temperature, T_{db} and wet-bulb temperature, T_{wb}.

Category II experiments

The purpose of the Category II experiments was to validate the ANN-based dynamic model developed. These experiments were carried out independent of those in Category I, so as to validate independently the ANN-based dynamic model to be developed. Three different variation patterns of input signals were designed: 1) varying P_C only, with P_F fixed; 2) varying P_F only, with P_C fixed; and 3) varying both P_C and P_F. Experimental data were collected at the above three patterns of input signals and compared to the corresponding predicted output results using the

ANN-based dynamic model. For the first variation pattern, the step changes in compressor speed, P_C, were 30%→90%→30%; for the second pattern, the step changes in supply fan speed, P_F, were 30%→90%→30%; and for the last one, the step changes in both compressor speed and supply fan speed, P_C and P_F, were 30%→60%→90%, respectively. The time interval for each step change was all set at 20 minutes, and the open-loop responses of the system were recorded correspondingly. Three experiments, corresponding to the three variation patterns, were carried out. Each lasted for one hour, and the sampling interval for experimental data was at 1 minutes. Thus, in each experiment, totally 60 sets of data were collected.

6.3 Development of the ANN-based dynamic model

When developing an ANN-based dynamic model for a complicated system or process, the previous/present outputs from the system, together with the previous/present inputs to the system, would be designated as inputs to the ANN. A network where the outputs at the previous time steps are used as the inputs to the network at the current time step is generally known as a recurrent network [Yang 2008]. The structure of the ANN used to develop the ANN-based dynamic model for the experimental DX A/C system is shown in Fig. 6.1. The first six inputs to the ANN are the indoor air dry-bulb and wet-bulb temperatures at the present time step (t) and two previous time steps ($t-1$) and ($t-2$), while the other six inputs are the

compressor and supply fan speeds at the present time step and two previous time steps. The two outputs of the ANN are the indoor air dry-bulb and wet-bulb temperatures at one time step ahead (t+1).

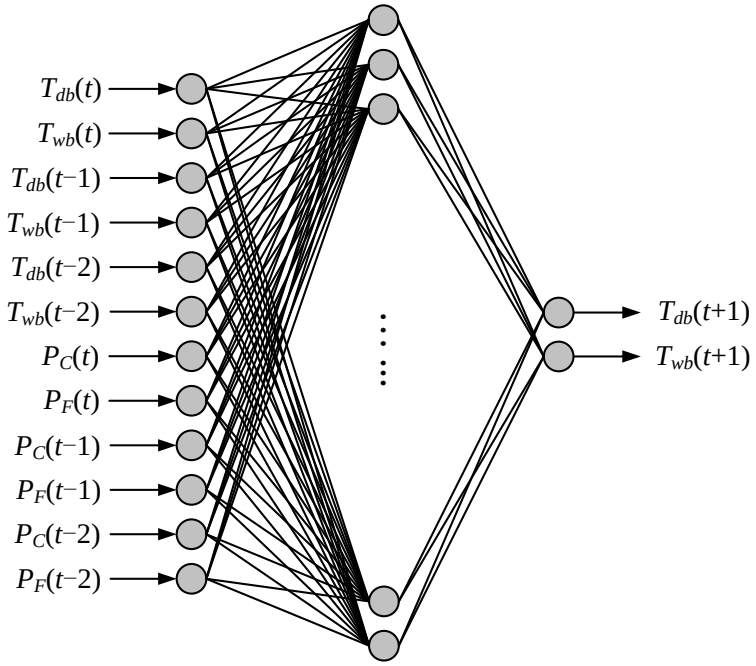

Fig. 6.1 The structure of the ANN-based dynamic model with inputs and outputs

This multilayer feedforward ANN was selected because of its capability of approximating any function after sufficient training. Feed-forward BP algorithm was used in the current study. In training of an ANN, if too much training was applied to a group of data, the ANN would eventually become over-fit. This meant that the ANN obtained would be fitted precisely to this group of training data, thereby losing its generality [Nissen 2003]. Therefore, part of experimental data sets should be reserved as testing data. By testing, it could be decided that how much training was

required for a trained ANN to perform well without over-fitting. This was the so called Early Stopping Strategy, which was derived from the fact that the errors for the training data decreased continuously, while that for the testing data decreased firstly and then increased when the ANN's generality was considered to start to diminish. Therefore, the training of the ANN should be stopped when the errors for the testing data started to increase, thus avoiding over-fitting [Ahmad and Zhang 2009, Asensio-Cuesta et al. 2010]. It was noted that there were no exact or specific guidelines readily available on allocating the percentage of the total data sets for either training or testing, with however some discussions seen in earlier literatures. For example, Pacheco-Vega et al. [2001b] mentioned when more than 60% of the experimental data sets were used for training, the final results would be indifferent. Others used 75% [Diaz et al. 1999] or 80% [Anderson et al. 1997] of the data sets for training. In the current study, with reference to these previously reported studies [Pacheco-Vega et al. 2001b, Diaz et al. 1999, Anderson et al. 1997], 80% of the total data sets were used for training and the remaining 20% for testing.

Two indices were used to evaluate the results of ANN training and testing, i.e., ARE and MRE, which similar to Equations (5.11) and (5.12), were evaluated by:

$$ARE = \frac{1}{J_I}\frac{1}{N}\sum_{j=1}^{J_I}\sum_{n=1}^{N} RE_j^n = \frac{1}{J_I}\frac{1}{N}\sum_{j=1}^{J_I}\sum_{n=1}^{N}\frac{\left|y_{I,j}^n - O_{I,j}^n\right|}{y_{I,j}^n} \tag{6.1}$$

$$MRE = Max\left(RE_j^n\right) \tag{6.2}$$

where J_I is the total number of neurons in the output layer (J_I=2 in the current study), N the total number of the data sets used in training or testing (N=960 for training and N=240 for testing in the current study), y the experimental results, and O the corresponding predicted results using the ANN trained.

During training, ARE for the testing data as defined by Equation (6.1), was evaluated to determine when the ANN training should be stopped following the Early Stopping Strategy. Furthermore, different ANN structures with one, two and three hidden layers and different combinations of number of neurons in the hidden layers have been tried and compared. It was shown that at different number of hidden layers, no clear difference in ARE may be observed. The ANN with single hidden layer was therefore chosen. Finally, the number of neurons in the hidden layer was determined by trial and error, which suggested that an ANN having a 12-30-2 structure be employed.

The ANN-based dynamic model for the experimental DX A/C system obtained after training and testing was a good representation of the dynamic characteristics between system inputs and outputs. Figure 6.2 shows the comparisons between the experimental training data (T_{db} and T_{wb}) and the corresponding predicted results using the ANN-based dynamic model developed for one of the four groups of

experimental data used for training.

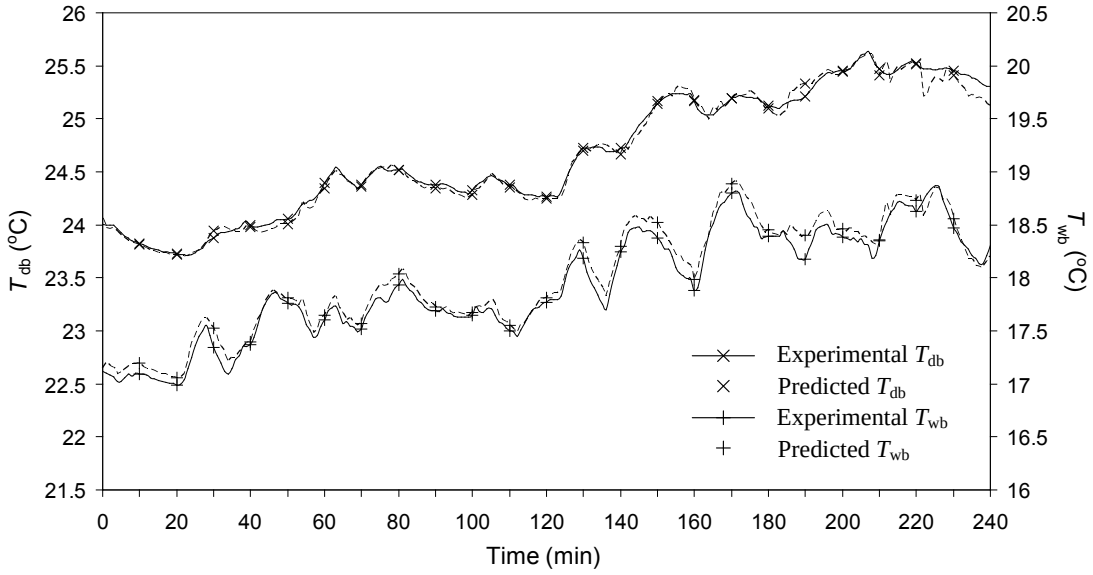

Fig. 6.2 Example comparisons between the experimental and the predicted dry-bulb and wet-bulb temperatures using the ANN-based dynamic model developed

For the ANN-based dynamic model developed, the values of ARE and MRE during training were 0.30% and 1.36%, respectively, indicating that the ANN-based dynamic model developed was able to model the dynamic relationship between the inputs and outputs for the experimental DX A/C system with a high accuracy.

6.4 Validation of the ANN-based dynamic model developed

Simulation results using the ANN-based dynamic model developed were compared with the Category II experimental results obtained using the experimental DX A/C system for the purpose of model validation. When validating the model, in addition to using ARE and MRE, two further evaluating indices, i.e., R and σ, were also used as follows:

$$R = \frac{1}{J_I}\sum_{j=1}^{J_I} R_j = \frac{1}{J_I}\frac{1}{N}\sum_{j=1}^{J_I}\sum_{n=1}^{N} R_j^n = \frac{1}{J_I}\frac{1}{N}\sum_{j=1}^{J_I}\sum_{n=1}^{N}\frac{y_{I,j}^n}{O_{I,j}^n} \tag{6.3}$$

$$\sigma = \frac{1}{J_I}\sum_{j=1}^{J_I}\sigma_j = \frac{1}{J_I}\sum_{j=1}^{J_I}\sqrt{\frac{1}{N}\sum_{n=1}^{N}(R_j - R_j^n)^2} \tag{6.4}$$

where N is the total number of the data sets used in validation (N=60 in the current study). R indicates the average accuracy of the model prediction while σ the degree of scatter of the model prediction. The accuracy of the prediction increases with R approaching unity and σ approaching zero, respectively.

Figures 6.3 and 6.4 show the comparison between experimental results and the corresponding predicted results using the ANN-based dynamic model developed when the compressor speed and supply fan speed were varied following the variation patterns 1) and 2) shown in Section 6.2 (Category II experiments). The calculated results of ARE for these two experiments were 0.33% and 0.27%, respectively, and

MRE were 0.89% and 0.99%, respectively. The calculated results of R and σ for the indoor air dry-bulb and wet-bulb temperature for pattern 1), i.e., R_{db}, R_{wb}, σ_{db}, σ_{wb}, were 1.0014, 0.9978, 2.9830×10^{-6} and 1.3904×10^{-5}, respectively, and the corresponding results for pattern 2) were 1.0008, 0.9966, 1.8776×10^{-6} and 1.0152×10^{-5}, respectively. The results of all these evaluating indices indicated the high prediction accuracy of the ANN-based dynamic model developed.

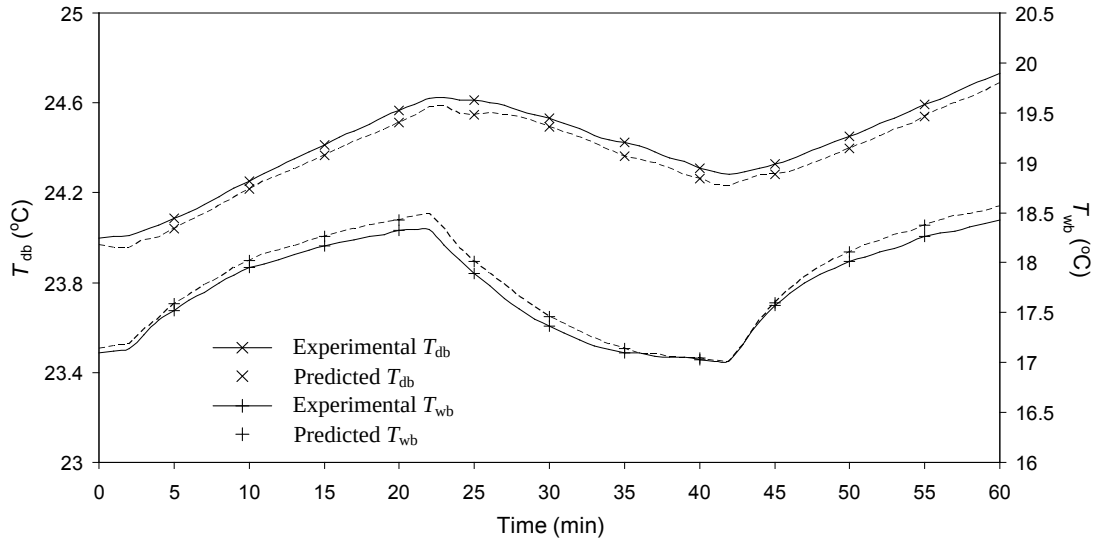

Fig. 6.3 Comparison between the experimental and the predicted dry-bulb and wet-bulb temperatures using the ANN-based dynamic model developed in validation (varying P_C)

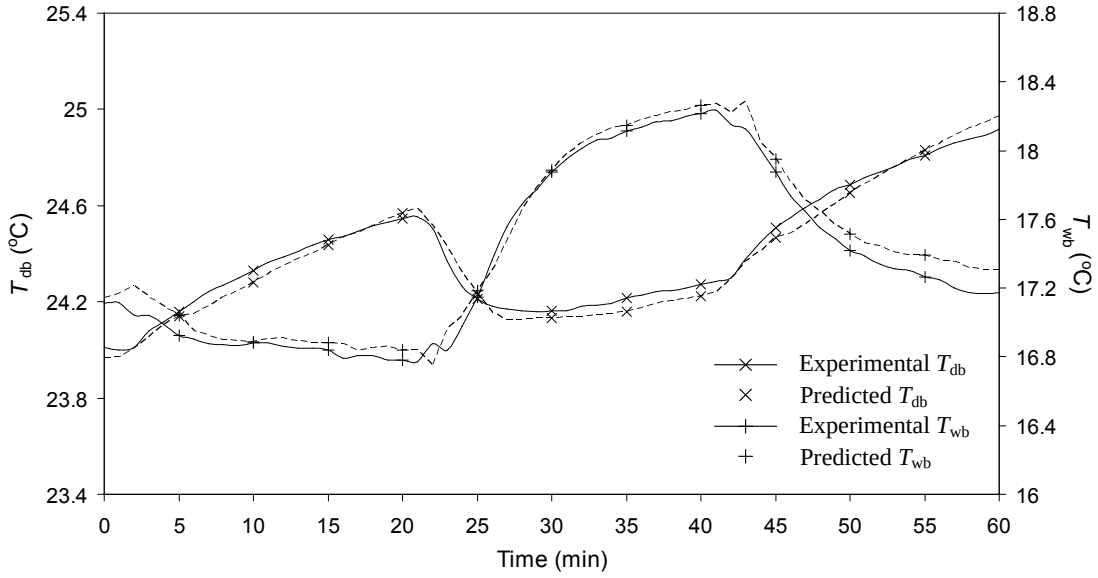

Fig. 6.4 Comparison between the experimental and the predicted dry-bulb and wet-bulb temperatures using the ANN-based dynamic model developed in validation (varying P_F)

The comparison between the experimental and predicted indoor air dry-bulb and wet-bulb temperatures when both the compressor speed and supply fan speed were varied following the variation pattern 3) as specified in Section 6.2 (Category II experiments) are shown in Fig. 6.5. The ARE was evaluated at 0.27%, and the MRE at 1.15% and the values of R_{db}, R_{wb}, σ_{db} and σ_{wb} were 1.0014, 0.9978, 2.9830×10^{-6} and 1.3904×10^{-5} respectively. The results of all these evaluating indices also suggested that the ANN-based dynamic model developed could represent the dynamic relationship between the inputs and outputs of the experimental DX A/C system with a high accuracy.

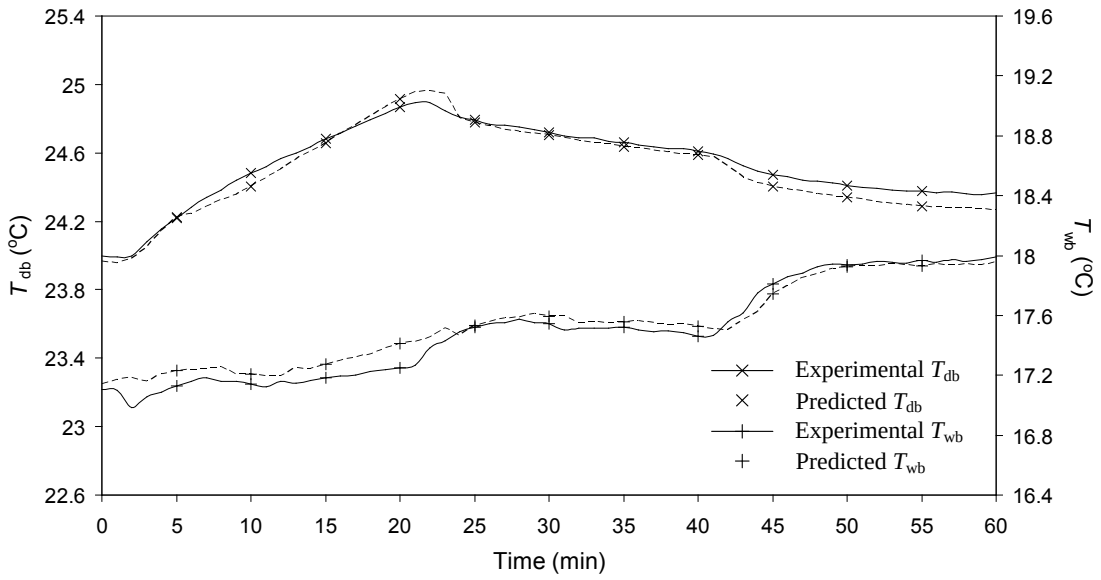

Fig. 6.5 Comparison between the experimental and the predicted dry-bulb and wet-bulb temperatures using the ANN-based dynamic model developed in validation (varying both P_C and P_F)

6.5 Conclusions

This Chapter reports on the development of an ANN-based dynamic model for the experimental DX A/C system linking its dynamic indoor air condition in terms of dry-bulb temperature and wet-bulb temperature with the variation of its compressor and supply fan speeds at a fixed indoor sensible and latent load. Totally 960 sets of experimental data were used for ANN training and 240 sets for testing. The ANN-based dynamic model has been validated experimentally by comparing the

measured results of indoor air dry-bulb and wet-bulb temperatures under Category II experiments conditions for the experimental DX A/C system, with the predicted results using the ANN-based dynamic model developed. The values of ARE and MRE when validating the ANN-based dynamic model developed under three different input patterns were 0.33%, 0.27%, 0.27% and 0.89%, 0.99%, 1.15%, respectively, suggesting the high prediction accuracy of the ANN-based dynamic model developed.

The ANN-based dynamic model developed helped to better understand the dynamic operating performance of a DX A/C system. Based on the ANN-based dynamic model developed, an ANN-based controller for the DX A/C system to simultaneously control indoor air temperature and humidity in a space served by the DX A/C system was developed and is reported in Chapter 7.

Chapter 7

ANN-based Controller for the Experimental DX A/C System for Simultaneous Control of Indoor Air Temperature and Humidity

7.1 Introduction

An ANN-based dynamic model for the experimental DX A/C system has been developed and is reported in Chapter 6. When developing the dynamic model, it was intended that the model would be used to assist the development of an ANN-based controller for the DX A/C system for simultaneous control over indoor air temperature and humidity.

This Chapter presents the development of an ANN-based controller for the experimental DX A/C system to control the indoor air temperature and humidity simultaneously by varying compressor speed and supply fan speed. In this Chapter, the ANN training algorithm used in developing the ANN-based controller for the DX A/C system is firstly introduced. Secondly, the development of the ANN-based controller for the experimental DX A/C system is detailed. Finally, the validation of the ANN-based controller developed by carrying out the controllability tests using the experimental DX A/C system is presented.

7.2 ANN training algorithm used to design the ANN-based controller

The ANN-based controller to be developed was composed of the ANN-based dynamic model reported in Chapter 6, and an ANN-based inverse model, whose details will be given later in Section 7.3. When developing the ANN-based controller, the DIC strategy following the ANN-based direct design method was used.

There were usually two methods for establishing an inverse model in the DIC strategy: an off-line method known as general training and an on-line method called specialized training [Norgaard et al. 2000, Saerens and Soquet 1989]. In the current study, both the general training and specialized training methods were used in training the ANN-based inverse model. The former is detailed Chapter 5 and the latter will be introduced as follows.

The specialized training method aims at minimizing the difference between the actual output from a controlled system and the control reference:

$$E = \frac{1}{2}\sum_i \left(y_i - r_i\right)^2 \tag{7.1}$$

Where, y is the output from the system and r, the control reference. The BP algorithm implements a gradient descent in E and upgrades the weights of the ANN-based inverse model, i.e., W, in such a way:

$$W(t+1) = W(t) - \eta \frac{\partial E}{\partial W(t)} \tag{7.2}$$

To obtain the value of $\frac{\partial E}{\partial \boldsymbol{W}}$, the chain rule can be used:

$$\frac{\partial E}{\partial \boldsymbol{W}} = \frac{\partial E}{\partial \boldsymbol{y}} \frac{\partial \boldsymbol{y}}{\partial \boldsymbol{u}} \frac{\partial \boldsymbol{u}}{\partial \boldsymbol{W}} \tag{7.3}$$

The value of $\frac{\partial E}{\partial \boldsymbol{y}}$ could be evaluated as follows:

$$\frac{\partial E}{\partial \boldsymbol{y}} = \sum_i \left(y_i - r_i \right) \tag{7.4}$$

The value of $\frac{\partial \boldsymbol{y}}{\partial \boldsymbol{u}}$, which is the Jacobian of the system, could be evaluated using the ANN-based dynamic model developed:

$$\frac{\partial y(t+1)}{\partial u(t)} \approx \frac{\partial y_m(t+1)}{\partial u(t)} \tag{7.5}$$

Where $y_m(t+1)$ refers to the outputs from the ANN-based dynamic model at time step $(t+1)$. It is the predicted result using the ANN-based dynamic model developed.

Compared to general training, specialized training has no training stage during which

the network is not operational. In specialized training, ANN learns directly towards the goal of the controller, which is that the system output should follow the reference signal closely and effectively, so as to improve the control performance of the ANN-based controller. Under specialized training, ANN could learn continuously and can therefore be used in processes with time varying characteristics. However, the evaluation of the error between the control reference and the output from the controlled system requires prior knowledge of the system, which means that the dynamic model of the system should be available first. In this study, the ANN-based dynamic model developed of the DX A/C system was used when updating of the ANN-based inverse model when the prior knowledge of the system was required.

7.3 Development of the ANN-based controller

The controller to be developed was expected to be able to achieve the simultaneous control over indoor air temperature and humidity, through simultaneously varying the speeds of compressor and supply fan in the experimental DX A/C system. As mentioned earlier, the controller consisted of the ANN-based dynamic model reported in Chapter 6 and an ANN-based inverse model for the experimental DX A/C system. The ANN-based inverse model, as opposed to the ANN-based model, was a dynamic model trained to simulate the inverse dynamic characteristics of the DX A/C system to be controlled and then acted as an actuator in the controller. The structure of the ANN-based inverse model was the same as that of the ANN-based

dynamic model presented in Chapter 6. The inputs and outputs of the ANN-based inverse model are shown in Fig. 7.1, in which r_{db} and r_{wb} are the control references, or settings, for indoor air dry-bulb temperature and wet-bulb temperature. Other inputs included the indoor air dry-bulb and wet-bulb temperatures at the present time step (t) and two previous time steps ($t-1$) and ($t-2$), the compressor and supply fan speeds at the two previous time steps. The two outputs of the ANN-based inverse model were the compressor and supply fan speeds at the present time step. With such an inverse model, the required compressor and supply fan speeds at the present time step may be evaluated, and implemented in the DX A/C system to be controlled.

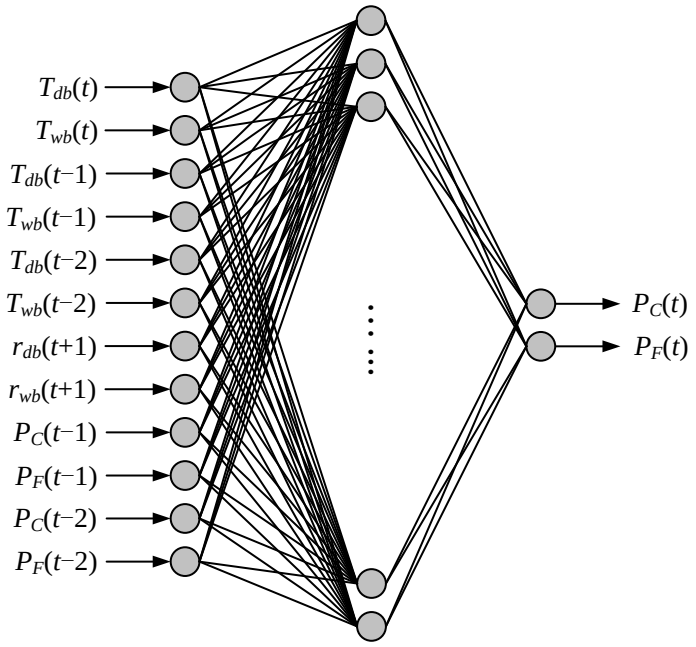

Fig. 7.1 The structure of the ANN-based inverse model with inputs and outputs

The development of the ANN-based controller was accomplished in the following

three steps:

Step (1): Building an ANN-based dynamic model for the experimental DX A/C system using the general training method, which is already presented in Chapter 6. After validation, this ANN-based dynamic model was included as part of the ANN-based controller to describe the dynamic relationship between inputs and outputs of the experimental DX A/C system. Since the indoor loads were fixed in this study with only small changes introduced in the disturbance rejection test as detailed in Section 7.4.2.2, the ANN-based dynamic model developed was directly used in the controller for estimating of the plant Jacobian and therefore no further on-line training was needed [Ng 1997, Wang and Bao 2000].

Step (2): Training an initial ANN-based inverse model with inputs and outputs shown in Fig. 7.1 using the experimental data collected in Chapter 6 by the general training method. The training and testing process for the initial ANN-based inverse model was similar to that for the ANN-based dynamic model presented in Chapter 6.

Step (3): However, when the initial ANN-based inverse model trained was used as an actuator in the ANN-based controller for the experimental DX A/C system, a large deviation between the control references and the outputs from the system was resulted in since the inverse model was off-line trained. Hence, the specialized training method was then used to update the initial ANN-based inverse model. Using

this on-line training method, the weights of the ANN-based inverse model were continuously updated according to changes in control references and real-time operating parameters of the experimental DX A/C system.

The operating principle of the ANN-based controller under the DIC strategy established following the above three steps is illustrated in Fig. 7.2. In this figure, $\boldsymbol{u}$ is the inputs to the system ($\boldsymbol{u}$=[P_C, P_F] in the current study), $\boldsymbol{y}$, the outputs from the system ($\boldsymbol{y}$=[T_{db}, T_{wb}] in the current study), $\boldsymbol{y}_m$, the outputs from the ANN-based model, $\boldsymbol{r}$, the control reference of the controller ($\boldsymbol{r}$=[r_{db}, r_{wb}] in the current study), and q, a time delay operator (for example, $q^{-2}\,\boldsymbol{u}(t)=\boldsymbol{u}(t\text{-}2)$).

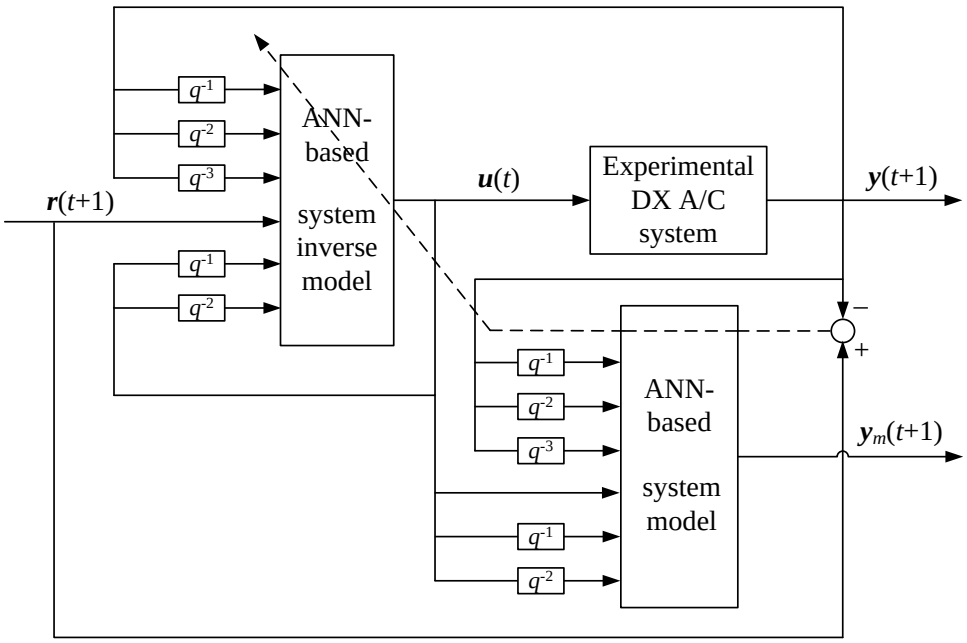

Fig. 7.2 The ANN-based controller under DIC strategy for the experimental DX A/C system

7.4 Controllability tests

7.4.1 Test types and conditions

After developing the ANN-based controller for the experimental DX A/C system as reported above, the controllability tests to examine its control performance were carried out using the experimental DX A/C system. When carrying out the tests, the controller was digitally implemented in the form of a computer program, with suitable interfaces for collecting data and outputting control actions such as varying speeds of compressor and supply fan via variable speed drives.

With the computerized instrumentation, all the measured data could be recorded for subsequent analysis, and the control inputs to the DX A/C system could be generated based on the feedback signals of measured indoor air temperature and humidity. The schematic diagram of the ANN-based controller implementation for the experimental DX A/C system is shown in Fig. 7.3.

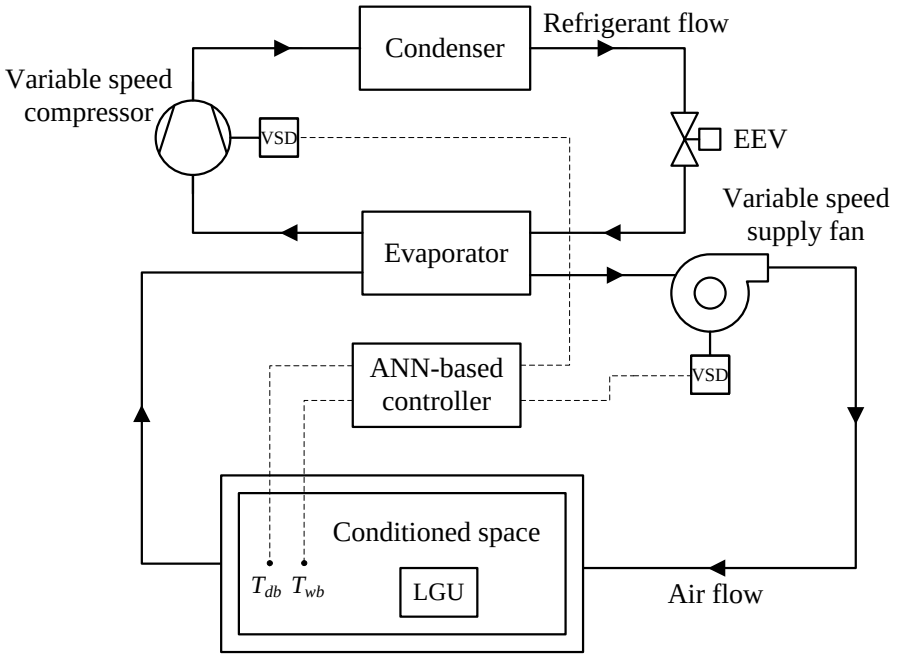

Fig. 7.3 Schematic diagram of the ANN-based controller arrangement

For all controllability tests using the experimental DX A/C system, indoor air temperature control was via controlling indoor air dry-bulb temperature, and indoor humidity control was via controlling indoor air wet-bulb temperature. During the controllability tests, the time interval between the changes in compressor and supply fan speeds (controller's outputs) was 1 minute.

The following two types of controllability tests were carried out:

(1) Command following: the output variables could track changes of their setpoints with stability. When the setpoints of indoor air dry-bulb temperature and wet-bulb temperature were changed, the controller was expected to react so that indoor air

temperature and moisture content could be maintained at their respective new setpoints. In the current study, the setpoints of indoor air dry-bulb temperature and wet-bulb temperature were altered from 24 ºC and 17.1 ºC, respectively, to 25 ºC and 18 ºC, respectively.

(2) Disturbance rejection: the output variables, i.e., indoor air dry-bulb temperature and wet-bulb temperature were to be maintained at their respective setpoints when space sensible load and latent load were subjected to disturbances. In the current study, this type of test was carried out under the indoor air setpoints of 24 ºC, dry-bulb temperature and 17.1 ºC, wet-bulb temperature. The disturbances introduced to the system were the changes in indoor sensible and latent cooling loads, from 4.1 kW and 2.3 kW, respectively, to 3.4 kW and 1.9 kW, respectively.

7.4.2 Test results

7.4.2.1 Command following test

Figure 7.4 shows the results of command following test for the ANN-based controller developed, following a change in the setpoints of indoor air dry-bulb temperature and wet-bulb temperature. As seen, indoor air temperature settings were at 24 ºC for dry-bulb temperature and 17.1 ºC for wet-bulb temperature initially. During the first 400 s of the test, the DX A/C system was stable, and both indoor air

temperature and humidity were maintained at their respective setpoints. At t = 400 s, the above settings were altered to 25 ºC and 18 ºC, respectively, and the ANN-based controller was immediately reacted by simultaneously varying the compressor and supply fan speeds, as shown in Fig. 7.5. The indoor air dry-bulb temperature and wet-bulb temperature reached their respective new setpoints after about 1000 s and was maintained steady during the following 2100 s, as shown in Fig. 7.4. Therefore, the ANN-based controller developed was able to track the changes in the indoor air dry-bulb temperature and wet-bulb temperature settings.

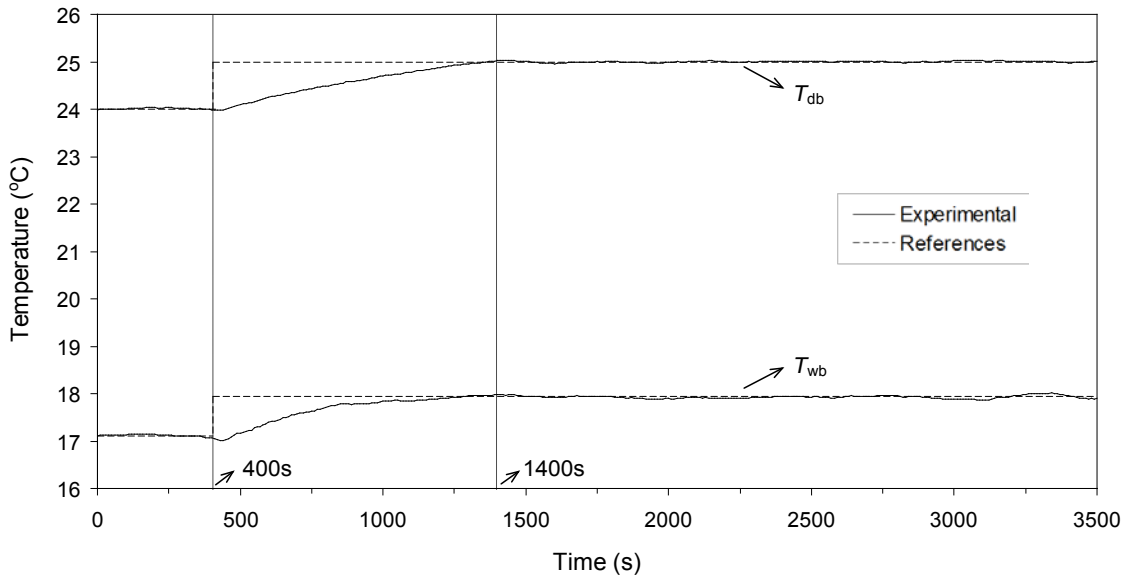

Fig. 7.4 The variations of the indoor air dry-bulb and wet-bulb temperatures in command following test

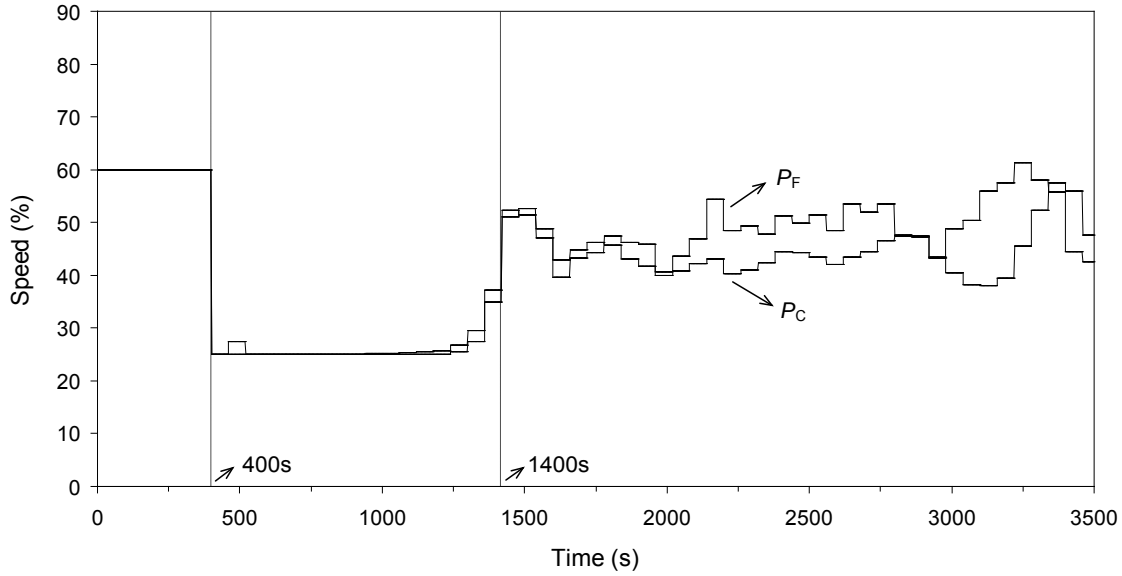

Fig. 7.5 The variations of compressor and supply fan speeds in command following test

7.4.2.2 Disturbance rejection test

During the disturbance rejection test, indoor settings were 24 ºC for air dry-bulb temperature, and 17.1 ºC for air wet-bulb temperature, respectively (or an equivalent of indoor air moisture content 0.00934 kg/(kg dry air) or relative humidity 50%). With the ANN-based controller, these settings were expected to be maintained after the disturbances in both space sensible and latent cooling loads were introduced. The ANN-based controller was enabled when the deviation for either the measured indoor air dry-bulb temperature or the measured indoor air wet-bulb temperature was greater than ± 0.5 ºC.

Figures 7.6 and 7.7 present the results of disturbance rejection test for the ANN-based controller. As seen, prior to the introduction of disturbance at t = 400 s, indoor air temperatures were stably maintained at their respective setpoints. At t = 400 s, space sensible load was reduced from 4.1 kW to 3.4 kW and space latent load from 2.3 kW to 1.9 kW, respectively. In response to the disturbance, both indoor air dry-bulb and wet-bulb temperatures gradually decreased. At about t = 1400 s, when indoor air dry-bulb temperature dropped to 23.5 ºC, the ANN-based controller was enabled. Figure 7.7 shows the variation profiles of compressor speed and supply fan speed. The indoor air dry-bulb temperature and wet-bulb temperature came back to their respective setpoints after about 720 s and were maintained steady during the following 1880 s, as shown in Fig. 7.6. Therefore, the ANN-based controller was able to bring back the indoor air dry-bulb and wet-bulb temperatures to their respective set points after indoor thermal loads were varied, achieving a satisfactory control performance in disturbance rejection test. As seen, at the end of test, the deviation between indoor air wet-bulb temperature and its setting was less than 0.2 ºC.

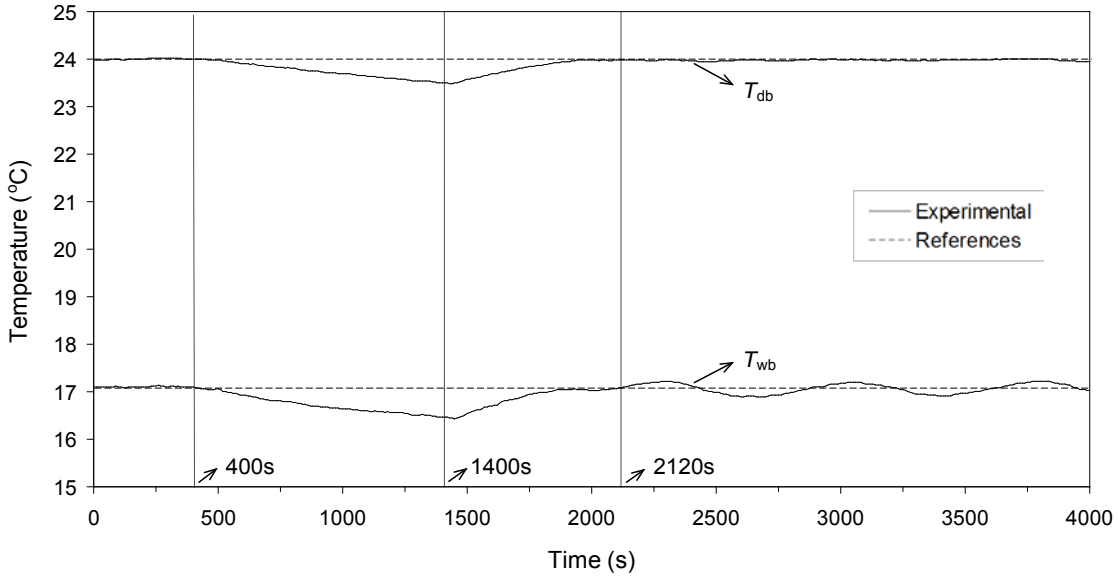

Fig. 7.6 The variations of the indoor air dry-bulb and wet-bulb temperatures in disturbance rejection test

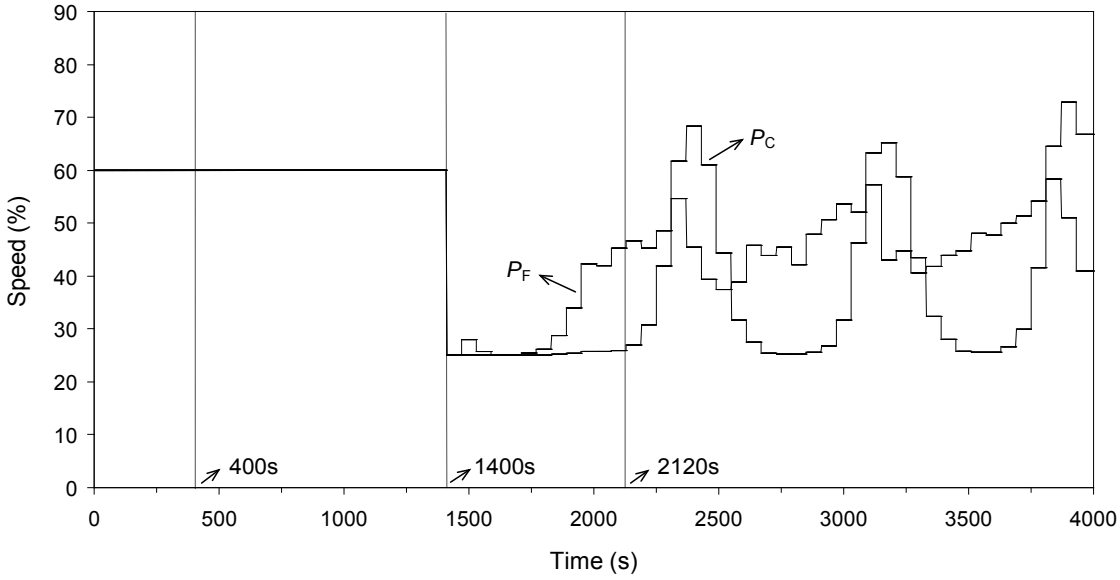

Fig. 7.7 The variations of compressor and supply fan speeds in disturbance rejection test

7.5 Conclusions

In this Chapter, an ANN-based controller to simultaneously control indoor air temperature and humidity in a space served by the experimental DX A/C system has been developed using the ANN-based dynamic model developed and reported in Chapter 6. This ANN-based controller was designed using the DIC strategy. Controllability tests including the command following test and disturbance rejection test were then carried out to examine the performance of the ANN-based controller developed. In the command following test, the indoor air dry-bulb temperature and wet-bulb temperature could be controlled to their respective new setpoints. In the disturbance rejection capability test, the results showed that the ANN-based controller can effectively control the indoor air dry-bulb temperature and wet-bulb temperature to their respective setpoints when there were sensible and latent load disturbances imposed. Therefore the results of the controllability tests showed that the ANN-based controller developed could simultaneously control indoor air temperature and humidity by varying compressor speed and supply fan speed of the experimental DX A/C system with an adequate control accuracy.

A novel feature of the ANN-based controller reported in this Chapter was that it dealt with a MIMO system which presented much difficulty for control in current literature. A possible approach of controlling a complex MIMO nonlinear dynamic system based on ANN-based techniques was illustrated. It was expected that this approach could be further developed to be applicable to more general complex

systems.

In the development of this ANN-based controller, it could be noted that the controller could only perform well in the vicinity of the operating points where the ANN-based dynamic model was originally trained. This is because that the weights of the ANN-based dynamic model in the ANN-based controller remained unchanged while the operating conditions of the system may continuously vary, leading to the problem of limited controllable range. In order to resolve this problem of limited controllable range, an ANN-based on-line adaptive controller has been developed and is reported in Chapter 8 in this thesis.

Chapter 8

ANN-based On-line Adaptive Controller for the Experimental DX A/C System for Simultaneous Control of Indoor Air Temperature and Humidity

8.1 Introduction

In Chapter 7, the development of an ANN-based controller, which was based on the ANN-based dynamic model, for the experimental DX A/C system, is reported. This ANN-based controller developed consist the ANN-based dynamic model, which was off-line trained beforehand and remained unchanged during control, and an ANN-based inverse model, which was updated during control to minimize the difference between control references and controlled variables. However, similar to all models developed through system identification, the ANN-based dynamic model used was off-line trained using the operating data collected at a particular operating point, or the training point, and would therefore fail to simulate system performance when the operating conditions drifted away from the training point, making the ANN-based inverse model incapable of being updated to correctly trace the control references. Therefore, the ANN-based controller can only work as expected near the system operating point at which the ANN-based dynamic model was off-line trained. In other words, the ANN-based controller developed had a problem of limited controllable range. In order to make the ANN-based controller workable at the entire

operating rang of the DX A/C system, the concept of adaptive control was applied to the ANN-based controller developed to turn it into an ANN-based on-line adaptive controller, in which an ANN-based dynamic model was trained on-line using the data collected and thus updated on a regular basis as the system operation went on. Consequently the model can represent the real-time dynamic operating performance of the DX A/C system. Then the ANN-based inverse model could be updated correctly to adapt to the change in operating conditions.

This Chapter reports on the development of the ANN-based on-line adaptive controller and the results of its controllability tests. Firstly, the development of the ANN-based on-line adaptive controller is detailed. Secondly, the results of controllability tests for the ANN-based on-line adaptive controller including initial start-up stage test, command following test, disturbance rejection test and commanding following with disturbances test using the experimental DX A/C system are presented. Finally, a discussion on related issues in the development of the ANN-based on-line adaptive controller for the experimental DX A/C system is detailed.

8.2 The development of the ANN-based on-line adaptive controller

The details of the ANN-based controller previously developed are reported in Chapter 7. Since the ANN-based dynamic model in the ANN-based controller was

off-line trained at a fixed operating point, satisfactory control performances were achieved using the ANN-based controller when the DX A/C system was operated in the vicinity of this training point. However, as commonly acknowledged, control performance still using such a controller would be likely to deteriorate, when the DX A/C system is operated away from the training point. It was therefore necessary that an ANN-based on-line adaptive controller should be developed to address and resolve the problem of limited controllable range, as discussed earlier.

The operating principle of the ANN-based on-line adaptive controller is illustrated in Fig. 8.1. In this figure, similar to those in Fig. 7.2, $\boldsymbol{u}$ is the inputs to the system ($\boldsymbol{u}$=[P_C, P_F], where P_C is the percentage of the maximum compressor speed, and P_F the percentage of the maximum supply fan speed), $\boldsymbol{y}$, the outputs from the system ($\boldsymbol{y}$=[T_{db}, T_{wb}], where T_{db} is the indoor air dry-bulb temperature and T_{wb} indoor air wet-bulb temperature), $\boldsymbol{y}_m$, the outputs from the ANN-based model, $\boldsymbol{r}$, the control references of the controller ($\boldsymbol{r}$=[r_{db}, r_{wb}]), q, a time delay operator (for example, q^{-2} $\boldsymbol{u}(t)=\boldsymbol{u}(t\text{-}2)$), and t, time instant (where t is the present time step, (t-1), the time instant at last time step and (t+1), the time instant at next time step, and the time interval between time instant t and (t+1) is Δt).

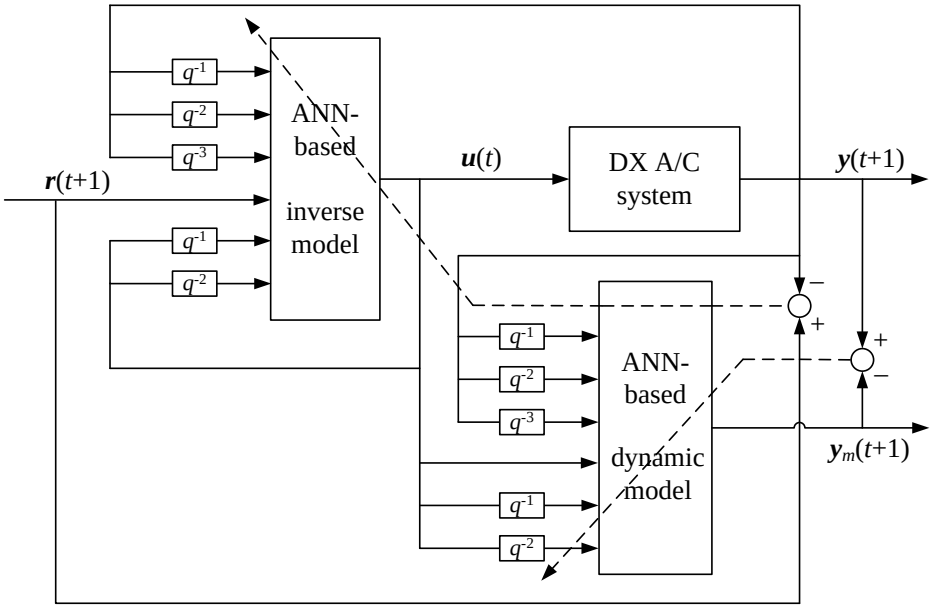

Fig. 8.1 The schematics of the ANN-based on-line adaptive controller

Comparing Fig 8.1 with Fig 7.2 in Section 7.3 in Chapter 7, the development of the ANN-based on-line adaptive controller was accomplished in four steps, with Steps (1) and (2) being the same as that of the developed ANN-based controller presented in Section 7.3 in Chapter 7. The two more steps were:

Step (3): Updating the ANN-based dynamic model on-line using the data collected during control using the general training method. The data used for on-line training were updated continuously every 60 s in the current study, so that the resulted updated ANN-based model could reflect the real-time operating performance of the DX A/C system;

Step (4): Updating the weights of the ANN-based inverse model using the specialized training method according to the changes in control references and real-time operating parameters of the DX A/C system. Since the ANN-based dynamic model would be trained using the latest collected data every time when the ANN-based inverse model was updated to calculate the control outputs, the updating of the ANN-based inverse model could use the Jacobian of the system which was evaluated by the last updated ANN-based dynamic model. In this way, the ANN-based on-line adaptive controller could adapt to the changes in actual operating conditions for the DX A/C system.

In the current study, both the ANN-based dynamic model and ANN-based inverse model were initially off-line trained around the indoor air dry-bulb temperature and wet-bulb temperature setpoints of 24 ^{o}C and 17.1 ^{o}C respectively (or 50% RH). The controllable ranges of the ANN-based on-line adaptive controller were designed to be extended to 20 ^{o}C to 28 ^{o}C for indoor air dry-bulb temperature and 13 ^{o}C to 21 ^{o}C for indoor air wet-bulb temperature, which were commonly required for indoor thermal comfort.

The flow chart of control process is illustrated in Fig. 8.2. In this figure, τ is the time duration starting from the beginning of control to the current time instant, t, Δt, the time interval between two consecutive control actions by the ANN-based on-line adaptive controller (Δt = 60 s in the current study), k, counter of control action by the

ANN-based on-line adaptive controller, *l*, the number of data sets used for on-line training of the ANN-based dynamic model (*l* was set at 10 in the current study).

In Figure 8.2, the judgment '$\tau \geq k \times \Delta t$?' suggests whether the present time interval, Δt, was satisfied so that the controller could act to change the speeds of compressor and supply fan according to the results calculated by the ANN-based on-line adaptive controller. If the answer to this judgment was 'Yes', the controller would act to adjust the speeds of compressor and supply fan. However, if a 'No' answer was obtained, the control program would do data logging periodically (every 2 s in the current study) and the speeds of compressor and supply fan were kept unchanged. During the period of data logging, the program was running continuously and the operating data were recorded. Although the data recorded during the period of data logging would not be used for control, they could be displayed to reflect the dynamic operating conditions of the DX A/C system under control.

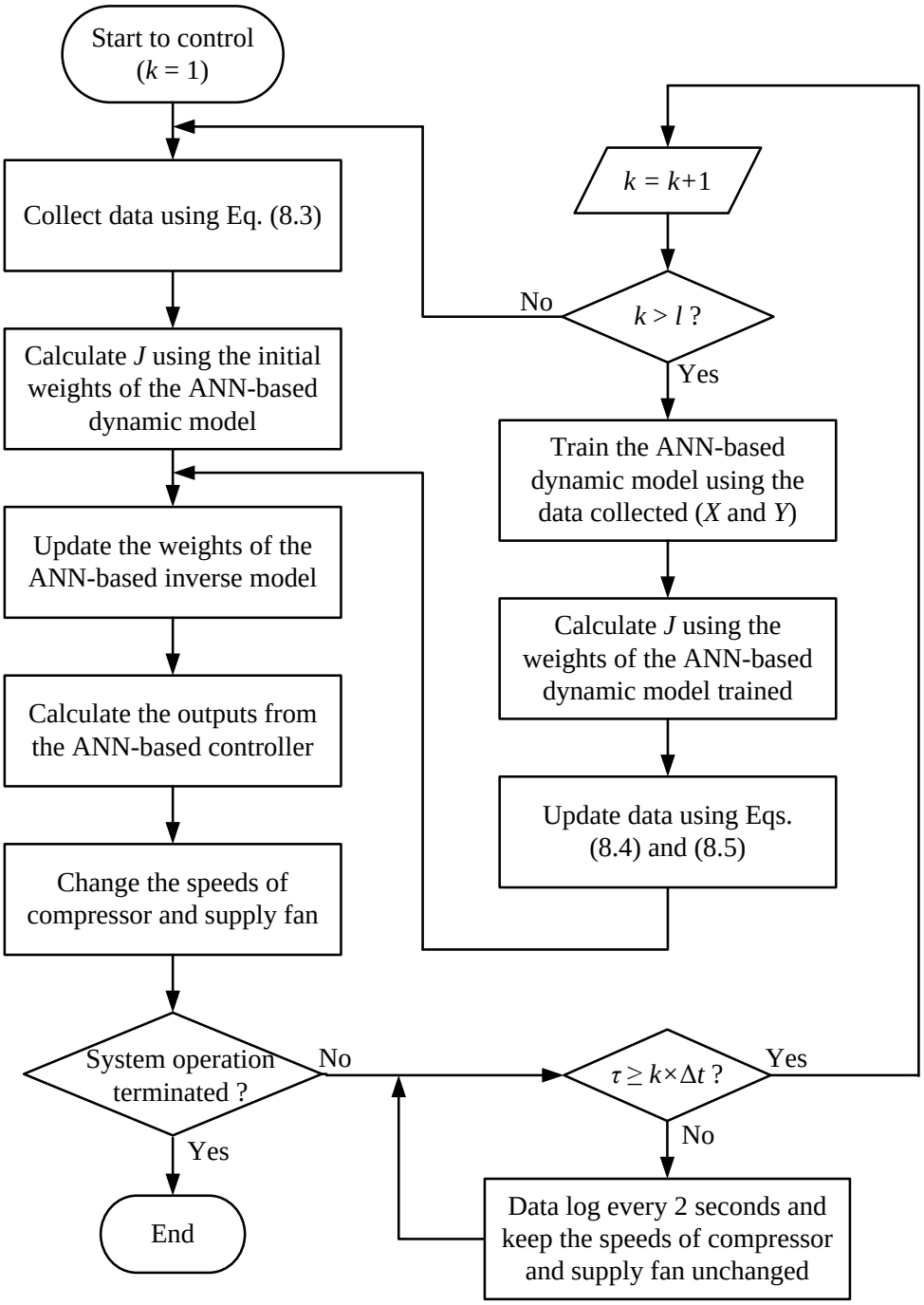

Fig. 8.2 Flow chart of the ANN-based on-line adaptive controller

In the current study, the data used for on-line training of the ANN-based dynamic model were collected every 60 s from the beginning of control. Thus, it would take

10 minutes for the controller to collect sufficient data sets to start on-line training of the ANN-based dynamic model. Therefore, in Fig.8.2 the judgment '$k > l$?' suggests whether the controller could start the on-line training of the ANN-based dynamic model. A 'No' answer means that the data sets collected were not adequate to train on-line the ANN-based dynamic model, then the controller would continue to collect data and the initially trained ANN-based dynamic model would still be used to calculate the Jacobian of the system so as to achieve updating the ANN-based inverse model. However, a 'Yes' answer means that the controller had collected adequate data sets to training the ANN-based dynamic model, so that it would be on-line trained using the data collected and used to calculate the Jacobian of the system to update the ANN-based inverse model. Once the condition of '$k > l$' was satisfied, a 'Yes' answer would always be obtained in this judgment, which meant the initial weights of the ANN-based dynamic model would never be used again in the remaining system operating period, and the data used for on-line training the ANN-based dynamic model would be updated every 60 s.

$\boldsymbol{X}$ and $\boldsymbol{Y}$ are the data collected to on-line train the ANN-based dynamic model, defined as follows:

$$\boldsymbol{X} = [\boldsymbol{X}(1), \boldsymbol{X}(2), \ldots \boldsymbol{X}(l)] \tag{8.1}$$

$$\boldsymbol{Y} = [\boldsymbol{Y}(1), \boldsymbol{Y}(2), \ldots \boldsymbol{Y}(l)] \tag{8.2}$$

During the initial period of control (10 minutes in the current study), when the data sets collected to train the ANN-based dynamic model were not sufficient (when $k \leq l$), the initial weights of the ANN-based dynamic model obtained through off-line training were used to calculate the Jacobian of the DX A/C system, so as to accomplish the updating of the ANN-based inverse model. Meanwhile, the data needed to train the ANN-based dynamic model were collected using:

$$\begin{aligned} \boldsymbol{X}(k) &= [P_C, P_F]_p \\ \boldsymbol{Y}(k) &= [T_{db}, T_{wb}]_p \end{aligned} \tag{8.3}$$

where, '$\boldsymbol{X}(k) = [P_C, P_F]_p$' means to collect the values of P_C and P_F at the present time.

When sufficient data sets were collected during control (when $k > l$), the ANN-based dynamic model was on-line trained and the weights so obtained were then used to calculate the Jacobian of the DX A/C system. Therefore, the size of the data sets used for on-line training the ANN-based dynamic model was fixed, with the newest data sets added and the oldest removed, as follows:

$$\begin{aligned} \boldsymbol{X}(i) &= \boldsymbol{X}(i+1) \\ \boldsymbol{Y}(i) &= \boldsymbol{Y}(i+1) \end{aligned} \tag{8.4}$$

where, $i = 1, 2, \ldots (l-1)$.

$$\boldsymbol{X}(l) = [P_C, P_F]_p$$
$$\boldsymbol{Y}(l) = [T_{db}, T_{wb}]_p \tag{8.5}$$

The determination of l should be made to ensure that adequate information on the operating conditions of the DX A/C system was collected for training the ANN-based dynamic model. On the other hand, although the ANN-based dynamic model performed better with an increase in l, the time duration required for training would be longer making the control program more complicated, and the waiting period would also be longer before sufficient data could be collected for on-line training the ANN-based dynamic model, lowering the control sensitivity. Therefore, the determination of l would be influenced by these two aspects, and a trial and error method, together with the knowledge of a controlled system, should be used in deciding the value of l.

8.3 Controllability tests

During the controllability tests, the time interval between two subsequent changes in compressor and supply fan speeds (controller's outputs) was 60 s. The following four types of controllability tests were carried out:

(1) Initial start-up stage test: to simulate the condition when the system was initially started up, making sure that the indoor air temperature and humidity could return to

the setpoints within the controllable ranges by the controller, from their starting points.

(2) Command following test: when the setpoints of indoor air dry-bulb temperature and wet-bulb temperature were changed, the controller was expected to respond so that indoor air temperature and moisture content could be maintained at their respective new setpoints.

(3) Disturbance rejection test: the output variables of the DX A/C system, i.e., indoor air dry-bulb temperature and wet-bulb temperature were to be maintained at their respective setpoints when space sensible and latent cooling loads were subjected to disturbances.

(4) Command following with disturbances test: when the setpoints of indoor air dry-bulb temperature and wet-bulb temperature were changed, and space sensible and latent cooling loads were also varied after being subjected to disturbances, the indoor air dry-bulb and wet-bulb temperatures could be maintained at their respective new setpoints by the controller.

8.3.1 Initial start-up stage test (Exp. I-1)

Figure 8.3 shows the results of initial start-up stage test for the ANN-based on-line adaptive controller developed. As seen, the initial indoor air temperature settings were the same as those outdoor conditions commonly seen in summer in Hong Kong (T_{db} = 30 ºC and T_{wb} = 27 ºC, or RH = 79%). At 300 s into the test, the indoor air settings were altered to commonly adopted setpoints of indoor air conditions (T_{db} = 24 ºC and T_{wb} = 17 ºC) and the controller was immediately responded by simultaneously varying the compressor and supply fan speeds, as shown in Fig. 8.3. T_{db} and T_{wb} reached their respective new setpoints at about 2220 s into the test and were maintained steadily for the remaining 2580 s of the testing period. The fluctuations of T_{db} and T_{wb} during the 2580 s period were within 0.1 ºC and 0.15 ºC, respectively. The ANN-based on-line adaptive controller could return the indoor air dry-bulb and wet-bulb temperatures to their setpoints within the controllable range from relatively high values outside the range. The test results clearly demonstrated that the controller can well control the DX A/C system over a wide operating range.

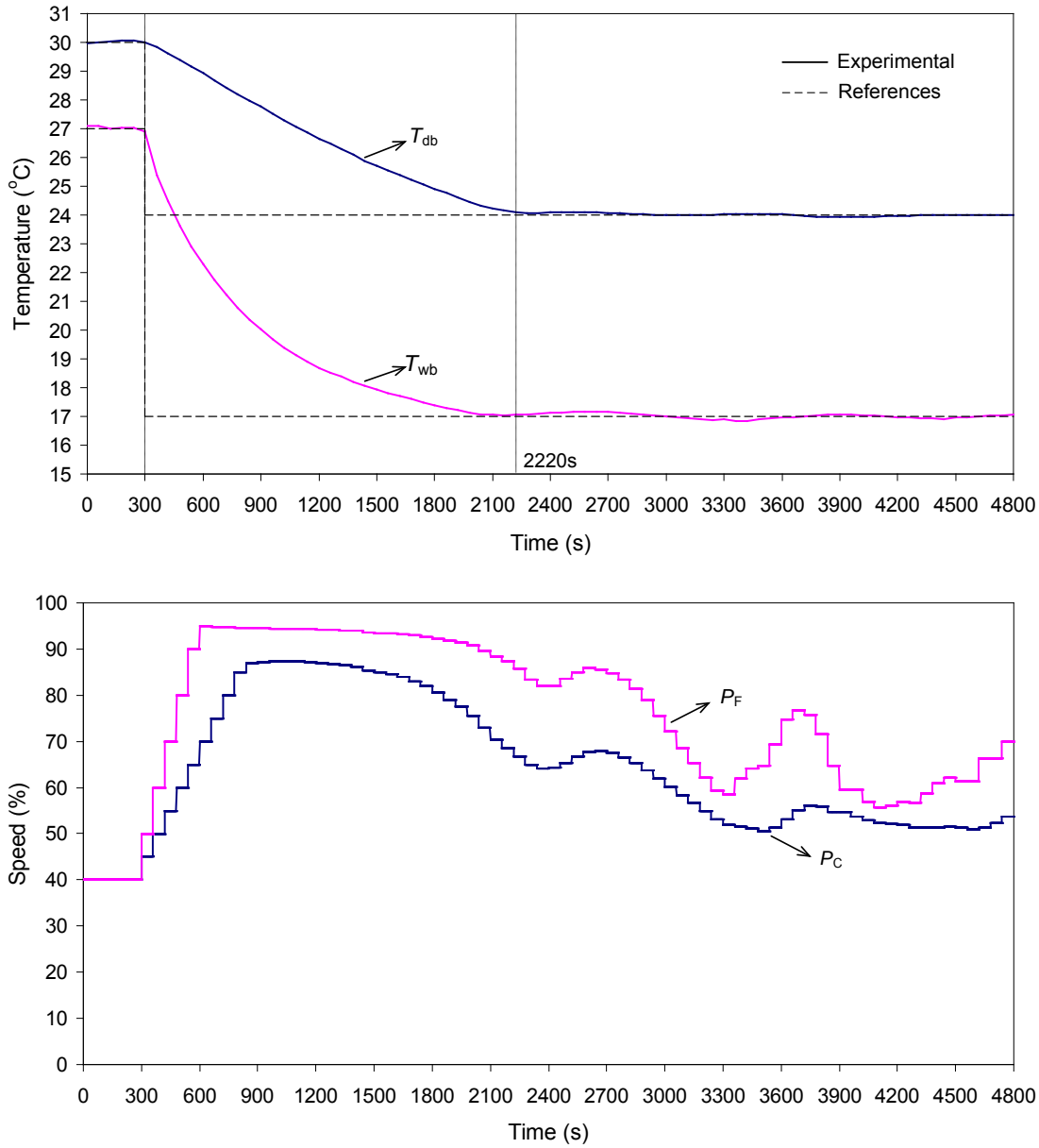

Fig. 8.3 The variations of the indoor air dry-bulb and wet-bulb temperatures and compressor and supply fan speeds in Exp. I-1

8.3.2 Command following tests (Exp. II-1, II-2 and II-3)

Figures 8.4 to 8.6 show the results of command following tests for the ANN-based on-line adaptive controller. The initial settings of indoor air conditions were T_{db} = 28 ºC and T_{wb} = 21 ºC in Exp II-1, T_{db} = 26 ºC and T_{wb} = 19 ºC in Exp II-2 and T_{db} = 21 ºC and T_{wb} = 14 ºC in Exp II-3. At 300 s into the test, the above settings were altered to T_{db} = 26 ºC and T_{wb} = 19 ºC, T_{db} = 23 ºC and T_{wb} = 16 ºC and T_{db} = 23 ºC and T_{wb} = 16 ºC, respectively, and the controller responded immediately by simultaneously varying the compressor and supply fan speeds. T_{db} and T_{wb} reached their respective new setpoints in about 1500 s, 1800 s and 3000 s, respectively, and were maintained steadily in the remaining3300 s, 3300 s and 3000 s, respectively, of the testing period. As seen in all tests, T_{db} was very stable and accurate during the steady periods, and the fluctuations of T_{wb} during the steady periods were all within 0.2 ºC. These suggested that the ANN-based on-line adaptive controller was able to track the changes in its indoor air dry-bulb temperature and wet-bulb temperature settings within their controllable ranges. Since both the ANN-based dynamic model and inverse model were on-line updated continuously, the speeds of compressor and supply fan would keep changing to deal with the disturbances even when the controlled parameters did not significantly fluctuate.

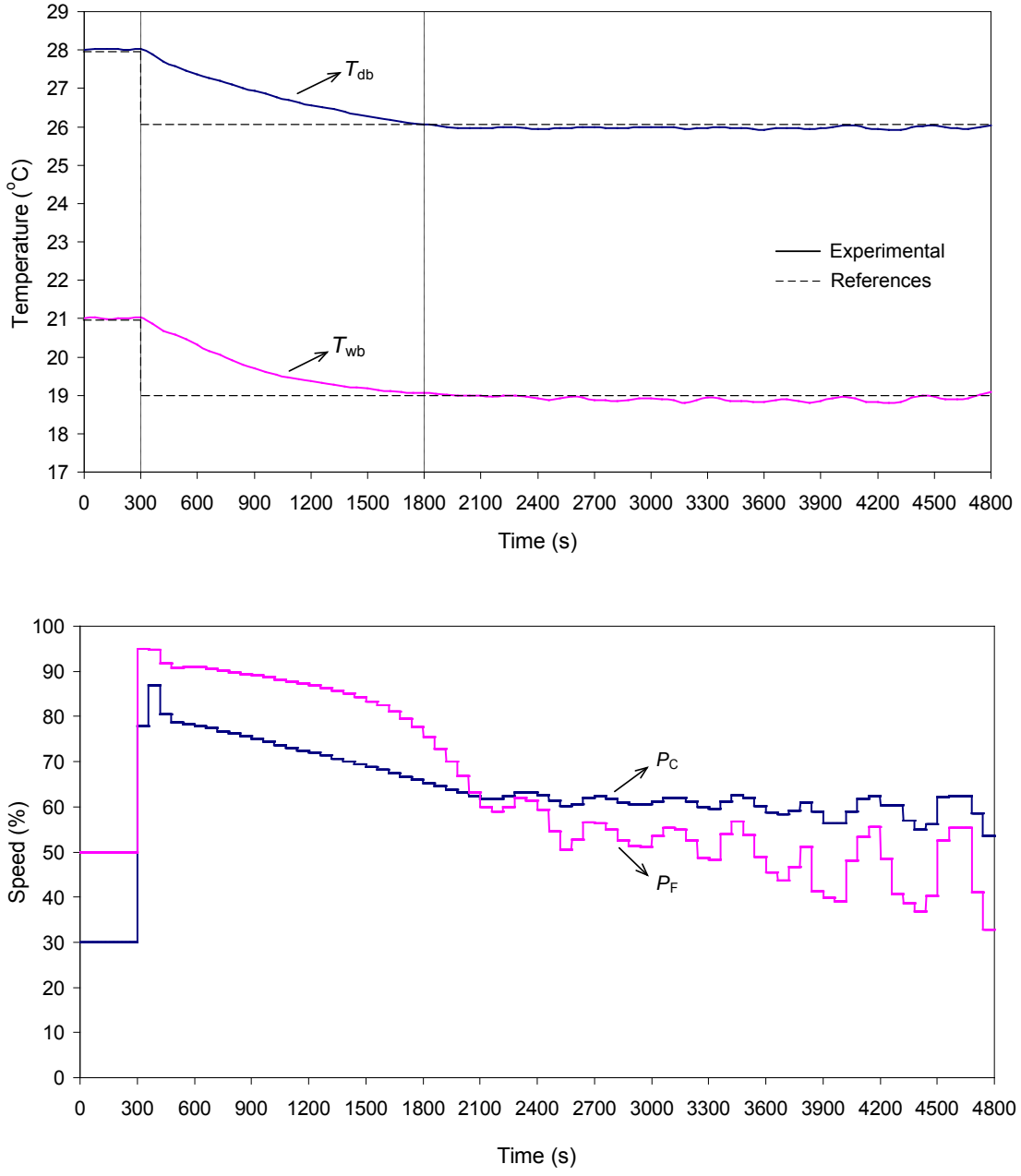

Fig. 8.4 The variations of the indoor air dry-bulb and wet-bulb temperatures and compressor and supply fan speeds in Exp. II-1

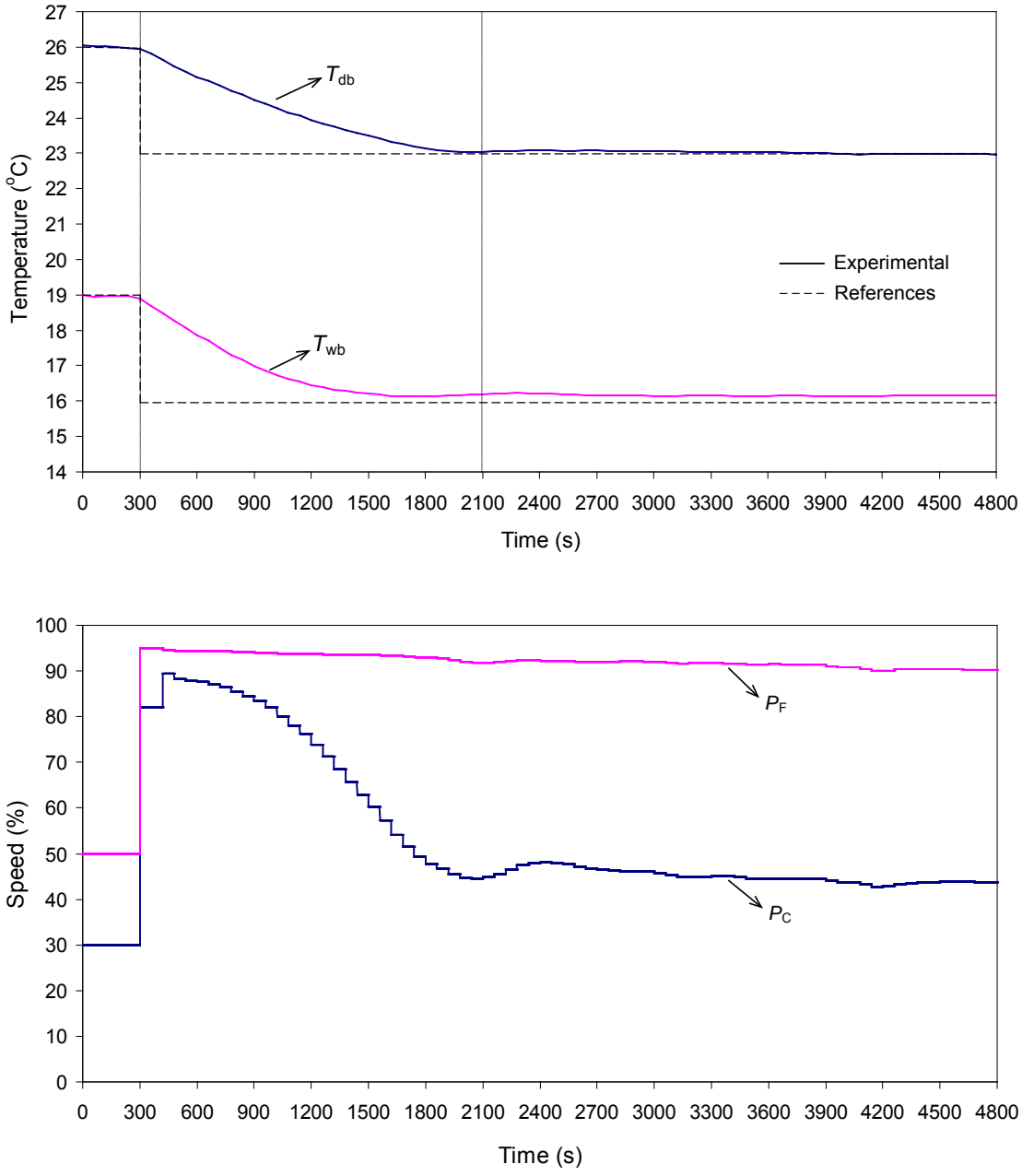

Fig. 8.5 The variations of the indoor air dry-bulb and wet-bulb temperatures and compressor and supply fan speeds in Exp. II-2

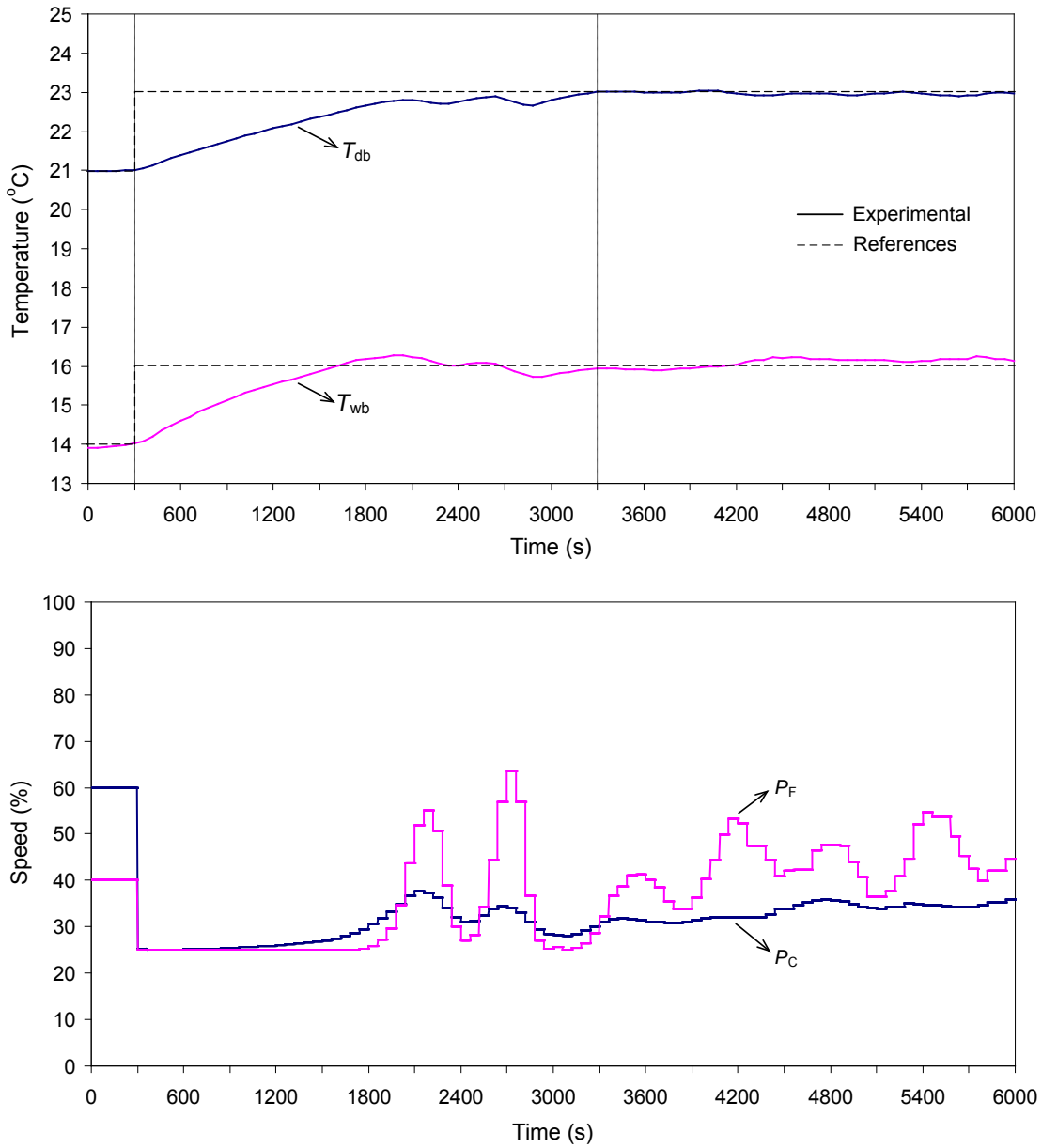

Fig. 8.6 The variations of the indoor air dry-bulb and wet-bulb temperatures and compressor and supply fan speeds in Exp. II-3

8.3.3 Disturbance rejection tests (Exp III-1 and III-2)

In these tests, the indoor air settings were T_{db} = 28 ºC and T_{wb} = 21 ºC in Exp III-1 and T_{db} = 25 ºC and T_{wb} = 18 ºC in Exp III-2, respectively. The ANN-based controller was enabled when the deviation for either the measured indoor air dry-bulb temperature or the measured indoor air wet-bulb temperature was greater than ± 0.5 ºC. Figures 8.7 and 8.8 present the results of disturbance rejection tests for the ANN-based on-line adaptive controller. As seen, prior to the introduction of disturbance at 300 s into the test, indoor air temperatures were steadily maintained at their respective setpoints. At 300 s into the test, space sensible load was reduced from 4.6 kW to 3.4 kW in Exp III-1 and 4.4 kW to 3.6 kW in Exp III-2, and space latent load from 2.5 kW to 1.9 kW in Exp III-1 and 3.4 kW to 3.0 kW in Exp III-2, respectively. In response to the disturbances, both T_{db} and T_{wb} were gradually decreased. At about 960 s into the test, when T_{db} dropped to 27.5 ºC in Exp III-1 and 24.5 ºC in Exp III-2, the controller was enabled. The variation profiles of compressor speed and supply fan speed are also shown in Figs. 8.7 and 8.8. Indoor air dry-bulb and wet-bulb temperatures went back to their respective setpoints in about 540 s in Exp III-1 and 1020 s in Exp III-2 and were maintained steadily thereafter for the rest of the test period. The fluctuations of T_{db} and T_{wb} during the steady period were both within 0.2 ºC. Therefore, the ANN-based on-line adaptive controller was able to maintain indoor air dry-bulb and wet-bulb temperatures at their respective set points after indoor thermal loads were varied, achieving a satisfactory control performance

in the disturbance rejection test.

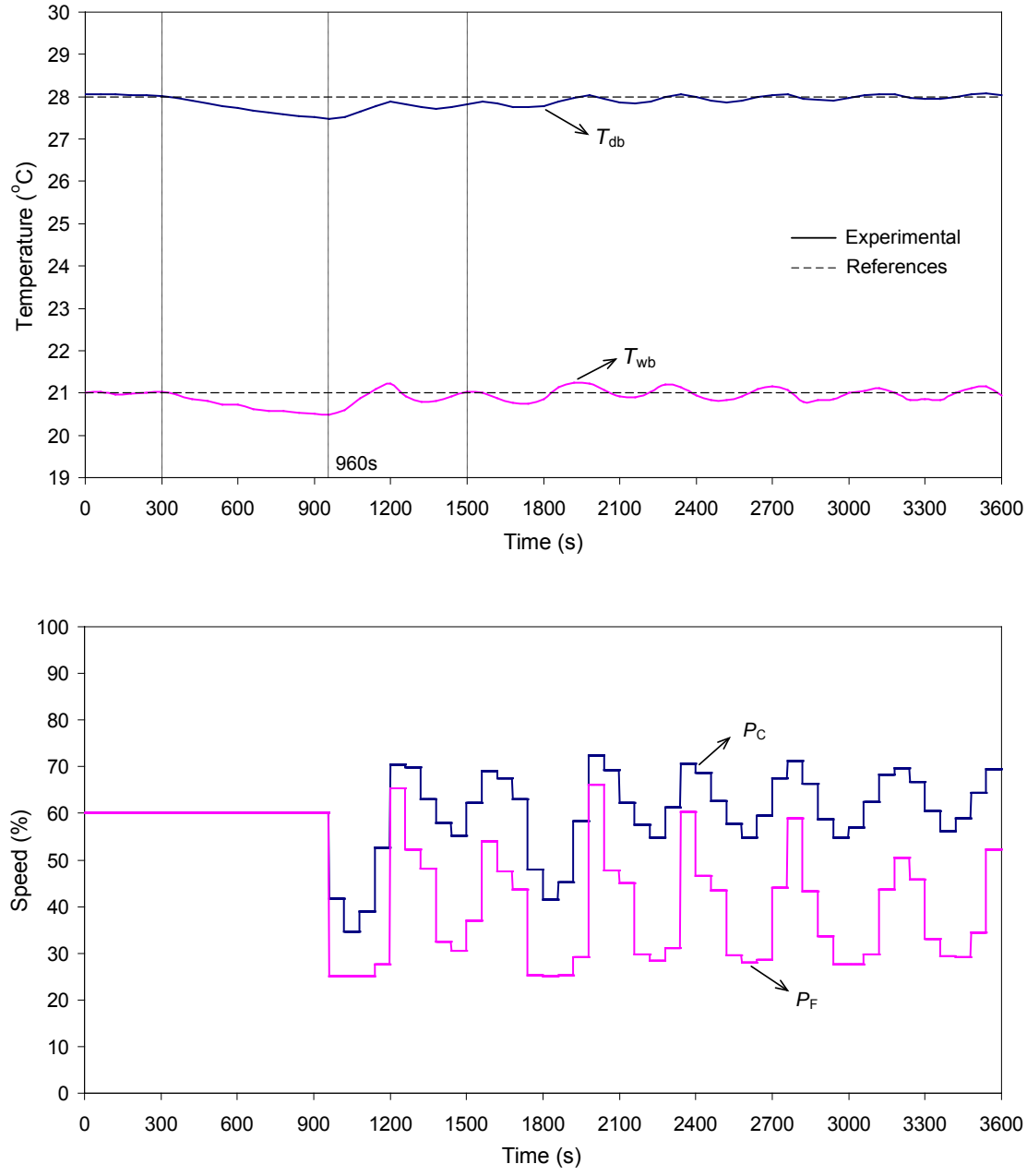

Fig. 8.7 The variations of the indoor air dry-bulb and wet-bulb temperatures and compressor and supply fan speeds in Exp. III-1

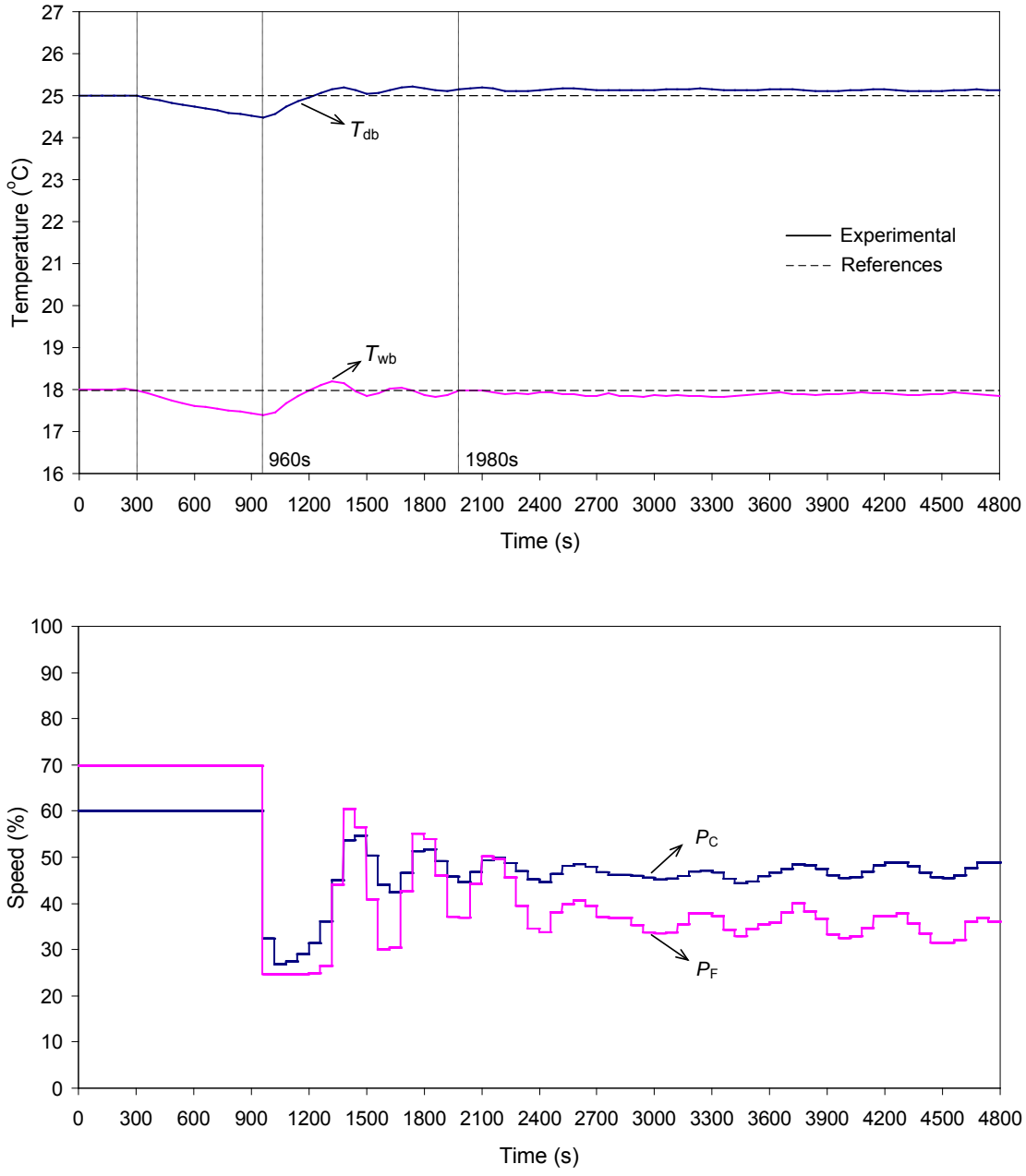

Fig. 8.8 The variations of the indoor air dry-bulb and wet-bulb temperatures and compressor and supply fan speeds in Exp. III-2

8.3.4 Command following with disturbances tests (Exp IV-1, IV-2 and IV-3)

Figures 8.9 to 8.11 show the results of command following with disturbances tests for the ANN-based on-line adaptive controller. Initially, indoor air settings were at 27 ºC dry-bulb temperature and 20 ºC wet-bulb temperature and the percentage outputs from the LGUs were 15% for sensible load and 30% for latent load, respectively, in all these three tests. At 300 s into the test, indoor air settings were changed to 25 ºC dry-bulb temperature and 18 ºC wet-bulb temperature, respectively. At the same time, the outputs of LGUs also started to vary in all the tests according to the following different patterns:

In Exp. IV-1: the outputs of LGUs were step changed from 15% to 18% for sensible load and 30% to 27% for latent load, and remained unchanged thereafter;

In Exp. IV-2: the outputs of LGUs were step changed from 15% to 12% for sensible load and 30% to 27% for latent load, as represented by the dashed lines in Fig 8.10, and then randomly varied within 3% around the dashed lines, respectively, till the end of the test, as shown in the figure;

In Exp. IV-3: the outputs of LGUs were reduced from 15% to 10% for sensible load, and 30% to 25% for latent load, at the end of the test, during which both were randomly varied within 3% around the dashed lines shown in Fig. 8.11.

As seen, after all the changes were introduced, the controller immediately responded by simultaneously varying the compressor and supply fan speeds, and T_{db} and T_{wb} reached their respective new setpoints in about 3000 s in Exp IV-1, 1620 s in Exp IV-2 and 1660 s in Exp IV-3, and were maintained steadily thereafter for the remaining test periods of 3300 s, 1980 s and 3240 s, respectively. It can be seen that the fluctuations of T_{db} and T_{wb} were all within 0.3 ºC. Therefore, the ANN-based on-line adaptive controller was able to function properly under the changes in both indoor air settings and thermal loads.

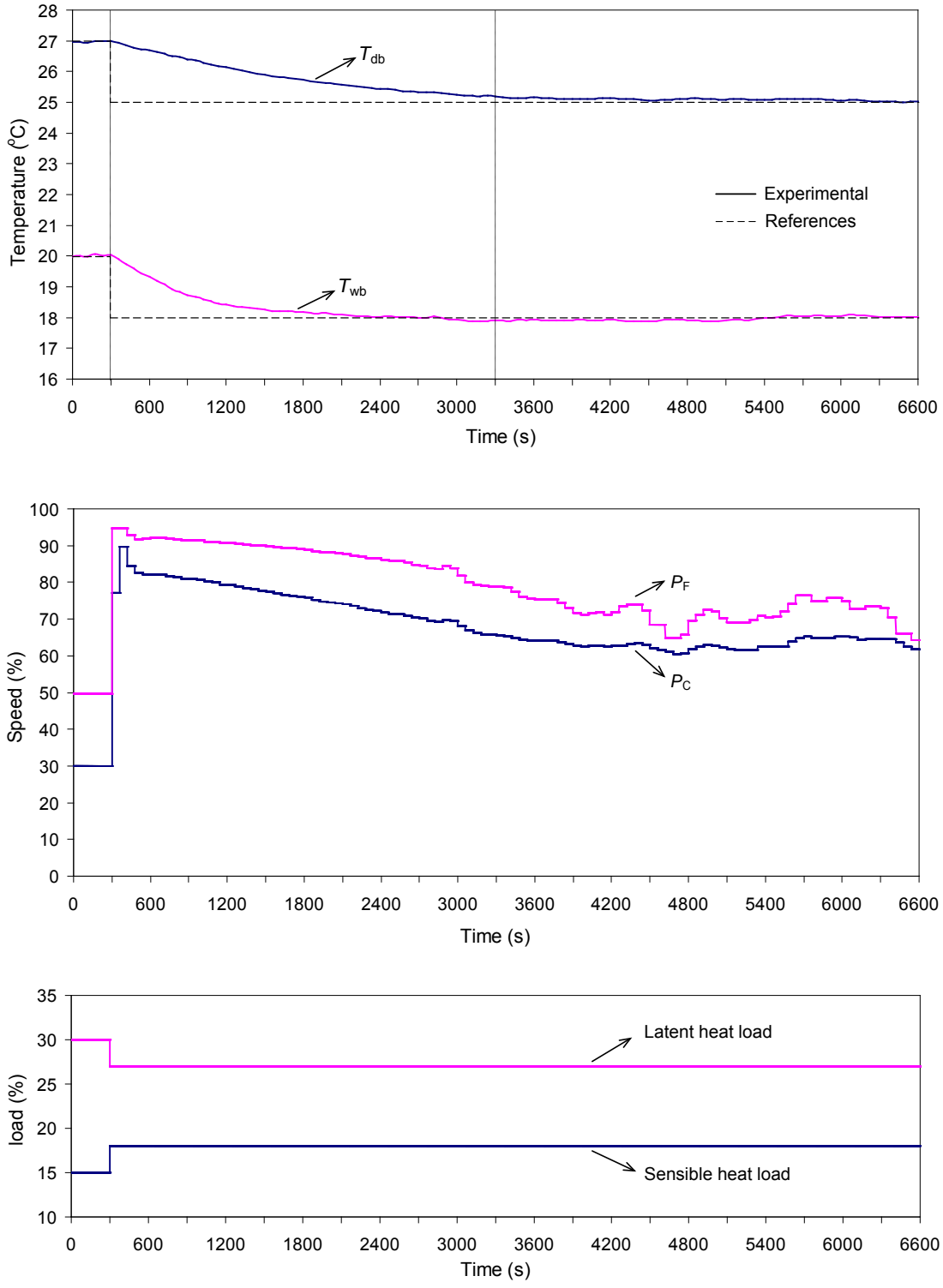

Fig. 8.9 The variations of the indoor air dry-bulb and wet-bulb temperatures, compressor and supply fan speeds and sensible and latent cooling loads in Exp. IV-1

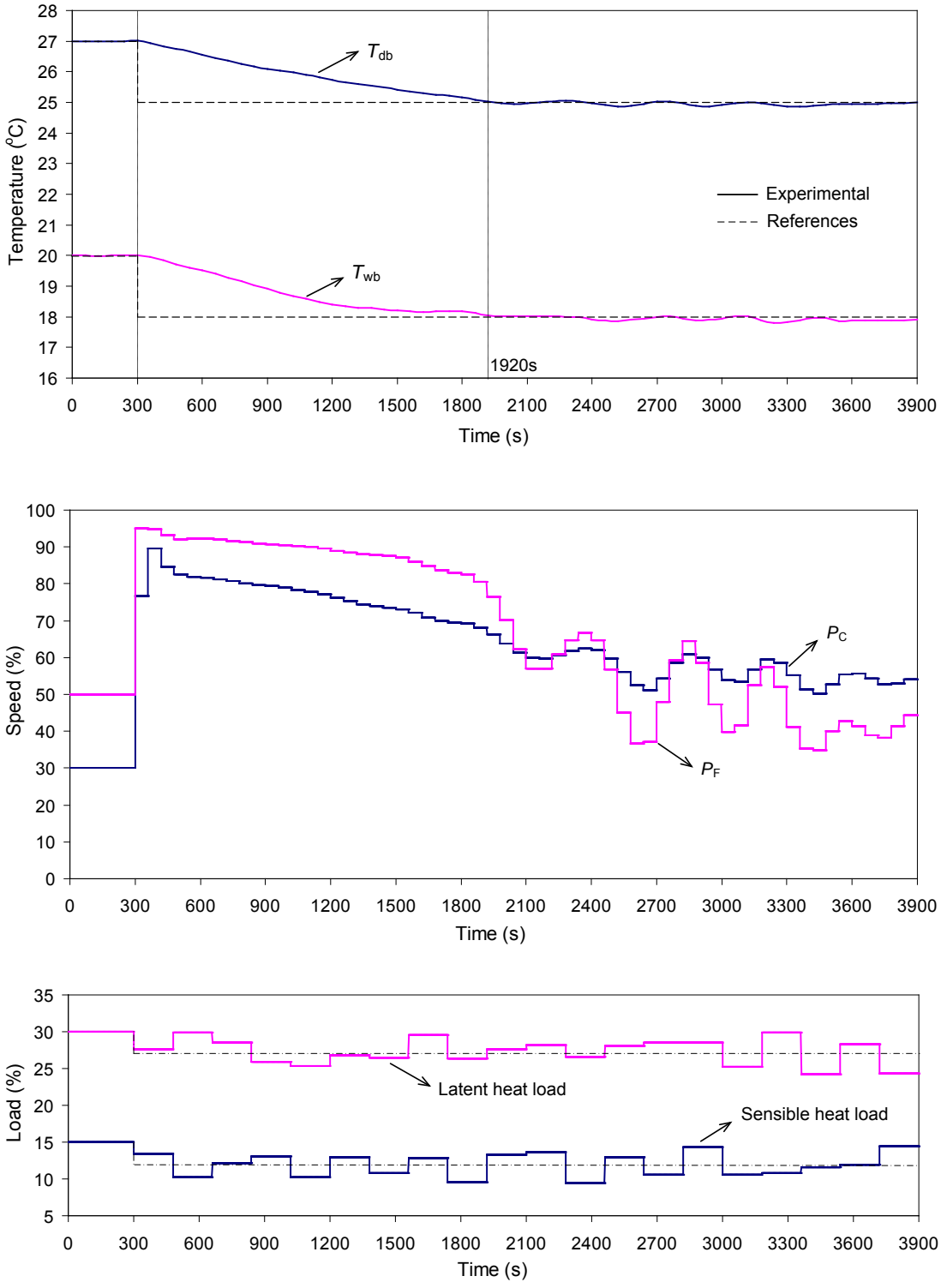

Fig. 8.10 The variations of the indoor air dry-bulb and wet-bulb temperatures, compressor and supply fan speeds and sensible and latent cooling loads in Exp. IV-2

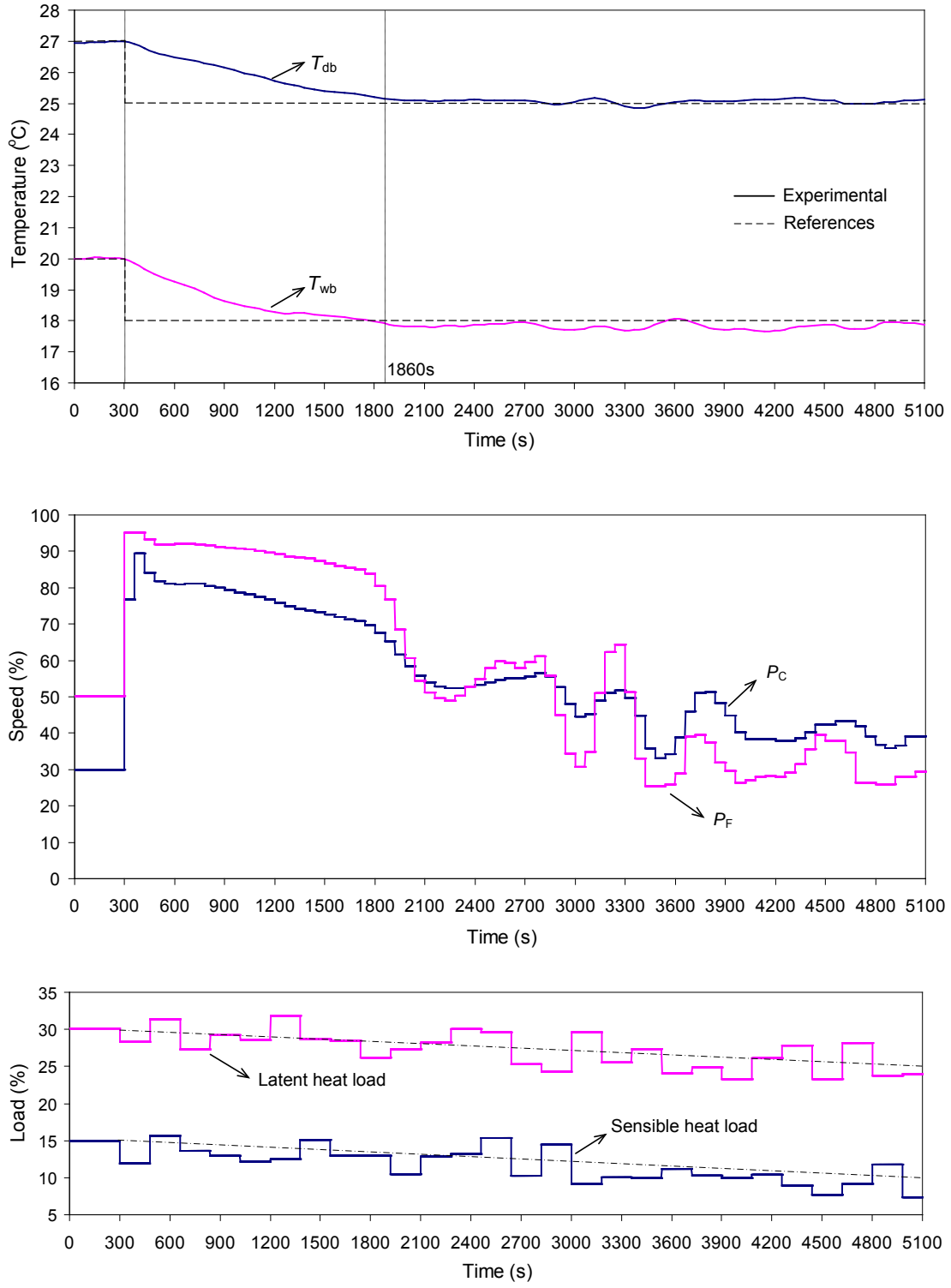

Fig. 8.11 The variations of the indoor air dry-bulb and wet-bulb temperatures, compressor and supply fan speeds and sensible and latent cooling loads in Exp. IV-3

8.4 Discussions

The feasibility of this ANN-based on-line adaptive controller has been proven through controllability tests using the experimental DX A/C system. The successful development of the ANN-based on-line adaptive controller may be attributed to the following reason.

The variations in the operating status of a DX A/C system were relatively slow because of the thermal inertia of indoor air. This allowed an ANN to have adequate time to be trained and updated for reflecting the changes in system operating status on-line using the latest operating data. Otherwise, there could be a deviation in the system operating status when the ANN training/updating was finished, leading to that the updated ANN might not be able to timely reflect the current system operating status. Therefore, it was expected that there existed a maximum rate of change in system operating status. The ANN-based on-line adaptive controller may not work properly once the rate of change was over its maximum value.

The issue of limited controllable range was encountered not only in an ANN-based control strategy, but also in all control strategies which were built based on a dynamic system model obtained through system identification. Since it was impossible to cover all possible operating conditions when carrying out system identification particularly when the system was complex, the data sets for system

identification were obtained under certain specific operating conditions. This explained why system control based on system identification would become ineffective as the operating conditions drifted away from the ones when system identification was carried out [Pintelon and Schoukens 2001]. With the successful development of the ANN-based on-line adaptive controller for the DX A/C system reported, it is believed that online adaptive control presented in this Chapter can be suitably employed to extend controllable range for all control strategies developed through system identification.

8.5 Conclusions

An ANN-based on-line adaptive controller for the DX A/C system has been developed, to address the issue of limited controllable range of a previously developed ANN-based controller for a DX A/C system, which is common to all controllers developed based on system identification. Using the experimental DX A/C system, controllability tests including the initial start-up stage test, command following test, disturbance rejection test and command following with disturbances test were carried out to examine the control performance of the ANN-based on-line adaptive controller developed. Tests results showed that the ANN-based on-line adaptive controller developed was able to control indoor air dry-bulb temperature and wet-bulb temperature both near and away from the operating condition at which the ANN-based model in the controller was initially trained, but within the entire range of operating conditions, with a high control accuracy.

Chapter 9

Conclusions and Future Work

9.1 Conclusions

A programmed research work on investigating the ANN-based modeling and control for an experimental DX A/C system having a variable speed compressor and a variable speed supply fan has been successfully carried out and is reported in this thesis. The conclusions of the thesis are as follows:

(1) A two-in two-out ANN-based steady-state model for the experimental DX A/C system has been developed using BP training algorithm linking its steady-state TCC and Equipment SHR with different combinations of its compressor and supply fan speeds at a fixed inlet air state of 24^{o}C and 50% RH, respectively. The ANN-based steady-state model has been validated experimentally by comparing the measured results of TCC and SHR at 10 additional sets of compressor speed and supply fan speed combinations using the experimental DX A/C system, with the predicted results using the ANN-based steady-state model developed. All the REs when using the developed ANN-based steady-state model for prediction were lower than 4%, with most of them being lower than 1%, suggesting the high prediction accuracy of the ANN-based model developed. Therefore, the ANN-based steady-state model for the experimental DX A/C system having multivariable inputs and multivariable outputs can be used to predict the steady-state operating performances of the DX A/C system, with a high accuracy.

(2) An ANN-based dynamic model for the experimental DX A/C system has been developed linking its output air dry-bulb temperature and wet-bulb temperature with the variation of its compressor and supply fan speeds at a fixed indoor sensible and latent load. The ANN-based dynamic model has been validated experimentally by comparing the measured results of dry-bulb and wet-bulb temperature under different variations of compressor speed and/or supply fan speed using the experimental DX A/C system, with the predicted results using the ANN-based dynamic model developed. The values of ARE and MRE when validating the ANN-based dynamic model developed under three different input patterns were 0.33%, 0.27%, 0.27% and 0.89%, 0.99%, 1.15%, respectively, suggesting the high prediction accuracy of the ANN-based dynamic model developed. The ANN-based dynamic model developed helped to better understand the dynamic operating performance of the DX A/C system and the development of an ANN-based controller for the simultaneous control of indoor air temperature and humidity.

(3) An ANN-based controller to simultaneously control the indoor air temperature and humidity in a space served by an experimental DX A/C system has been developed using the ANN-based dynamic model developed. This ANN-based controller was designed using the DIC strategy. Controllability tests including the command following test and disturbance rejection test were carried out to

examine the performance of the ANN-based controller developed. In the command following test, the indoor air dry-bulb temperature and wet-bulb temperature could be controlled to their respective new setpoints. In the disturbance rejection capability test, the results showed that the ANN-based control strategy can effectively control the indoor air dry-bulb temperature and wet-bulb temperature to their respective setpoints when there were sensible and latent load disturbances imposed. Therefore, the results of the controllability tests showed that the ANN-based controller developed could simultaneously control indoor air temperature and humidity by varying compressor speed and supply fan speed of the experimental DX A/C system with an adequate control accuracy. With the successful controller development, a possible approach of controlling a complex MIMO nonlinear dynamic system based on ANN has been illustrated.

(4) An ANN-based on-line adaptive controller for the DX A/C system has been developed to address the issue of limited controllable range of the ANN-based controller developed, which is common to all controllers developed based on system identification. Using the experimental DX A/C system, controllability tests including the initial start-up stage test, command following test, disturbance rejection test and command following with disturbances test were carried out to examine the control performance of the ANN-based on-line adaptive controller developed. Tests results showed that the ANN-based

on-line adaptive controller developed was able to control indoor air dry-bulb temperature and wet-bulb temperature both near and away from the operating condition at which the ANN-based model in the controller was initially trained, but within the entire range of operating conditions, with a high control accuracy.

The research work reported in this Thesis has made important contributions to the modeling and control of DX A/C systems. Better indoor thermal comfort for occupants, and reduced energy use can be achieved when using variable speed DX A/C systems. The ANN-based steady-state model, ANN-based dynamic model, ANN-based controller and ANN-based on-line adaptive controller developed and reported in this Thesis for the experimental DX A/C system are all the first of its kind. Furthermore, the ANN-based on-line adaptive controller developed for the DX A/C system could address the problem of limited controllable range of the ANN-based controller developed, which is common to controllers developed based on system identification. The long-term significance of the research work is that it will encourage a wider application of A/C systems to better control indoor thermal environment, leading to a better indoor thermal comfort and more energy saving.

9.2 Proposed future work

A number of future studies following on the successful completion of the research work reported in this thesis are proposed as follows:

Firstly, future studies may be directed to improving indoor thermal comfort using a DX A/C system. In this thesis, the controlled variables were the indoor air temperature and humidity. Although indoor air temperature and humidity are greatly important to indoor thermal comfort, it would not be enough as far as indoor thermal comfort is concerned, as comfort is a cognitive process influenced by different kinds of processes, such as physical, physiological or even psychological aspects [ASHRAE 2005]. Conventionally, thermal comfort indices are widely used to reflect the level of indoor thermal comfort, such as PMV, which is affected by six parameters, including four environmental and two personal. Therefore, when it intends to control a DX A/C system directly based on PMV, the number of controlled variables of a new ANN-based controller will be changed from the current two to six.

The concept of PMV based on a homogeneous whole volume thermal environment was used in the conventional comfort theory, which is somehow outdated. In recent years, the research into non-uniform thermal environment has been prevailing and fruitful. One of the significant research outcomes is ASHRAE 55-2010, which allows elevated air movement to broadly offset the need to cool the air in warm conditions for energy saving.

One way of improving indoor thermal comfort is to account for the thermal sensation of specific occupants. Thermal comfort is based on human response to a thermal environment, and those thermal comfort indices may just be statistically meaningful. Therefore, including the thermal sensations of occupants as part of controllers' profile can be interesting. A similar idea was implemented by Federspiel and Asada [1994] in their user adaptable comfort controller, in which the parameters of a thermal sensation prediction model could be adjusted with respect to the actual thermal sensation of a specific occupant. Liang and Du [2008] also developed a user adaptable controller, in which three types of user commands were considered: on/off, cooler and warmer, so that the thermal sensations of a specific user could influence system control. With regard to the developed ANN-based controller reported in this thesis, users' sensations could be used to adjust the weights of an ANN, so that the controller could predict the actual comfort conditions and help achieve a more effective and intelligent control.

Secondly, as reported in this thesis, the purpose of the ANN-based controller developed was to simultaneously control the indoor air temperature and humidity by varying the compressor speed and supply fan speed. However, the energy consumption of the DX A/C system under control was not yet considered. Therefore, a further development to ANN-based controller for the DX A/C system is to maximize system's operating efficiency in terms of coefficient of performance (COP).

Thirdly, using the ANN-based controller developed through varying compressor speed and supply fan speed in the DX A/C system, indoor air temperature and

humidity may be controlled to their respective setpoints. However, the fluctuation of operating degree of superheat (DS), which was controlled by a built-in conventional PID controller, can be observed from the experimental data while varying compressor speed and supply fan speed. The PID controller would not respond to take control actions until it received the feedback information of the change in DS, so that EEV's opening can be correspondingly adjusted. However, such a feedback process would take time before the opening of the EEV can be regulated in order to return the DS to its setpoint. To solve this problem, Qi et al. [2010] developed a new DS controller in which the information of the changes in both compressor speed and supply fan speed were used for predicting the changes in DS, thus appropriate control actions by the EEV may be timely taken. Therefore, such a DS controller may be integrated into the ANN-based controller to obtain a modified ANN-based controller to simultaneously control indoor air temperature, humidity and DS by varying the compressor speed, supply fan speed and EEV's opening.

Finally, the principle of this ANN-based control strategy could be implemented in other thermal engineering systems, to demonstrate its applicability to different thermal systems. Further development work in this aspect should be carried out.

Appendix A

Photos of the Experimental DX A/C system

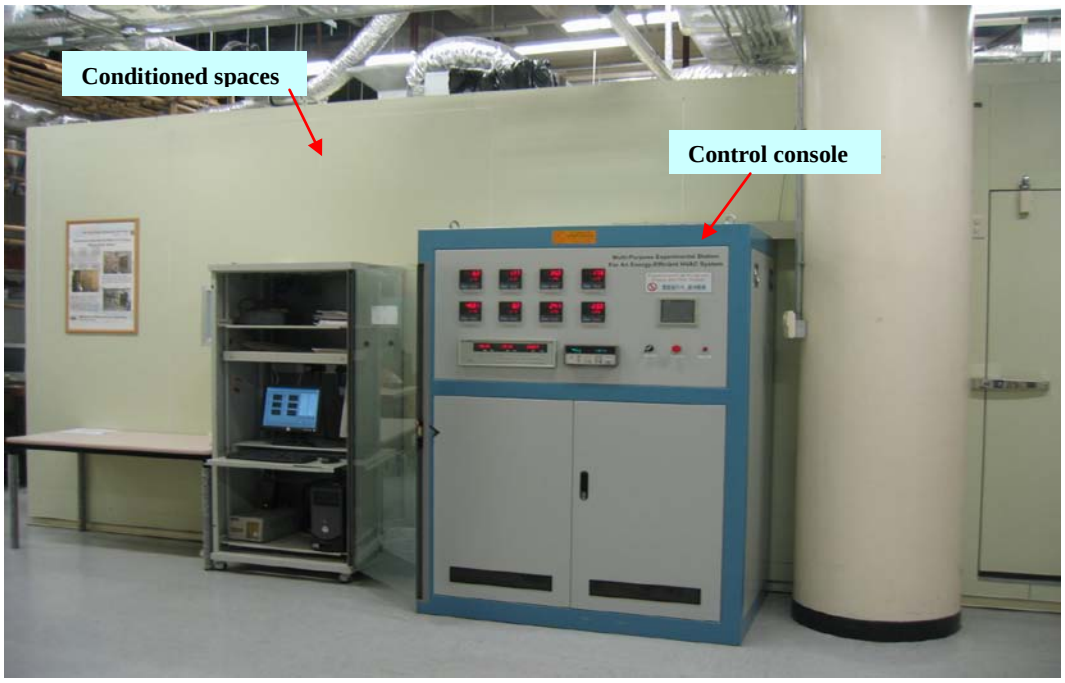

Photo 1 Overview of the experimental rig (1)

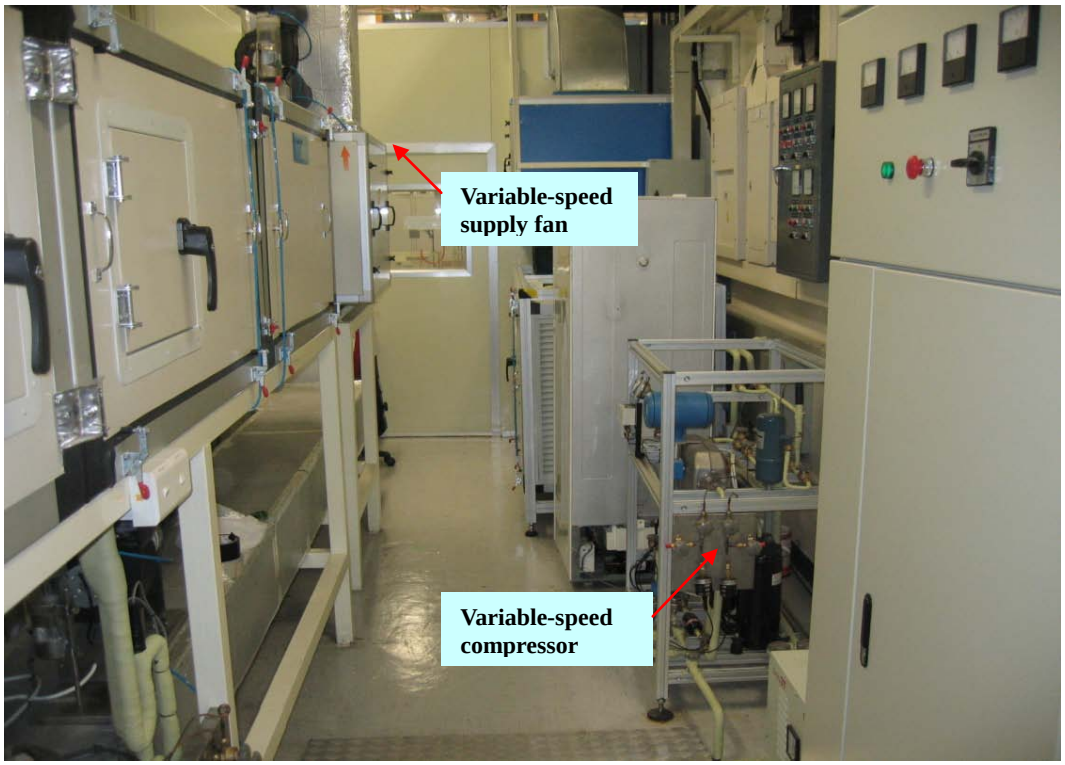

Photo 2 Overview of the experimental rig (2)

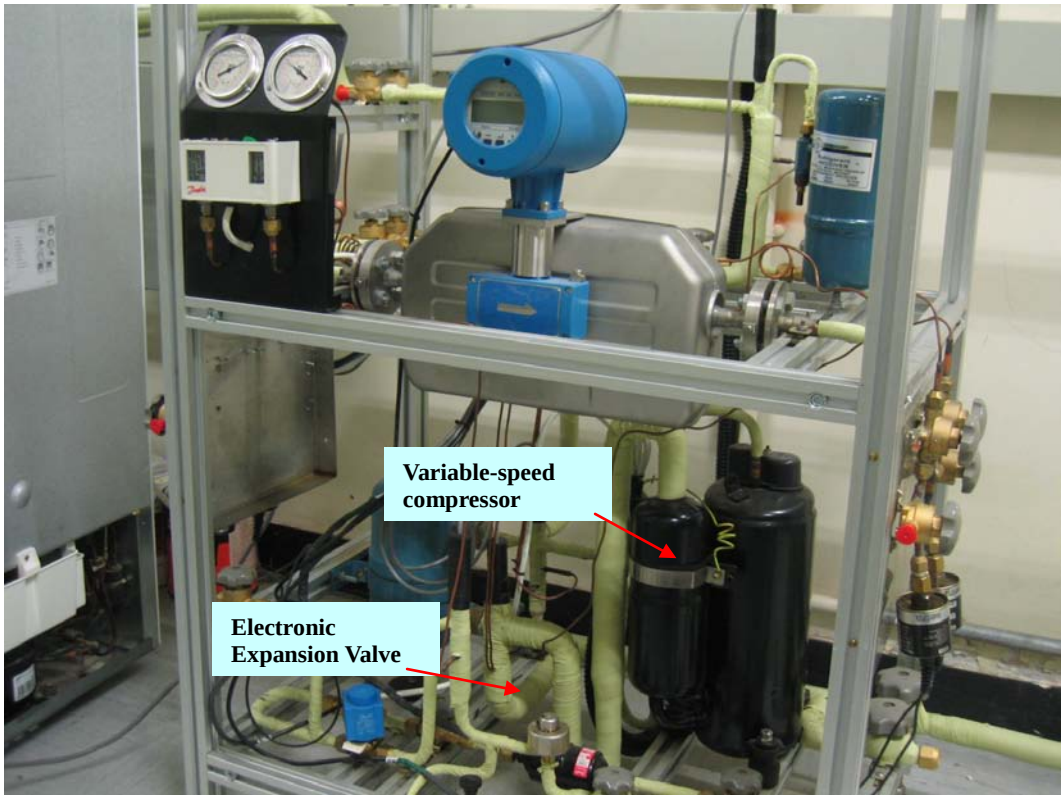

Photo 3 Variable-speed compressor in the DX A/C system

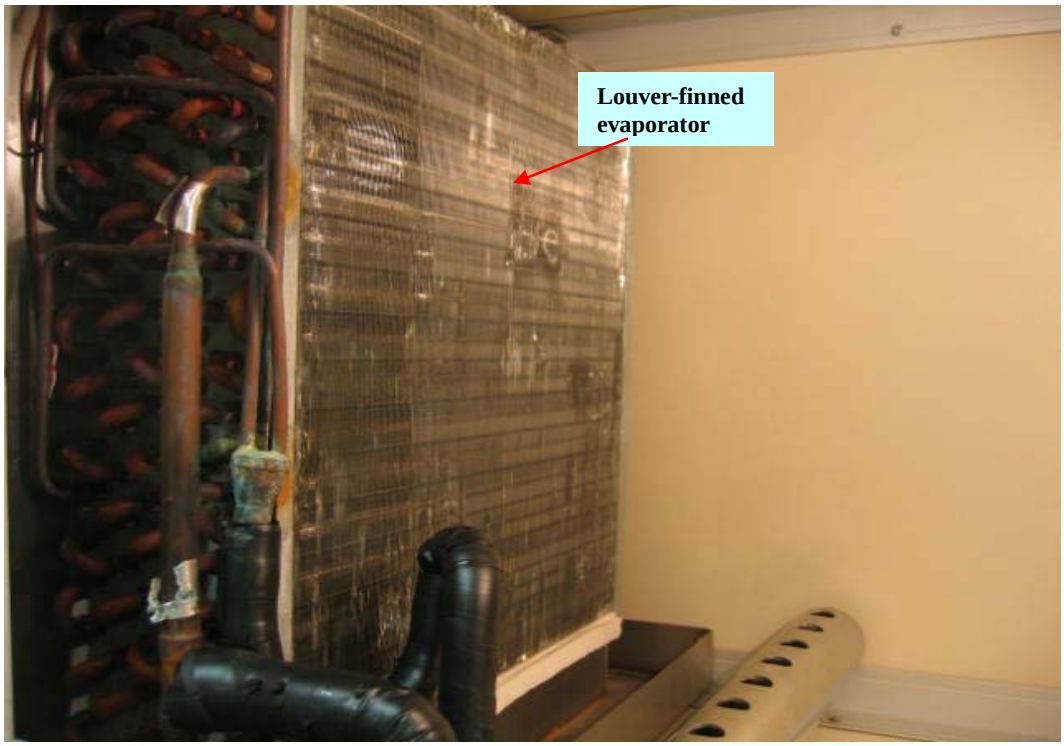

Photo 4 DX cooling coil in the DX A/C system

Photo 5　Load generation units inside conditioned space

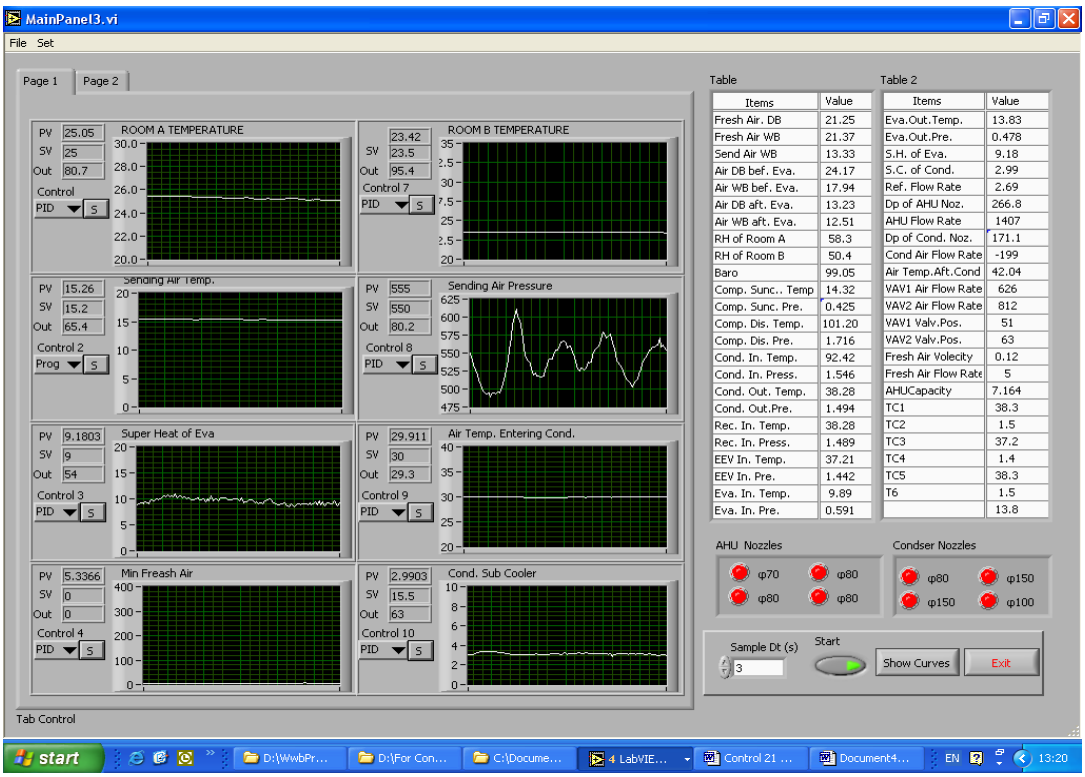

Photo 6　Logging & control supervisory program

References

1 Abbassi and Bahar 2005
Abbassi, A. and Bahar, L.
Application of neural network for the modeling and control of evaporative condenser cooling load. *Applied Thermal Engineering*, Vol. 25, No. 17-18, pp. 3176-3186 (2005)

2 Aggelogiannaki et al. 2007
Aggelogiannaki, E., Sarimveis, H. and Koubogiannis, D.
Model predictive temperature control in long ducts by means of a neural network approximation tool. *Applied Thermal Engineering*, Vol. 27, No. 14-15, pp. 2363-2369 (2007)

3 Ahmad and Zhang 2009
Ahmad, Z. and Zhang, J.
Selective combination of multiple neural networks for improving model prediction in nonlinear systems modelling through forward selection and backward elimination. *Neurocomputing*, Vol.72, pp. 1198-204 (2009)

4 Amaral and Ottino 2004
Amaral, L.A.N. and Ottino, J.M.
Complex systems and networks: challenges and opportunities for chemical and biological engineers. *Chemical Engineering Science*, Vol. 59, pp. 1653-1666. (2004)

5 Amrane et al. 2003
Amrane, K., Hourahan, G.C. and Potts, G.
Latent performance of unitary equipment. *ASHRAE Journal*, Vol. 45, No. 1, pp. 28-31 (2003)

6 Anderson et al. 1997
Anderson, C.W., Hittle, D.C., Katz, A.D. and Kretchmar, R.M.
Synthesis of reinforcement learning, neural networks and PI control applied to a simulated heating coil. *Artificial Intelligence in Engineering*, Vol. 11, No. 4, pp. 421-429 (1997)

7 Andrade et al. 2002
Andrade, M.A., Bullard, C.W., Hancock, S. and Lubliner, M.
Modulating blower and compressor capacities for efficient comfort control. *ASHRAE Transactions*, Vol. 108, Part. 1, pp. 631-637 (2002)

8 Angeline et al. 1994
Angeline, P.J., Saunder, G.M. and Pollack, J.B.
Complete introduction of recurrent neural networks. Proceedings of the Third Annual Conference on Evolutionary Programming, Sebald A.V. and Fogel L.J. eds., *World Scientific*, Singapore, pp. 1-8, (1994)

9 Ao and Palade 2011
Ao, S.I. and Palade, V.
Ensemble of Elman neural networks and support vector machines for reverse engineering of gene regulatory networks. *Applied Soft Computing*, Vol. 11, No. 2, pp. 1718-1726 (2011)

10 Arcaklioglu et al. 2004
Arcaklioglu, E., Cavusoglu, A. and Erisen, A.
Thermodynamic analyses of refrigerant mixtures using artificial neural networks. *Applied Energy*, Vol. 78, No. 2, pp. 219-230 (2004)

11 Arens and Baughman 1996
Arens, E.A. and Baughman, A.V.
Indoor humidity and human health: part II-buildings and their systems. *ASHRAE Transactions*, Vol. 102, No. 1, pp. 212-221 (1996)

12 Argiriou et al. 2000
Argiriou, A.A., Bellas-Velidis, I. and Balaras, C.A.
Development of a neural network heating controller for solar buildings. *Neural Networks*, Vol. 13, pp. 811-820 (2000)

13 Argiriou et al. 2004
Argiriou, A.A., Bellas-Velidis, I., Kummert. M. and Andre, P.
A neural network controller for hydronic heating systems of solar buildings. *Neural Networks*, Vol. 17, pp. 427-440 (2004)

14 Asensio-Cuesta et al. 2010
Asensio-Cuesta, S., Diego-Mas, J.A. and Alcaide-Marzal, J.
Applying generalised feedforward neural networks to classifying industrial jobs in terms of risk of low back disorders. International Journal of Industrial Ergonomics, Vol. 40, pp. 629-635 (2010)

15 ASHRAE 2000
ASHRAE
Handbook-HVAC Systems and Equipment (2000)

16 ASHRAE 2005
ASHRAE
ASHRAE Handbook - Fundamentals, Refrigerating American Society of Heating and Air-Conditioning Engineers (2005)

17 Atik et al. 2010
Atik, K., Aktas, A. and Deniz, E.
Performance parameters estimation of MAC by using artificial neural network. *Expert Systems with Applications*, Vol. 37, No. 7, pp. 5436-5442 (2010)

18 Atthajariyakul and Leephakpreeda 2005
Atthajariyakul, S. and Leephakpreeda, T.
Neural computing thermal comfort index for HVAC systems. *Energy Conversion and Management*, Vol. 46, No. 15-16, pp. 2553-2565 (2005)

19 Bao et al. 2006
Bao, C., Ouyang, M. and Yi, B.
Modeling and optimization of the air system in polymer exchange membrane fuel cell system. *Journal of Power Sources*, Vol. 156, No. 2, pp. 232-243 (2006)

20 Barringer and McGugan 1989
Barringer, C.G. and McGugan, C.A.
Development of a dynamic model for simulating indoor air temperature and humidity. *ASHRAE Transactions*, Vol. 95, Part. 2, pp. 449-460 (1989)

21 Bacthler et al. 2001
Bacthler, H., Browne, M.W., Bansal, P.K. and Kecman, V.
Neural-networks – A new approach to model vapour compression heat pumps. *International Journal of Energy Research*, Vol. 25, pp. 591-599 (2001)

22 Becerikli et al. 2003
Becerikli, Y., Konar, A.F. and Samad, T.
Intelligent optimal control with dynamic neural networks. *Neural Networks*, Vol. 16, No. 2, pp. 251-259 (2003)

23 Bechtler et al. 2001
Bechtler, H., Browne, M.W., Bansal, P.K. and Kecman, V.
New approach to dynamic modelling of vapour-compression liquid chillers: artificial neural networks. *Applied Thermal Engineering*, Vol. 21, No. 9, pp. 941-953 (2001)

24 Ben-Nakhi and Mahmoud 2002
Ben-Nakhi, A.E. and Mahmoud, M.A.
Energy conservation in buildings through efficient A/C control using neural networks. *Applied Energy*, Vol. 73, No. 1, pp. 5-23 (2002)

25 Berbari 1998
Berbari, G. J.
Fresh air treatment in hot and humid climates. *ASHRAE Journal*, Vol. 40, No. 10, pp. 64-70 (1998)

26 Berglund 1998
Berglund, L.G.
Comfort and humidity. *ASHRAE Journal*, Vol. 40, No. 8, pp. 35-41 (1998)

27 Blunier et al. 2009
Blunier, B., Cirrincione, G., Herve, Y. and Miraoui, A.
A new analytical and dynamical model of a scroll compressor with experimental validation.*International Journal of Refrigeration*, Vol. 32, No. 5, pp. 874-891 (2009)

28 Bordick and Gilbride 2002
Bordick, J. and Gilbride, T.L.
Focusing on buyer's needs: DOE's engineering technology programme. *Energy Engineering*, Vol. 99, No. 6, pp. 18-38 (2002)

29 Brandemuehl and Katejanekarn 2004
Brandemuehl, M.J. and Katejanekarn, T.
Dehumidification characteristics of commercial building applications. *ASHRAE Transactions*, Vol. 114, Part. 2, pp. 65-76 (2004)

30 Broomhead and Lowe 1988
Broomhead, D.S. and Lowe, D.
Multivariable functional interpolation and adaptive networks. *Complex system*, Vol. 2, pp. 321-355 (1988)

31 Carrado and Mazza 1991
Carrado, V. and Mazza, A.
Axial fan. IEA Annex 17 Report, Politecnico di Torino, Italy (1991)

32 Cavallini et al. 1996
Cavallini, A., Doretti, L., Longo, G.A., Rossetto, L., Bella, B. and Zannerio, A.
Thermal analysis of a hermetic reciprocating compressor. *International Compressor Engineering Conference*, Purdue University, USA, 1996

33 Chang 2007
Chang, Y.C.
Sequencing of chillers by estimating chiller power consumption using artificial neural networks. *Building and Environment*, Vol. 42, No. 1, pp. 180-188 (2007)

34 Chang and Chen 2009
Chang, Y.C. and Chen, W.H.
Optimal chilled water temperature calculation of multiple chiller systems using Hopfield neural network for saving energy. *Energy*, Vol. 34, No. 4, pp. 448-456 (2009)

35 Chen and Deng 2006
Chen, W. and Deng, S.M.
Development of a dynamic model for a DX VAV air conditioning system. *Energy Conversion and Management*, Vol. 47, No. 18-19, pp. 2900-2924 (2006)

36 Chen et al. 2002a
Chen, Y., Halm, N.P., Groll, E.A. and Braun, J.E.
Mathematical modeling of scroll compressors. Part I: compression process modeling. *International Journal of Refrigeration*, Vol. 25, pp.731-750(2002).

37 Chen et al. 2002b
Chen, Y., Halm, N.P., Groll, E.A. and Braun, J.E.
Mathematical modeling of scroll compressors. Part II: overall scroll compressor modeling, *International Journal of Refrigeration*, Vol. 25, pp. 751-764 (2002).

38 Chow et al. 2002
Chow, T.T., Zhang, G.Q., Lin, Z. and Song, C.L.
Global optimization of absorption chiller system by genetic algorithm and neural network. *Energy and Buildings*, Vol. 34, No. 1, pp. 103-109 (2002)

39 Chua et al. 2007
Chua, K.J., Ho, J.C. and Chou, S.K.
A comparative study of different control strategies for indoor air humidity. *Energy and Buildings*, Vol. 39, pp. 537-545 (2007)

40 Chuah et al. 1998
Chuah, Y.K., Hung, C.C. and Tseng, P.C.
Experiments on the dehumidification performance of a finned tube heat exchanger. *HVAC&R Research*, Vol. 4, No. 2, pp. 167-178 (1998)

41 Cortes et al. 2009
Cortes, O., Urquiza, G. and Hernandez, J.A.
Optimization of operating conditions for compressor performance by means of neural network inverse. *Applied Energy*, Vol. 86, No. 11, pp. 2487-2493 (2009)

42 Damasceno and Rooke 1990
Damasceno, G. S. and Rooke, S. P.
Comparison of three steady-state heat pump computer models. *ASHRAE Transaction*, Vol. 96, part 2, pp. 191-204 (1990)

43 Daosud et al. 2005
Daosud, W., Thitiyasook, P., Arpornwichanop, A., Kittisupakorn, P. and Hussain, M.A.
Neural network inverse model-based controller for the control of a steel pickling process. *Computers & Chemical Engineering*, Vol. 29, No. 10, pp. 2110-2119 (2005)

44 Deng 2000
Deng, S. M.
A dynamic mathematical model of a direct expansion (DX) water-cooled air conditioning plant. *Building and Environment*, Vol. 35, No. 7, pp. 603-613 (2000)

45 Deng et al. 2009
Deng, H., Xu, Z. and Li, H.X.
A novel neural internal model control for multi-input multi-output nonlinear discrete-time processes. *Journal of Process Control*, Vol. 19, No. 8, pp. 1392-1400 (2009)

46 Diaz et al. 1996
Diaz, G., Yanes, J., Sen, M., Yang, K.T. and McClain, R.L.
Analysis of data from single-row heat exchanger experiments using an artificial neural network. *Proceedings of the ASME Fluids Engineering Division FED-242*, pp. 45-52 (1996)

47 Diaz et al. 1999
Diaz, G., Sen, M., Yang, K.T. and McClain, R.L.
Simulation of Heat Exchanger Performance by Artificial Neural Networks. *HVAC&R Research*, Vol. 5, No. 3, pp. 195-208 (1999)

48 Diaz et al. 2001a
Diaz, G., Sen, M., Yang, K.T. and McClain, R.T.
Dynamic prediction and control of heat exchangers using artificial neural networks. *International Journal of Heat Mass Transfer*, Vol. 45, pp. 1671-1679 (2001)

49 Diaz et al. 2001b
Diaz, G., Sen, M., Yang, K.T. and McClain, R.T.
Adaptive neuro-control of heat exchangers. *ASME Journal of Heat Transfer*, Vol. 123, pp. 417-612 (2001)

50 Diaz et al. 2004
Diaz, G., Sen, M., Yang, K.T. and McClain, R.L.
Stabilization of thermal neurocontrollers. *Applied Artificial Intelligence*, Vol. 18, No. 5, pp. 447-466 (2004)

51 Ding et al. 2002
Ding, G.L., Zhang, C.L. and Liu, H.
A fast simulation model combining with artificial neural networks for fin-and-tube condenser. *Heat Transfer - Asian Research*, Vol. 31, No. 7, pp. 551-557 (2002)

52 Ding et al. 2004
Ding, G.L., Zhang, C.L. and Zhan, T.
An approximate integral model with an artificial neural network for heat exchangers. *Heat Transfer-Asia Research*, Vol. 33, No. 3, pp. 153-160 (2004)

53 Egilegor et al. 1997
Egilegor, B., Uribe, J.P., Arregi, G., Pradilla, E. and Susperregi, L.
A fuzzy control adapted by a neural network to maintain a dwelling within thermal comfort. *Proceedings of Building Simulation* 97, Vol. II, pp 87-94 (1997)

54 Ekici and Aksoy 2009
Ekici, B.B. and Aksoy, U.T.
Prediction of building energy consumption by using artificial neural networks. *Advances in Engineering Software*, Vol. 40, No. 5, pp. 356-362 (2009)

55 Ekren et al. 2010
Ekren, O., Sahin, S. and Isler, Y.
Comparison of different controllers for variable speed compressor and electronic expansion valve. *International Journal of Refrigeration*, Vol. 33, No. 6, pp. 1161-1168 (2010)

56 Ertunc and Hosoz 2006
Ertunc, H.M. and Hosoz, M.
Artificial neural network analysis of a refrigeration system with an evaporative condenser. *Applied Thermal Engineering*, Vol. 26, pp. 627-635 (2006)

57 Ertunc and Hosoz 2008
Ertunc, H.M. and Hosoz, M.
Comparative analysis of an evaporative condenser using artificial neural network and adaptive neuro-fuzzy inference system. *International Journal of Refrigeration*, Vol. 31, pp. 1426-1436 (2008)

58 Escriva-Escriva et al. 2011
Escriva-Escriva, G., Alvarez-Bel, C., Roldan-Blay, C. and Alcazar-Ortega, M.
New artificial neural network prediction method for electrical consumption forecasting based on building end-uses. *Energy and Buildings*, Vol. 43, No. 11, pp. 3112-3119 (2011)

59 Esen and Inalli 2009
Esen, H. and Inalli, M.
Modelling of a vertical ground coupled heat pump system by using artificial neural networks. *Expert Systems with Applications*. Vol. 36, pp. 10229-11038 (2009)

60 Esen et al. 2008a
Esen, H., Inalli, M., Sengur, A. and Esen, M.
Performance prediction of a ground coupled heat pump system using artificial neural networks. *Expert Systems with Applications*, Vol. 35, pp. 1940-1948 (2008)

61 Esen et al. 2008b
Esen, H., Inalli, M., Sengur, A. and Esen, M.
Forecasting of a ground-coupled heat pump performance using neural networks with statistical data weighting preprocessing. *International Journal of Thermal Sciences*, Vol. 47, pp. 431-441 (2008)

62 Esen et al. 2008c
Esen, H., Inalli, M., Sengur, A. and Esen, M.
Artificial neural networks and adaptive neuro-fuzzy assessments for ground-coupled heat pump system. *Energy and Buildings*, Vol. 40, pp. 1074-1083 (2008)

63 Fahlman and Lebiere 1990
Fahlman, S.E. and Lebiere, C.
The cascade-correlation learning architecture. Advances in Neural Information Processing System 2, D. Touretzky (eds), Morgan Kaufmann, San Mateo, CA, pp. 534-542, 1990

64 Fanger 2001
Fanger, P.O.
Human requirements in future air-conditioned environments. *International Journal of Refrigeration*, Vol. 24, pp. 148-153 (2001)

65 Fargus and Chapman 1998
Fargus, R.S. and Chapman, C.
Commercial PI-neural controller for the control of building services plant. *IEE Conference Publication*, Vol. 455, No. 2, pp. 1688-1693, Stevenage, England (1998)

66 Federspiel and Asada 1994
Federspiel, C.C. and Asada, H.
User-Adaptable Comfort Control for HVAC Systems. *Journal of Dynamic Systems, Measurement and Control*, Vol. 116, No. 3, pp. 474-486 (1994)

67 Friedrich et al. 2008
Friedrich, M., Fankhauser, M., Oyeyemi, E. and McKinnell, L.A.
A neural network-based ionospheric model for Arecibo. *Advances in Space Research*, Vol. 42, No. 4, pp. 776-781 (2008)

68 Galindo et al. 2008
Galindo, J., Serrano, J.R., Climent, H. and Tiseira, A.
Experiments and modelling of surge in small centrifugal compressor for automotive engines. *Experimental Thermal and Fluid Science*, Vol. 32, No. 3, pp. 818-826 (2008)

69 Gao et al. 2009
Gao, M., Sun, F.Z., Zhou, S.J., Shi, Y.T., Zhao, Y.B. and Wang, N.H.
Performance prediction of wet cooling tower using artificial neural network under cross-wind conditions. *International Journal of Thermal Science*, Vol. 48, pp. 583-589 (2009)

70 Graupe 2007
Daniel, G.
Principles of artificial neural networks. 2nd ed. Singapore: World Scientific Publishing Co. Pte. Ltd. 2007

71 Gurney 1997
Gurney, K.
An introduction to neural networks. London: UCL Press; 1997

72 Harriman Ⅲ and Judge 2002
Harriman, Ⅲ L.G. and Judge, J.
Dehumidification equipment advances. *ASHRAE Journal*, Vol. 44, No. 8, pp. 22-29 (2002)

73 Hayashi et al. 2010
Hayashi, Y., Hsieh, M.H. and Setiono, R.
Understanding consumer heterogeneity: A business intelligence application of neural networks. *Knowledge-Based Systems*, Vol. 23, No. 8, pp. 856-863 (2010)

74 Hayati et al. 2009
Hayati, M., Rezaei, A. and Seifia, M.
Prediction of the heat transfer rate of a single layer wire-on-tube type heat exchanger using ANFIS. *International Journal of Refrigeration*, Vol. 32, pp. 1914-1917 (2009)

75 Haykin 1999
Haykin, S.
Neural Networks, A Comprehensive Foundation. 2nd ed. London: Prentice-Hall; 1999

76 He et al. 1997
He, X.D., Liu, S. and Asada, H.H.
Modeling of vapor compression cycles for multivariable feedback control of HVAC systems. *Transaction of the ASME: Journal of Dynamic Systems, Measurement, and Control*, Vol. 119, pp. 183-191 (1997)

77 Henderson 1998
Henderson, H.I. Jr.
The impact of part-load air conditioner operation on dehumidification performance: Validating a latent capacity degradation model. *Proceeding of the 1998 ASHRAE Indoor Air Quality Conference*. (1998)

78 Henderson et al. 1992
Henderson, H.I.Jr., Rengarjan, K. and Shirey, D.B.
The impact of comfort control on air conditioner energy use in humid climates. *ASHRAE Transactions*, Vol. 98, No. Part. 2, pp. 104-112 (1992)

79 Holman 1994
Holman, J.P.
Experimental methods for engineers. New York: McGraw-Hill, 1994

80 Hopfield 1982
Hopfield, J.J.
Neural networks and physical systems with emergent collective computational abilities. *Proceedings of the National Academy of Science*, USA, Vol. 79, pp. 2554-2558 (1982)

81 Hosoz and Ertunc 2006a
Hosoz, M. and Ertunc, H.M.
Modeling of a cascade refrigeration system using artificial neural networks. *International Journal of Energy Research*, Vol. 30, pp. 1200-1215 (2006)

82 Hosoz and Ertunc 2006b
Hosoz, M. and Ertunc, H.M.
Artificial neural network analysis of an automobile air conditioning system. *Energy Conversion and Management*, Vol. 47, No. 11-12, pp. 1574-1587 (2006)

83 Hosoz et al. 2007
Hosoz, M., Ertunc, H.M. and Bulgurcu, H.
Performance prediction of a cooling tower using artificial neural network. *Energy Conversion and Management*, Vol. 48, pp. 1349-1359 (2007)

84 Hou et al. 2006
Hou, Z., Lian, Z., Yao, Y. and Yuan, X.
Cooling-load prediction by the combination of rough set theory and an artificial neural-network based on data-fusion technique. *Applied Energy*, Vol. 83, pp. 1033-1046 (2006)

85 Hourahan 2004
Hourahan, G.C.
How to properly size unitary equipment. *ASHRAE Journal*, Vol. 46, No. 2, pp. 15-18 (2004)

86 Huang et al. 2004
Huang, S.N, Tan, K.K. and Tang, K.Z.
Neural network control: theory and applications. Baldock, Hertfordshire, England: Research Studies Press, 2004

87 Huang et al. 2010
Huang, Y, Lan, Y, Thomson, S.J., Fang, A, Hoffmann, W.C. and Lacey, R.E.
Development of soft computing and applications in agricultural and biological engineering. *Computers and Electronics in Agriculture*, Vol. 71, No. 2 (2010)

88 Islamoglu et al. 2005
Islamoglu, Y., Kurt, A. and Parmaksizoglu, C.
Performance prediction for non-adiabatic capillary tube suction line heat exchanger: an artificial neural network approach. *Energy Conversion and Management*, Vol. 46, No. 2, pp. 223-232 (2005)

89 Jacobs et al. 1991
Jacobs, R.A., Jordan, M.I. and Barto, A.G.
Task decomposition through competition in a modular connectionist architecture: the what and where vision tasks. *Cognitive Science*, Vol. 15, pp. 219-250 (1991)

90 Jeannette et al. 1998
Jeannette, E., Assawamartbunlue, K., Curtiss, P. and Kreider, J.
Experimental results of a predictive neural network HVAC controller. *ASHRAE Transactions*, Vol. 104, No. 2, pp. 192-197, ASHRAE, Atlanta, GA, USA (1998)

91 Jia et al. 1995
Jia, X., Tso, C. P., Chia, P. K. and Jolly, P.
A distributed model for prediction of the transient response of an evaporator. *International Journal of Refrigeration*, Vol. 18, No. 5. pp. 336-342(1995)

92 Jiang et al. 2006
Jiang, W., Khan, J and Dougal, R.A.
Dynamic centrifugal compressor model for system simulation. *Journal of Power Sources*, Vol. 158, No. 2, pp. 1333-1343 (2006)

93 Jordan and Jacobs 1993
Jordan, M. and Jacobs, R.
Hierarchical mixtures of experts and the EM algorithm. Technical report 9301, MIT computational cognitive science (1993)

94 Kanarachos and Geramanis 1998
Kanarachos, A. and Geramanis, K.
Multivariable control of single zone hydronic heating systems with neural networks. *Energy Conversion and Management*, Vol. 39, No. 13, pp. 1317-1336 (1998)

95 Karlaftis and Vlahogianni 2011
Karlaftis, M.G. and Vlahogianni, E.I.
Statistical methods versus neural networks in transportation research: Differences, similarities and some insights. *Transportation Research Part C: Emerging Technologies*, Vol. 19, No. 3, pp. 387-399 (2011)

96 Khayyam et al. 2011
Khayyam, Hamid, Kouzani, A.Z., Hu, E.J. and Nahavandi, S.
Coordinated energy management of vehicle air conditioning system. *Applied Thermal Engineering*, Vol. 31, No. 5, pp. 750-764 (2011)

97 Kim et al. 2010
Kim, M.Y., Charles, P.G. and Christopher, Y.C.
Assessment of physically-based and data-driven models to predict microbial water quality in open channels. *Journal of Environmental Sciences*, Vol. 22, No. 6, pp. 851-857 (2010)

98 Kittisupakorn et al. 2009
Kittisupakorn, P., Thitiyasook, P., Hussain, M.A. and Daosud, W.
Neural network based model predictive control for a steel pickling process. *Journal of Process Control*, Vol. 19, No. 4, pp. 579-590 (2009)

99 Kittler 1996
Kittler, R.
Mechanical Dehumidification Control Strategies and Psychromatrics. *ASHRAE Transactions*, Vol. 102, No. 2, pp. 613-617 (1996)

100 Kizilkan 2011
Kizilkan, O.
Thermodynamic analysis of variable speed refrigeration system using artificial neural networks. *Expert Systems with Applications*, Vol. 38, No. 9, pp. 11686-11692 (2011)

101 Kohonen 1982
Kohonen, T.
Self-organized formation of topologically correct feature maps. *Biological Cybernetics*, Vol. 43, pp. 59-69 (1982)

102 Kosar 2006
Kosar, D.
Dehumidification system enhancements. *ASHRAE Journal*, February, pp. 48-58 (2006)

103 Krakow et al. 1995
Krakow, K.I., Lin, S. and Zeng, Z.S.
Temperature and humidity control during cooling and dehumidifying by compressor and evaporator fan speed variation. *ASHRAE Transactions*, Vol. 101, No. 1, pp. 292-304 (1995)

104 Krichel and Sawodny 2011
Krichel, S.V. and Oliver, Sawodny
Dynamic modeling of compressors illustrated by an oil-flooded twin helical screw compressor. *Mechatronics*, Vol. 21, No. 1, pp. 77-84 (2011)

105 Kurt and Kayfeci 2009
Kurt, H. and Kayfeci, M.
Prediction of thermal conductivity of ethylene glycol-water solutions by using artificial neural networks. *Applied Energy*, Vol. 86, pp. 2244-2248 (2009)

106 Kusiak et al. 2010
Kusiak, A., Li, M. and Zhang, Z.
A data-driven approach for steam load prediction in buildings. *Applied Energy*, Vol. 87, No. 3, pp. 925-933 (2010)

107 Kwok et al. 2011
Kwok, S.S.K., Yuen, R.K.K. and Lee, E.W.M.
An intelligent approach to assessing the effect of building occupancy on building cooling load prediction. *Building and Environment*, Vol. 46, No. 8, pp. 1681-1690 (2011)

108 Labus et al. 2012
Labus, J., Hernandez, J.A., Bruno, J.C. and Coronas, A.
Inverse neural network based control strategy for absorption chillers. *Renewable Energy*, Vol. 39, No. 1, pp. 471-482 (2012)

109 Lam 1996
Lam, J.C.
An analysis of residential sector energy use in Hong Kong. *Energy*, Vol. 21, pp.1-8 (1996)

110 Lenarduzzi and Yap 1998
Lenarduzzi, F. J. and Yap, S. S.
Measuring the performance of a variable-speed drive retrofit on a fixed-speed centrifugal chiller. *ASHRAE Transaction*, Vol. 104, part 2, pp. 658-667 (1998)

111 Li and Deng 2007a
Li, Z. and Deng, S.M.
An experimental study on the inherent operational characteristics of a direct expansion (DX) air conditioning (A/C) unit. *Building and Environment*, Vol. 42, No. 1, pp. 1-10 (2007)

112 Li and Deng 2007b
Li, Z. and Deng, S.M.
A DDC-based capacity controller of a direct expansion (DX) air conditioning (A/C) unit for simultaneous indoor air temperature and humidity control - Part I: Control algorithms and preliminary controllability tests. *International Journal of Refrigeration*, Vol. 30, No. 1, pp. 113-123 (2007)

113 Li and Deng 2007c
Li, Z. and Deng, S.M.
A DDC-based capacity controller of a direct expansion (DX) air conditioning (A/C) unit for simultaneous indoor air temperature and humidity control – Part II: Further development of the controller to improve control sensitivity. *International Journal of Refrigeration*, Vol. 30, No. 1, pp. 124-133 (2007)

114 Liang and Du 2008
Liang, J. and Du, R.
Design of intelligent comfort control system with human learning and minimum power control strategies. *Energy Conversion and Management*, Vol. 49, No. 4, pp. 517-528 (2008)

115 Liang et al. 1999
Liang, S.Y., Liu, M., Wong, T.N., and Nathan, G.K.
Analytical study of evaporator coil in humid environment, *Applied Thermal Engineering*, Vol. 19, pp.1129-1145(1999)

116 Li et al. 2009
Li, Q., Meng, Q., Cai, J., Yoshino, H. and Mochida, A.
Predicting hourly cooling load in the building: a comparison of support vector machine and different artificial neural networks. *Energy Conversion and Management*, Vol. 50, pp. 90-96 (2009)

117 Yamamoto et al. 1982
Yamamoto, T., Hibi, H. and Kuroda, T.
Development of an energy-saving-oriented variable capacity system heat pump. *ASHRAE Transaction*, Vol. 88, part 1, pp. 441-450 (1982)

118 Lin et al. 2008
Lin, C.S, Chiu, J.S., Hsieh, M.H., Mok, M.S., Li, Y.C. and Chiu, H.W.
Predicting hypotensive episodes during spinal anesthesia with the application of artificial neural networks, *Computer Methods and Programs in Biomedicine*, Vol. 92, No. 2, pp. 193-197 (2008)

119 Link and Deschamps 2011
Link, R. and Deschamps, C.J.
Numerical modeling of startup and shutdown transients in reciprocating compressors. *International Journal of Refrigeration*, Vol. 34, No. 6, pp. 1398-1414 (2011)

120 Liu et al. 2007
Liu, W.W., Lian, Z.W. and Zhao, B.
A neural network evaluation model for individual thermal comfort. *Energy and Buildings*, Vol. 39, No. 10, pp. 1115-1122 (2007)

121 Loannou and Pitsillides 2008
Loannou, P.A., Pitsillides, A.
Modeling and control of complex systems. London, New York: CRC Press, Tayor & Francis Group; 2008.

122 Lu 2003
Lu, X.
Estimation of indoor moisture generation rate from measurement in buildings. *Building and Environment*, Vol. 38, No. 5, pp. 665-675 (2003)

123 Lu and Viljanen 2009
Lu, T. and Viljanen, M.
Prediction of indoor temperature and relative humidity using neural network models: model comparison. *Neural Computing and applications*, Vol. 18, pp. 345-357 (2009)

124 Lu et al. 2004
Lu, W.Z., Wang, W.J., Wang, X.K., Yan, S.H. and Lam, J.C.
Potential assessment of a neural network model with PCA/RBF approach for forecasting pollutant trends in Mong Kok urban air, Hong Kong. *Environmental Research*, Vol. 96, No. 1, pp. 79-87 (2004)

125 Lucas and Miranville 2004
Lucas, F. and Miranville, F.
Indoor humidity modeling and evaluation of condensation on interior surfaces. *ASHRAE Transactions*, Vol. 110, Part. 2, pp. 300-308 (2004)

126 Mahmoud and Alajmi 2010
Mahmoud, M.A. and Alajmi, A.F.
Quantitative assessment of energy conservation due to public awareness campaigns using neural networks. *Applied Energy*, Vol. 87, No. 1, pp. 220-228 (2010)

127 Manohar et al. 2006
Manohar, H.J., Saravanan, R. and Renganarayanan, S.
Modelling of steam fired double effect vapour absorption chiller using neural network. *Energy Conversion and Management*, Vol. 47, No. 15-16, pp. 2202-2210 (2006)

128 Marini et al. 2008
Marini, F., Bucci, R., Magri, A.L. and Magri, A.D.
Artificial neural networks in chemometrics: History, examples and perspectives. *Microchemical Journal*, Vol. 88, No. 2, pp. 178-185 (2008)

129 Mazzei et al. 2005
Mazzei, P., Minichiello, F. and Palma, D.
HVAC dehumidification systems for thermal comfort: a critical review. *Applied Thermal Engineering*, Vol. 25, pp. 677-707 (2005)

130 Mehrotra et al. 1996
Mehrotra, K., Mohan, C.K. and Ranka, S.
Elements of artificial neural networks. London, England: MIT Press, 1996

131 Mei and Levermore 2002
Mei, L. and Levermore, G. J.
Simulation and validation of a VAV system with an ANN fan model and a non-linear VAV box model. *Building and Environment*, Vol. 37, No. 3, pp. 277-284 (2002)

132 McGahey 1998
McGahey, K.
New commercial applications for desiccant-based cooling. *ASHRAE Journal*, Vol. 40, No. 7, pp. 41-45 (1998)

133 McCulloch and Pitts 1943
McCulloch, W.S. and Pitts, W.
A logical calculus of the ideas immanent in nervous activity. *Bulletin of Mathematical Biophysics*, Vol. 5, pp. 115-133 (1943)

134 McNelis 2005
McNelis, P.D.
Neural Networks in Finance: Gaining Predictive Edge in the Market. London: Elsevier; 2005.

135 Miro 2005
Miro, C.
ASHRAE issues guidance on minimizing mold, mildew. *ASHRAE Journal*, Vol. 47, No. 3, pp. 86 (2005)

136 Moghaddam et al. 2011
Moghaddam, J.J., Farahani, M.H. and Amanifard, N.
A neural network-based sliding-mode control for rotating stall and surge in axial compressors. *Applied Soft Computing*, Vol. 11, No. 1, pp. 1036-1043 (2011)

137 Mohanraj et al. 2009a
Mohanraj, M., Jayaraj, S. and Muraleedharan, C.
Performance prediction of a direct expansion solar assisted heat pump using artificial neural networks. *Applied Energy*, Vol. 86, pp. 1441-1449 (2009)

138 Mohanraj et al. 2009b
Mohanraj, M., Jayaraj, S. and Muraleedharan, C.
Exergy analysis of a direct expansion solar assisted heat pump using artificial neural networks. *International Journal of Energy Research*, Vol. 33, pp. 1005-1020 (2009)

139 Mohanraj et al. 2010
Mohanraj, M., Jayaraj, S. and Muraleedharan, C.
Exergy assessment of direct expansion solar assisted heat pump working with R22 and R407C/LPG mixture. *International Journal of Green Energy*, Vol. 7, pp. 65-83 (2010)

140 Morel et al. 2001
Morel, N., Bauer, M., El-Khoury, M. and Krauss, J.
Neurobat, a predictive and adaptive heating-control system using artificial neural networks. *International Journal of Solar Energy*, Vol. 21, No. 2-3, pp. 161-202 (2001)

141 Mustafaraj et al. 2010
Mustafaraj, G., Chen, J. and Lowry, G.
Thermal behaviour prediction utilizing artificial neural networks for an open office. *Applied Mathematical Modelling*, Vol. 34, No. 11, pp. 3216-3230 (2010)

142 Mustafaraj et al. 2011
Mustafaraj, G., Lowry, G. and Chen, J.
Prediction of room temperature and relative humidity by autoregressive linear and nonlinear neural network models for an open office. *Energy and Buildings*, Vol. 43, No. 6, pp. 1452-1460 (2011)

143 Nagaya et al. 2006
Nagaya, K., Senbongi, T., Li, Y., Zheng, J. and Murakami, I.
High energy efficiency desiccant assisted automobile air-conditioner and its temperature and humidity control system. *Applied Thermal Engineering* , Vol. 26, pp. 1545-1551 (2006)

144 Nanayakkara et al. 2002
Nanayakkara, V.K., Ikegami, Y. and Uehara, H.
Evolutionary design of dynamic neural networks for evaporator control, *International Journal of Refrigeration*, Vol. 25, No. 6, pp. 813-826 (2002)

145 Narendra and Parthasarathy 1990
Narendra, K.S. and Parthasarathy, K.
Identification and control of dynamical systems using neural networks. *IEEE Transactions on Neural Networks*, Vol. 3, pp. 4-27 (1990)

146 Navarro-Esbri et al. 2007
Navarro-Esbri, J., Berbegall, V., Verdu, G., Cabello, R. and Llopis, R.
A low data requirement model of a variable-speed vapour compression refrigeration system based on neural networks. *International Journal of Refrigeration*, Vol. 30, No. 8, pp. 1452-1459 (2007)

147 Navarro et al. 2007
Navarro, E., Granryd, E., Urchueguia, J.F. and Corberan, J.M.
A phenomenological model for analyzing reciprocating compressors. *International Journal of Refrigeration*. Vol. 30, No. 7, pp. 1254-1265 (2007)

148 Ndiaye and Bernier 2010
Ndiaye, D. and Bernier, M.
Dynamic model of a hermetic reciprocating compressor in on-off cycling operation (Abbreviation: Compressor dynamic model). *Applied Thermal Engineering*, Vol. 30, No. 8-9, pp. 792-799 (2010)

149 Negrao et al. 2011
Negrao, C.O.R., Erthal, R.H., Andrade, D.E.V. and Silva, L.W.
A semi-empirical model for the unsteady-state simulation of reciprocating compressors for household refrigeration applications. *Applied Thermal Engineering*, Vol. 31, No. 6-7, pp. 1114-1124 (2011)

150 Neto and Fiorelli 2008
Neto, A.H. and Fiorelli, F.A.S.
Comparison between detailed model simulation and artificial neural network for forecasting building energy consumption. *Energy and Buildings*, Vol. 40, No. 12, pp. 2169-2176 (2008)

151 NG 1997
NG, G.W.
Application of neural networks to adaptive control of nonlinear systems. Taunton, Somerset, England: Research studies press ltd, 1997

152 Nissen 2003
Nissen, S.
Implementation of a Fast Artificial Neural Network Library (FANN), Report, Department of Computer Science University of Copenhagen (DIKU), 2003

153 Norgaard et al. 2000
Norgaard. M., Ravn, O., Poulsen, N.K. and Hansen, L.K.
Neural Networks for Modelling and Control of Dynamic Systems. Springer, London, 2000

154 Ovaska 2004
Ovaska, S.J.
Computationally Intelligent Hybrid Systems: The Fusion of Soft Computing and Hard Computing. John Wiley & Sons, Inc. NY, 2004

155 Pacheco-Vega et al. 2001a
Pacheco-Vega, A., Diaz, G., Sen, M., Yang, K.T. and McClain, R.T.
Neural network analysis of fin-tube refrigerating heat exchanger with limited experimental data. *International Journal of Heat Mass Transfer*, Vol. 44, pp. 763-770 (2001)

156 Pacheco-Vega et al. 2001b
Pacheco-Vega, A., Diaz, G., Sen, M., Yang, K.T. and McClain, R.T.
Heat Rate Predictions in Humid Air-Water Heat Exchanger Using Correlations and Neural Networks. *ASME Journal of Heat Transfer*, Vol. 123, No. 2, pp. 348-354 (2001)

157 Palau et al. 1999
Palau, A., Velo, E. and Puigjaner, L.
Use of neural networks and expert systems to control a gas/solid sorption chilling machine. *International Journal of Refrigeration*, Vol. 22, No. 1, pp. 59-66 (1999)

158 Park 2010
Park, Y.C.
Transient analysis of a variable speed rotary compressor. *Energy Conversion and Management*, Vol. 51, No. 2, pp. 277-287 (2010)

159 Park et al. 2007
Park, C., Cho, H., Lee, Y. and Kim, Y.
Mass flow characteristics and empirical modeling of R22 and R410A flowing through electronic expansion valves. *International Journal of Refrigeration*, Vol. 30, pp.1401-1407(2007)

160 Perez-Segarra et al. 2003
Perez-Segarra, C.D., Rigola, J. and Oliva, A.,
Modeling and numerical simulation of the thermal and fluid dynamic behavior of hermetic reciprocating compressors. Part 1: theoretical basis, *HVAC & R Research*, Vol. 9, No. 2, pp. 215-235 (2003)

161 Pintelon and Schoukens 2001
Pintelon, R. and Schoukens, J.
System identification: a frequency domain approach, IEEE Press, New York, 2001

162 Porkhial et al. 2004
Porkhial, S., Khastoo, B. , Saffar-Avval, M.
Transient response of dry expansion evaporator in household refrigerators. *Applied Thermal Engineering*, Vol. 24, pp. 1465-1480 (2004)

163 Qi and Deng 2008
Qi, Q., Deng, S.M.
Multivariable control-oriented modeling of a direct expansion (DX) air conditioning (A/C) system. *International Journal of Refrigeration*, Vol. 31, pp. 841-849 (2008)

164 Qi and Deng 2009
Qi, Q., Deng, S.M.
Multivariable control of indoor air temperature and humidity in a direct expansion (DX) air conditioning (A/C) system. *Building Environment*, Vol. 44, pp. 1659-1667 (2009)

165 Qi et al. 2010
Qi, Q., Deng, S.M., Xu X.G. and Chan, M.Y.
Improving degree of superheat control in a direct expansion (DX) air conditioning (A/C) system. *International Journal of Refrigeration*, Vol. 33, No. 1, pp. 125-134 (2010)

166 Qureshi and Tassou 1996
Qureshi, T. Q. and Tassou, S. A.
Variable-speed capacity control in refrigeration systems. *Applied Thermal Engineering*, Vol. 16, No. 2, pp. 103-113(1996)

167 Rigola et al. 2003
Rigola, J., Perez-Segarra, C.D. and Oliva, A.,
Modeling and numerical simulation of the thermal and fluid dynamic behavior of hermetic reciprocating compressors. Part 2: experimental investigation, *HVAC & R Research*, Vol. 9, No. 2, pp. 237-249 (2003)

168 Rock and Wu 1998
Rock, B.A. and Wu, C.T.
Performance of fixed, air-side economizer, and neural network demand-controlled ventilation in CAV systems. *ASHRAE Transactions*, Vol. 104, No. 2, pp. 234-245, ASHRAE, Atlanta, GA, USA (1998)

169 Rode et al. 2004
Rode, C., Mendes, N. and Grau, K.
Evaluation of moisture buffer effects by performing whole-building simulations. *ASHRAE Transactions*, Vol. 110, No. 2, pp. 783-794 (2004)

170 Rosenblatt 1958
Rosenblatt, F.
The perceptron: a probabilistic model for information storage and organization in the brain, *Psychological Review*, Vol. 65, No. 6, pp. 386-408 (1958)

171 Rosiek and Batlles 2010
Rosiek, S. and Batlles, F.J.
Modelling a solar-assisted air-conditioning system installed in CIESOL building using an artificial neural network. *Renewable Energy*, Vol. 35, pp. 2894-2901 (2010)

172 Rosiek and Batlles 2011
Rosiek, S. and Batlles, F.J.
Performance study of solar-assisted air-conditioning system provided with storage tanks using artificial neural networks. *International Journal of Refrigeration*, Vol. 34, No. 6, pp. 1446-1454 (2011)

173 Rumelhart et al. 1986
Rumelhart, D.E., Hinton, G.E. and Williams, R.J.
Learning representations of back-propagation errors. *Nature (London)*, Vol. 323, pp. 533-536 (1986)

174 Saerens and Soquet 1989
Saerens, M. and Soquet, A.
A neural controller. In: Proceeding of the first international conference of artificial neural networks, London, pp. 211-215 (1989)

175 Sahin 2011
Sahin, A.S.
Performance analysis of single-stage refrigeration system with internal heat exchanger using neural network and neuro-fuzzy. *Renewable Energy*, Vol. 36, No. 10, pp. 2747-2752 (2011)

176 Saidur et al. 2006
Saidur, R., Masjuki, H.H. and Jamiludhin, M.Y.
A new method to investigate the energy performance of a household refrigerator-freezer. *International Energy Journal*, Vol. 7, pp. 9-15 (2006)

177 Sainlez and Heyen 2011
Sainlez, M. and Heyen, G.
Recurrent neural network prediction of steam production in a Kraft recovery boiler. *Computer Aided Chemical Engineering*, Vol. 29, pp. 1784-1788 (2011)

178 Sanaye et al. 2011
Sanaye, S., Dehghandokht, M., Beigi, H.M. and Bahrami, S.
Modeling of rotary vane compressor applying artificial neural network. *International Journal of Refrigeration*, Vol. 34, pp. 764-772 (2011)

179 Scalabrin and Bianco 1994
Scalabrin, G. and Bianco, G.
Experimental and thermodynamic analysis of a variable-speed open reciprocating refrigeration compressor. *International Journal of Refrigeration*, Vol. 17, No. 1, pp. 68-75 (1994)

180 Schalkoff 1997
Schalkoff, R.J.
Artificial neural networks. USA: McGraw-Hill; 1997

181 Sen and Yang 2000
Sen, M. and Yang, K.T.
Applications of artificial neural networks and genetic algorithms in thermal engineering. Kreith F. (Ed.), *The CRC Handbook of Thermal Engineering*, CRC Press, Boca Raton, FL, 2000

182 Sencan 2006
Sencan, A.
Artificial intelligent methods for thermodynamic evaluation of ammonia-water refrigeration systems. *Energy Conversion and Management*, Vol. 47, pp. 3319-3332 (2006)

183 Sencan 2007
Sencan, A.
Performance of ammonia-water refrigeration systems using artificial neural networks. *Renewable Energy*, Vol. 32, pp. 314-328 (2007)

184 Sencan et al. 2011
Sencan, A., Kose, I.I. and Selbas, R.
Prediction of thermophysical properties of mixed refrigerants using artificial neural network. *Energy Conversion and Management*, Vol. 52, pp. 958-974 (2011)

185 Seshaiah et al. 2007
Seshaiah, N., Ghosh, S.K., Sahoo, R.K. and Sarangi, S.K.
Mathematical modeling of the working cycle of oil injected rotary twin screw compressor. *Applied Thermal Engineering*, Vol. 27, No. 1, pp. 145-155 (2007)

186 Shakun 1992
Shakun, W.
The causes and control of mold and mildew in hot and humid climates. *ASHRAE Transactions*, Vol. 98, No. 1, pp. 1282-1292 (1992)

187 Shaw and Luxton 1988
Shaw, A. and Luxton, R.E.
A comprehensive method of improving part-load air-conditioning performance. *ASHRAE Transactions*, Vol. 94, Part. 1, pp. 442-457 (1988)

188 Sherman 1999
Sherman, M.
Indoor air quality for residential buildings. *ASHRAE Journal*, Vol. 41, No. 5, pp. 26-30 (1999)

189 Shirey and Henderson 2004
Shirey, D.B.Ⅲ. and Henderson, H.I.Jr.
Dehumidification at part load. *ASHRAE Journal*, Vol. 46, No. 3, pp. 42-47 (2004)

190 Silver et al. 1990
Silver, S.C., Fine, P.J. and Rose, F.
Performance monitoring of DX rooftop cooling equipment. Energy Engineering: *Journal of the Association of Energy*, Vol. 87, No. 5, pp. 32-41 (1990)

191 Sofuoglu 2008
Sofuoglu, S.C.
Application of artificial neural networks to predict prevalence of building-related symptoms in office buildings. *Building and Environment*, Vol. 43, No. 6, pp. 1121-1126 (2008)

192 Soyguder 2011
Soyguder, S.
Intelligent system based on wavelet decomposition and neural network for predicting of fan speed for energy saving in HVAC system. *Energy and Buildings*, Vol. 43, pp. 814-822 (2011)

193 Sozen and Akcayol 2004
Sozen, A. and Akcayol, M.A.
Modelling (using artificial neural networks) the performance parameters of a solar-driven ejector-absorption cycle. *Applied Energy*, Vol. 79, pp. 309-325 (2004)

194 Sozen et al. 2004a
Sozen, A., Arcaklioglu, E. and Ozalp, M.
Performance analysis of ejector absorption heat pump using ozone safe fluid couple through artificial neural networks. *Energy Conversion and Management*, Vol. 45, pp. 2233-2253 (2004)

195 Sozen et al. 2004b
Sozen, A., Ozalp, M. and Arcaklioglu, E.
Investigation of thermodynamic properties of refrigerant/absorbent couples using artificial neural networks. *Chemical Engineering and Processing*, Vol. 43, pp. 1253-1264 (2004)

196 Sozen et al. 2005
Sozen, A., Arcaklioglu, E. and Ozalp, M.
Formulation based on artificial neural network of thermodynamic properties of ozone friendly refrigerant/absorbent couples. *Applied Thermal Engineering*, Vol. 25, pp. 1808-1820 (2005)

197 Sozen et al. 2007
Sozen, A., Ozalp, M. and Arcaklioglu, E.
Calculation for the thermodynamic properties of an alternative refrigerant (R508b) using artificial neural network. *Applied Thermal Engineering*, Vol. 27, No. 2-3, pp. 551-559 (2007)

198 Sozen et al. 2009
Sozen, A., Arcaklioglu, E., Menlik, T. and Ozalp, M.
Determination of thermodynamic properties of an alternative refrigerant (R407c) using artificial neural network. *Expert Systems with Applications*, Vol. 36, No. 3, pp. 4346-4356 (2009)

199 Sozen et al. 2010
Sozen, A., Arcaklioglu, E. and Menlik, T.
Derivation of empirical equations for thermodynamic properties of a ozone safe refrigerant (R404a) using artificial neural network. *Expert Systems with Applications*, Vol. 37, No. 2, pp. 1158-1168 (2010)

200 Sterling et al. 1985
Sterling, E.M., Arundel, A. and Sterling, T.D.
Criteria for human exposure to humidity in occupied buildings. *ASHRAE Transactions*, Vol. 91, No. Part. 1B, pp. 611-622 (1985)

201 Straube 2002
Straube, J.F.
Moisture in buildings. *ASHRAE Journal*, Vol. 44, No. 1, pp. 15-19 (2002)

202 Swider et al. 2001
Swider, D.J., Browne, M.W., Bansal, P.K. and Kecman, V.
Modeling of vapour compression liquid chillers with neural networks. *Applied Thermal Engineering*, Vol. 21, pp. 311-329 (2001)

203 Tian et al. 2008
Tian, J., Feng, Q. and Zhu, R.Q.
Analysis and experimental study of MIMO control in refrigeration system. *Energy Conversion and Management*, Vol. 49, No. 5, pp. 933-939 (2008)

204 Tirnovan et al. 2008
Tirnovan, R., Giurgea, S., Miraoui, A., Cirrincione, M.
Surrogate modelling of compressor characteristics for fuel-cell applications. *Applied Energy*, Vol. 85, No. 5, pp. 394-403 (2008)

205 Toftum and Fanger 1999
Toftum, J. and Fanger, P.O.
Air Humidity Requirements for Human Comfort. *ASHRAE Transactions*, Vol. 105, No. 2, pp. 641-647 (1999)

206 Vargas and Parise 1995
Vargas, J.V.C. and Paris, J.A.R.
Simulation in transient regime of a heat pump with closed-looped and on-off control. *International Journal of Refrigeration*, Vol. 18, No. 4, pp. 25-243 (1995)

207 Varshney and Panigrahi 2005
Varshney, K. and Panigrahi, P.K.
Artificial neural network control of a heat exchanger in a closed flow air circuit, *Applied Soft Computing*, Vol. 5, No. 4, pp. 441-465 (2005)

208 Vasickaninova et al. 2011
Vasickaninova, A., Bakosova, M., Meszaros, A. and Klemes, J.J.
Neural network predictive control of a heat exchanger, *Applied Thermal Engineering*, Vol. 31, No. 13, pp. 2094-2100 (2011)

209 Vins and Vacek 2009
Vins, V. and Vacek, V.
Mass flow rate correlation for two-phase flow of R218 through a capillary tube. *Applied Thermal Engineering*, Vol. 29, pp. 2816-2823 (2009)

210 Wang and Bao 2000
Wang, D. and Bao, P.
Enhancing the estimation of plant Jacobian for adaptive neural inverse control. *Neurocomputing*, Vol. 34, pp. 99-115 (2000)

211 Wang and Touber 1991
Wang, H. and Touber, S.
Distributed and non-steady-state modeling of an air cooler. *International Journal of Refrigeration*, Vol.14, pp. 98-111(1991)

212 Wang et al. 2006
Wang, Q.W., Xie, G.N., Zeng, M. and Luo, L.Q.
Prediction of heat transfer rates for shell-and-tube heat exchangers by artificial neural network approach. *Journal of Thermal Science*, Vol. 15, pp. 257-262 (2006)

213 Winandy et al. 2002
Winandy, E., Saavedra, O.C. and Lebrun, J.
Simplified modeling of an open-type reciprocating compressor, *International Journal of Thermal Science*, Vol. 41, pp.183-192(2002).

214 Widrow 1962
Widrow, B.
Generalization and information storage in networks of adeline neurons. in M.C. Yovitz, G.T. Jacobi, and G.D. Goldstein, eds., *Self-Organizing Systems*, pp. 435-461, Washington DC: Spartan Books (1962)

215 Widrow and Hoff 1960
Widrow, B. and Hoff, M.E.
Adaptive switching circuits. *Proc. IRE WESCON Conference*, New York, pp. 96-104 (1960)

216 Wong et al. 2010
Wong, S.L., Wan, K.K.W. and Lam, T.N.T.
Artificial neural networks for energy analysis of office buildings with daylighting. *Applied Energy*, Vol. 87, No. 2, pp. 551-557 (2010)

217 Wu et al. 2011
Wu, J.S., Zhang, G.Q., Zhang, Q., Zhou, J. and Wang, Y.
Artificial neural network analysis of the performance characteristics of a reversibly used cooling tower under cross flow conditions for heat pump heating system in winter. *Energy and Buildings*, Vol. 43, No. 7, pp. 1685-1693 (2011)

218 Xia et al. 2008
Xia, L., Chan, M.Y. and Deng, S.M.
Development of a method for calculating steady-state equipment sensible heat ratio of direct expansion air conditioning units. *Applied Energy*, Vol. 85, No. 12, pp. 1198-1207 (2008)

219 Xie et al. 2007
Xie, G.N., Wang, Q.W., Zeng, M. and Luo, L.Q.
Heat transfer analysis for shell-and-tube heat exchangers with experimental data by artificial neural networks approach. *Applied Thermal Engineering*, Vol. 27, pp. 1096-1104 (2007)

220 Xu et al. 2008
Xu, X.G., Deng, S.M. and Chan, M.Y.
A new control algorithm for direct expansion air conditioning systems for improved indoor humidity control and energy efficiency. *Energy Conversion and Management*, Vol. 49, No. 4, pp. 578-586 (2008)

221 Yang 2008
Yang, K.T.
Artificial Neural Networks (ANNs): A New Paradigm for Thermal Science and Engineering. *Journal of Heat Transfer*, Vol. 130, pp. 1-18 (2008)

222 Yang and Lee 1991
Yang, K. H and Lee, M. L.
Analysis of an inverter-driven air-conditioning system and its application in a hot and humid area. *International Journal of Energy Research*, Vol. 15, No. 5, pp. 357-365 (1991)

223 Yang and Sen 2000
Yang, K.T. and Sen, M.
Artificial neural network-based dynamic modeling thermal systems and their control. Wang B.X. (Ed.), *Heat Transfer Science and Technology*, Higher Education Press, Beijing (2000)

224 Yang et al. 2003
Yang, I.H., Yeo, M.S. and Kim, K.W.
Application of artificial neural network to predict the optimal start time for heating system in building. *Energy Conversion and Management*, Vol. 44, No. 17, pp. 2791-2809 (2003)

225 Yang et al. 2005
Yang, B.S., Hwang, W.W., Kim, D.J. and Tan, A.C.
Condition classification of small reciprocating compressor for refrigerators using artificial neural networks and support vector machines. *Mechanical Systems and Signal Processing*, Vol. 19, No. 2, pp. 371-390 (2005)

226 Yang et al. 2009
Yang, L., Zhao, L.X., Zhang, C.L. and Gu, B.
Loss-efficiency model of single and variable-speed compressors using neural networks. *International Journal of Refrigeration*, Vol. 32, No. 6, pp. 1423-1432 (2009)

227 Yao et al. 2006
Yao, Y., Lian, Z., Hou, Z. and Liu, W.
An innovative air conditioning load forecasting model based on RBF neural network and combined residual error correction. *International Journal of Refrigeration*, Vol. 29, pp. 528-538 (2006)

228 Yaqub and Zubair 2001
Yaqub, M. and Zubair, S.M.
Capacity Control for Refrigeration and Air-Conditioning Systems: A Comparative Study. *Transactions of the ASME*, Vol. 123, pp. 92-99 (2001)

229 Yau 2007
Yau, Y.H.
Application of a heat pipe heat exchanger to dehumidification enhancement in a HVAC system for tropical climates--a baseline performance characteristics study. *International Journal of Thermal Sciences*, Vol. 46, pp. 164-171(2007)

230 Yigit and Ertunc 2006
Yigit, K.S. and Ertunc, H.M.
Prediction of the air temperature and humidity at the outlet of a cooling coil using neural networks. *International Communications in Heat and Mass Transfer*, Vol. 33, pp. 898-907 (2006)

231 Youn et al. 2002
Youn, C.P., Kim, Y., and Cho, H.
Thermodynamic analysis on the performance of a variable speed scroll compressor with refrigerant injection. *International Journal of Refrigeration*, Vol. 25, No. 8, pp.1072-1082 (2002)

232 Zadeh 1994
Zadeh, L.A.
Fuzzy Logic, Neural Networks, and Soft Computing. *Communications of the ACM*, Vol. 37, No. 3, pp. 77-84 (1994)

233 Zadeh 1996
Zadeh, L.A.
The roles of soft computing and fuzzy logic in the conception, design and deployment of intelligent systems. IIZUKA'96, in: *Proceedings of the Fourth International Conference on Soft Computing*, pp. 3-4 (1996)

234 Zavala-Rio and Santiesteban-Cos 2007
Zavala-Rio, A. and Santiesteban-Cos, R.
Reliable compartmental models for double-pipe heat exchangers: An analytical study. *Applied Mathematical Modelling*, Vol. 31, No. 9, pp. 1739-1752 (2007)

235 Zhang 2002
Zhang, G.Q.
China HVACR Annual Business VolumeⅡ. *Chinese Construction Industry Press*, pp. 44-45 (2002)

236 Zhang 2005
Zhang, C.L.
Generalized correlation of refrigerant mass flow rate through adiabatic capillary tubes using artificial neural network. *International Journal of Refrigeration*, Vol. 28, pp. 506-514 (2005)

237 Zhang and Zhang 2006
Zhang, W.J. and Zhang, C.L.
A generalized moving-boundary model for transient simulation of dry-expansion evaporators under larger disturbances. *International Journal of Refrigeration*, Vol. 29, pp. 1119-1127 (2006)

238 Zhao and Zhang 2010
Zhao, L.X. and Zhang, C.L.
Fin-and tube condenser performance evaluation using neural networks. *International Journal of Refrigeration*, Vol. 33, pp. 625-634 (2010)

239 Zhao et al. 2007
Zhao, L.X., Zhang, C.L., Shao, L.L. and Yang, L.
A generalized neural network model of refrigerant mass flow through adiabatic capillary tubes and short tube orifices. *ASME Journal of Fluids Engineering*, Vol. 129, pp. 1559-1564 (2007)